
# NAVAL POSTGRADUATE SCHOOL

**MONTEREY, CALIFORNIA**

# THESIS

**DETECTION AND JAMMING LOW PROBABILITY OF INTERCEPT (LPI) RADARS**

by

Aytug Denk

September 2006

| | |
|---|---|
| Thesis Advisor: | Edward Fisher |
| Second Reader: | Orin Marvel |

**Approved for public release; distribution is unlimited.**

THIS PAGE INTENTIONALLY LEFT BLANK

| REPORT DOCUMENTATION PAGE | | Form Approved OMB No. 0704-0188 |
|---|---|---|

Public reporting burden for this collection of information is estimated to average 1 hour per response, including the time for reviewing instruction, searching existing data sources, gathering and maintaining the data needed, and completing and reviewing the collection of information. Send comments regarding this burden estimate or any other aspect of this collection of information, including suggestions for reducing this burden, to Washington headquarters Services, Directorate for Information Operations and Reports, 1215 Jefferson Davis Highway, Suite 1204, Arlington, VA 22202-4302, and to the Office of Management and Budget, Paperwork Reduction Project (0704-0188) Washington DC 20503.

| 1. AGENCY USE ONLY | 2. REPORT DATE | 3. REPORT TYPE AND DATES COVERED |
|---|---|---|
| | September 2006 | Master's Thesis |

**4. TITLE AND SUBTITLE** Detection and Jamming Low Probability of Intercept (LPI) Radars

**5. FUNDING NUMBERS**

**6. AUTHOR(S)** Aytug Denk

**7. PERFORMING ORGANIZATION NAME(S) AND ADDRESS(ES)**
Naval Postgraduate School
Monterey, CA 93943-5000

**8. PERFORMING ORGANIZATION REPORT NUMBER**

**9. SPONSORING /MONITORING AGENCY NAME(S) AND ADDRESS(ES)**
N/A

**10. SPONSORING/MONITORING AGENCY REPORT NUMBER**

**11. SUPPLEMENTARY NOTES** The views expressed in this thesis are those of the author and do not reflect the official policy or position of the Department of Defense or the U.S. Government.

**12a. DISTRIBUTION / AVAILABILITY STATEMENT**
Approved for public release; distribution is unlimited

**12b. DISTRIBUTION CODE**

**13. ABSTRACT**

An increasing number of LPI radars are integrated into integrated air defense systems (IADS) and modern platforms and weapons, such as anti-ship missiles, and littoral weapon systems. These LPI radars create a requirement for modern armed forces to develop new techniques, strategies, and equipment.

The primary objective of this thesis is to investigate methods and means to counter LPI radar threats integrated into a modern platforms and weapons and focus on the related techniques, strategies, and technology. To accomplish this objective both platform centric and network centric approaches will be examined thoroughly.

**14. SUBJECT TERMS**

detection, interception, classification, jamming, LPI Radar, low probability of intercept radar

**15. NUMBER OF PAGES**
123

**16. PRICE CODE**

| 17. SECURITY CLASSIFICATION OF REPORT | 18. SECURITY CLASSIFICATION OF THIS PAGE | 19. SECURITY CLASSIFICATION OF ABSTRACT | 20. LIMITATION OF ABSTRACT |
|---|---|---|---|
| Unclassified | Unclassified | Unclassified | UL |

NSN 7540-01-280-5500

Standard Form 298 (Rev. 2-89)
Prescribed by ANSI Std. 239-18

THIS PAGE INTENTIONALLY LEFT BLANK

**Approved for public release; distribution is unlimited**

**DETECTION AND JAMMING LOW PROBABILITY OF INTERCEPT (LPI) RADARS**

Aytug Denk
Captain, Turkish Air Force
B.S., Turkish Air Force Academy, 1997

Submitted in partial fulfillment of the
requirements for the degree of

**MASTER OF SCIENCE IN SYSTEMS ENGINEERING**

from the

**NAVAL POSTGRADUATE SCHOOL**
**September 2006**

Author: Aytug Denk

Approved by: Edward Fisher
Thesis Advisor

Orin Marvel
Second Reader

Dan Boger
Chairman, Department of Information Sciences

THIS PAGE INTENTIONALLY LEFT BLANK

# ABSTRACT

An increasing number of LPI radars are integrated into integrated air defense systems (IADS) and modern platforms and weapons, such as anti-ship missiles, and littoral weapon systems. These LPI radars create a requirement for modern armed forces to develop new techniques, strategies, and equipment.

The primary objective of this thesis is to investigate methods and means to counter LPI radar threats integrated into a modern platforms and weapons and focus on the related techniques, strategies, and technology. To accomplish this objective both platform centric and network centric approaches will be examined thoroughly.

THIS PAGE INTENTIONALLY LEFT BLANK

# TABLE OF CONTENTS

THIS PAGE INTENTIONALLY LEFT BLANK

# LIST OF FIGURES

# LIST OF TABLES

THIS PAGE INTENTIONALLY LEFT BLANK

# ACKNOWLEDGMENTS

Initially I would like to thank Mr. Edward Fisher and Professor Orin Marvel for their support, guidance and patience during this thesis preparation. Without their help, this work would not be possible.

I further would like to express my gratitude to my wife, Aydan, for her unconditional love, support, and understanding throughout our entire stay here in beautiful Monterey.

I would also like to thank to my brothers in arms, Lt.J.G Aykut Kertmen Turkish Navy, and 1st Lt. Ali Can Kucukozyigit, Turkish Army for their valuable contributions and support to this work.

Finally, I would like to thank the Turkish Air Force for giving me the opportunity to study at the Naval Postgraduate School.

THIS PAGE INTENTIONALLY LEFT BLANK

# I. INTRODUCTION

## A. BACKGROUND

Most radars, such as surveillance and target tracking radars, have to contend with very capable and advanced threats on today's battlefields. These threats range from anti-radiation missiles (ARMs), radar warning receivers (RWRs), electronic warfare support (ES) interception capabilities, and electronic attack (EA) systems. All of these are designed to contribute to the degradation of radar performance by jamming, evasion, or destruction.

To survive these countermeasures and accomplish their missions, radars have to hide their emissions from hostile receivers. For this purpose, and to mask their presence, radars use power management, wide operational bandwidth, frequency agility, antenna side lobe reduction, and advanced scan patterns (modulations). These types of radars are called Low Probability of Intercept (LPI) radars and they use techniques *"to see and not to be seen"*[1] by modern and capable intercept receivers.

Some receivers using conventional interception techniques can not efficiently detect and identify LPI radars. Mismatched waveforms used by LPI radar cause RWRs and conventional ES systems to detect the LPI radar at very short ranges, if at all. In these cases the RWR/ES system's detection range is much shorter than the operational range of the LPI radar, providing a detection disadvantage for the RWR/ES systems and a lethal advantage for the radar versus a potential target platform.

An increasing number of LPI radars are incorporated into integrated air defense systems (IADS) and modern platforms and weapons, such as anti-ship missiles, and littoral weapon systems. These LPI radars create a requirement for modern armed forces to develop new techniques, strategies, and equipment to counter them.

[1] (Fuller 1990, 1-10)

## B. SCOPE OF THE THESIS

The primary objective of this thesis is to investigate methods and means to counter LPI radar threats integrated into a modern platforms and weapons and focus on the related techniques, strategies, and technology. To accomplish this objective both platform centric and network centric approaches will be examined thoroughly.

## C. RESEARCH QUESTIONS

Primary Question

- Can LPI radars be jammed?

Subsidiary Questions

- How does LPI radar gain its advantage?
- What methods can be used to intercept LPI radars?
- What methods can be used to jam LPI radars?

## D. METHODOLOGY

Articles, books, periodicals, thesis, IEEE, and DoD documents related to the subject will be collected and thoroughly examined. The answers to questions stated in the above section will be established in a reasonable fashion. In order to do this, comprehensive knowledge of LPI radar systems, detection and jamming methods will be studied and explained.

## E. BENEFITS OF THE STUDY

The results from this thesis will be used to support ongoing efforts by the Turkish Armed Forces. This thesis will enhance the perspective and knowledge of Electronic Warfare officers, related project officers, and technical personnel. Furthermore, research and results will assist the Turkish Armed Forces in evaluating future needs and requirements of Electronic Warfare systems.

## F. THESIS OUTLINE

Chapter II briefly describes the LPI radar techniques, characteristics and waveforms used in this thesis work. Examples of airborne, maritime, and land-based LPI radars are given.

Chapter III describes detection methods of LPI radars. For this purpose ES receivers and signal processing algorithms are examined in detail. Examples of ES receiver systems used in real operational environment are also given.

Chapter IV analyzes both platform and network centric classification and jamming methods for LPI radars. LPI radar jammer requirements and jamming of LPI radars are discussed.

Finally, conclusions are summarized in Chapter V.

THIS PAGE INTENTIONALLY LEFT BLANK

# II. LOW PROBABILITY OF INTERCEPT (LPI) RADAR

## A. LPI RADAR PRINCIPLES

In the modern battlefield, radars face increasingly serious threats from Electronic Attack and ARMs. An important feature of modern radar systems is the ability "to see and not to be seen". Low Probability of Intercept radar has a powerful detection capability while simultaneously itself being not easily detected by electronic reconnaissance equipment. (Hou Jiangang et al. 2004, 2070; 2070-3 vol.3; 3o.3).

Whether or not a radar is LPI depends on the purpose or mission of the radar, the kind of receiver that is trying to detect it, and the applicable engagement geometry (Adamy 2001, ).. These types of radars are also described as "quiet" radars.

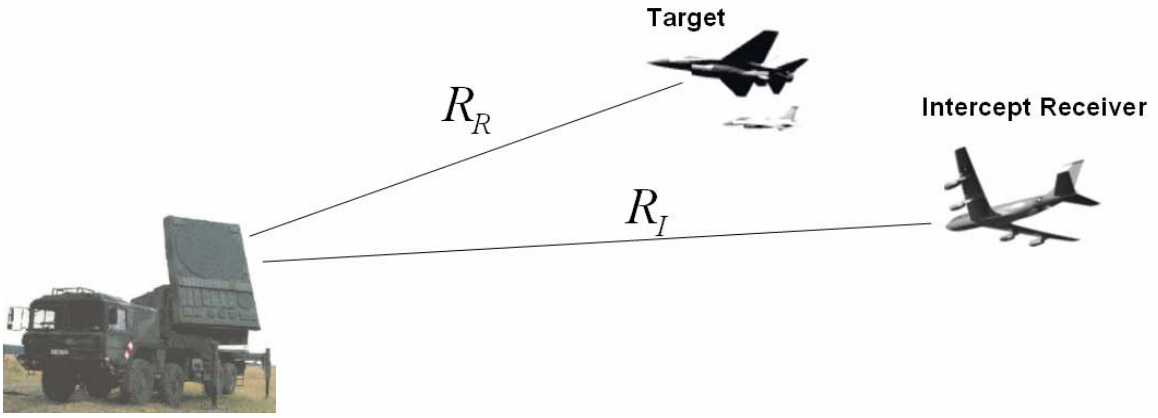


Figure 1. The Geometry of Radar, Target and Intercept Receiver[2]

In order to hide itself from the interception of ES systems and RWRs, the detection range of radar $R_R$ should be longer than that of intercept receiver $R_I$. From Figure 1, a range factor α can be defined as $\alpha = \frac{R_I}{R_R}$. If $\alpha > 1$, the radar will be detected by the intercept receiver. On the contrary, if $\alpha \leq 1$ the radar can detect the platform while the intercept receiver platform can not detect the radar. In fact, so called LPI performance is a probability event (GuoSui Liu et al. 2001, 120; 120-124; 124).

[2] (GuoSui Liu et al. 2001, 120; 120-124; 124)

## B. CHARACTERISTICS OF LPI RADAR

Many features distinguish LPI radar from conventional radar. These include:

- Low sidelobe antennas,
- Irregular antenna scan patterns,
- High duty cycle/wide band transmission,
- Accurate power management,
- Carrier frequency,
- Very high sensitivity,
- High processing gain,
- Coherent detection,
- Monostatic/bistatic configurations.

### 1. Low Sidelobe Antennas

The LPI radar antenna must have a transmit radiation pattern with very low sidelobes. The low sidelobes in the transmit pattern reduce the possibility of an intercept receiver detecting the radio frequency (RF) emissions from the sidelobe structures of the antenna pattern. By applying a tapered illumination, the sidelobe level can be lowered below -13 dB. For an LPI radar, ultra low sidelobes are required (-45 dB) (Pace 2004, 455)

The mainlobe can not be suppressed in the same manner, so the transmitting beam should be wide with the radiated energy spread over a wide area. This increases the difficulty to intercept the radar energy and determine direction of the signal. On the other hand, the radar receiving antenna should use a narrow beam for high resolution and detection. It is common to use adaptive arrays for leakage cancellation, multiple receiving beams, and electronic scanning (GuoSui Liu et al. 2001, 120; 120-124; 124).

### 2. Irregular Antenna Scan Patterns

Intercept receivers can use scan type and scan rate information to search for, detect, and identify radars. With confusing radar scan techniques, such as changing the scan parameters randomly, LPI radar will have a greater chance to avoid interception. Phased array Electronically Scanned Antennas (ESAs) can be used to produce irregular

scan patterns by creating multiple beams to search different scan volumes at different frequencies. Electronic scanning with software control also helps the LPI radar limit its illumination time.

The F/A-22 Raptor's AN/APG-77, Patriot's AN/MPQ-53, and SA-10 Grumble's Tombstone radars shown in Figure 2 have an ability to use irregular antenna scan patterns to reduce the probability of interception by hostile receivers.


Figure 2. Examples of Radars That Use Irregular Scan Patterns

Omnidirectional LPI (OLPI) radars use another antenna technique related to the scan pattern. They use a non-scanning, wide beam transmitting antenna and multiple receiving beams as shown in Figure 3. This technique increases target dwell time and reduces radar vulnerability to ES receivers.

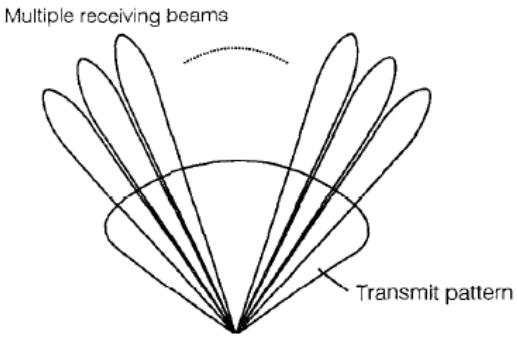


Figure 3. OLPI Antenna Pattern[3]

[3] (Wirth 1995, 698-703)

The German Floodlight radar is an example of OLPI radar. For transmitting, eight dipoles in a column are combined by a micro strip feed network resulting in a horizontal fan beam pattern about 20° in elevation and 120° in azimuth. The receiving antenna consists of an array of 64 columns, each column containing 8 dipoles combined by a micro strip network similar to the transmitting antenna (GuoSui Liu et al. 2001, 120; 120-124; 124).

### 3. High Duty Cycle/Wide Band Transmission

LPI radars escape detection by spreading the radiated energy over a wide spectrum of frequencies. The ES receiver must search a large bandwidth to find the LPI radar. The LPI radar is thus able to exploit the time bandwidth product by reducing its peak transmitted power to bury itself in the environmental noise. Due to the mismatch in waveforms for which the ES receiver is tuned, the LPI radar is effectively invisible to the ES receiver (Ong and Teng 2001, ).Since the high peak power transmitted by the pulsed radar can easily be detected by ES receivers; continuous wave (CW) radars can transmit very low power while maintaining the same energy profile (Taboada 2002, 271). A comparison is shown in Figure 4.

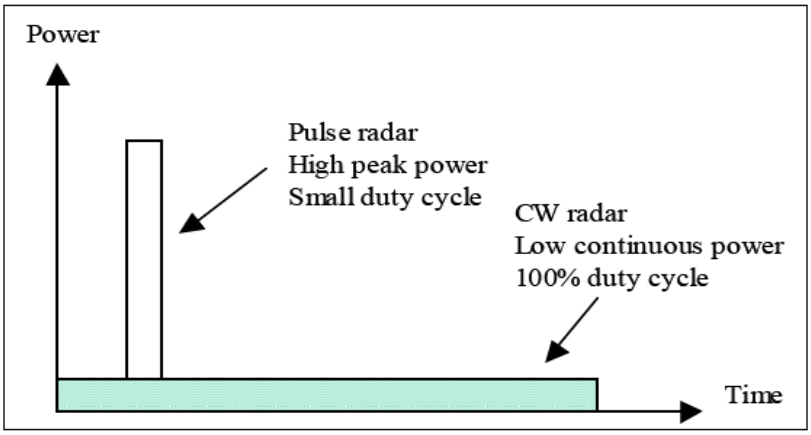


Figure 4. Comparison of Pulsed and CW Radar[4]

Consequently, most LPI emitters use periodically modulated CW signals resulting in large bandwidths and small resolution cells, and are ideally suited for pulse compression (Pace 2004, 455).

[4] (Pace 2004, 455)

### 4. Accurate Power Management

Power management is a radar technique that is becoming more practical with improvements in digital signal processing. Power management encompasses a host of techniques including:

- Antenna sidelobe control/suppression
- Pseudo-random illumination of a target
- Dynamic control of transmitter power to maintain a minimal SNR

The French CROTALE system makes effective use of power management. Shortly after lock on, the tracking radar reduces its transmitter power such that the SNR of the received level is kept to a minimal value. This process is continued during the course of engagement reducing the range at which the radar can be detected (McRitchie and McDonald 1999, ). This LPI technique causes some ES receivers to calculate the range of the threat incorrectly and categorize the threat as a low priority

### 5. Carrier Frequency

An LPI radar can use frequencies of 22, 60, 118, 183, and 320 GHz at which peak absorption occurs. This will serve to maximize attenuation in order to mask the transmit signal and limit reception by hostile receivers (atmospheric attenuation shielding). Because of the high absorption of the emitter's energy, this technique is always limited to short range systems.

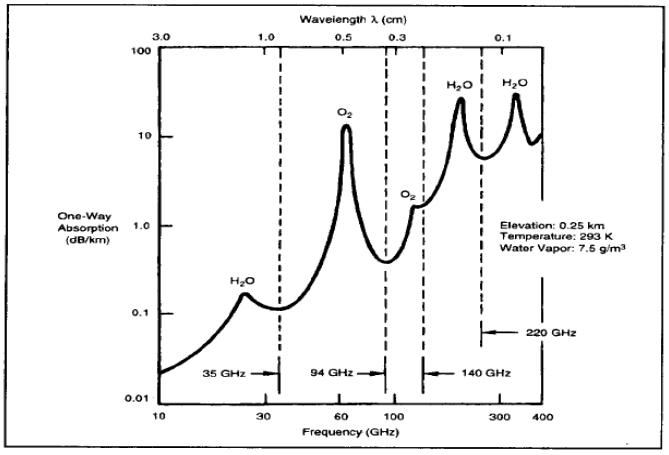


Figure 5. Atmospheric Absorption for Millimeter Wave Spectrum[5]

[5] (Klein 1997, )

Using a radar frequency that is outside of the current ES receivers' working band (generally between 0.5 GHz and 20 GHz) is another option for LPI radar carrier frequencies.

A final carrier frequency approach to achieving a lower probability of interception is to interleave the LPI radar with an infrared sensor (dual mode approach), reducing the amount of time that the RF transmitter radiates (Pace 2004, 455).

**6. Very High Sensitivity**

As shown in Figure 6, sensitivity is a function of the bandwidth, noise figure, and required SNR. The sensitivity factor is a crucial parameter that must be evaluated for a successful LPI radar design. The thermal noise is based on the formula KTB where T is the temperature in Kelvin, K is the Boltzmann's constant, and B represents the bandwidth. The sensitivity in dBm is the sum of the thermal noise (in dBm), noise figure (in dB), and required signal-to-noise ratio (in dB). If we set the value of the SNR to 13 dB as an example, then KTB is usually taken as

$$KTB=-114dBm+10\log(B) \qquad (2.1)$$

where KTB is the thermal noise in dBm and B is the bandwidth on Hz (Adamy 2001, ).

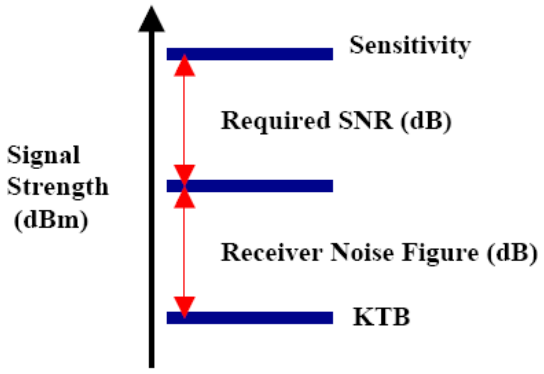


Figure 6. Receiver Sensitivity[6]

[6] (Adamy 2001, )

It is clear that reduction of the radar noise temperature and losses will improve LPI radar performance.

### 7. High Processing Gain

Processing gain has the effect of narrowing the effective bandwidth of the radar receiver by taking advantage of the signal modulation. Thus, the radar receiver achieves a processing gain while the hostile receiver cannot. An LPI radar achieves bandwidth advantage over an intercept receiver because the radar knows its own signal. In contrast, the intercept receiver must accept a wide range of signals and must typically make detailed parametric measurements to identify the type of signal it is receiving (Taboada 2002, 271).

### 8. Coherent Detection

Coherent detection is another technique used by LPI radars to avoid interception. An Electronic Warfare Support (ES) receiver cannot achieve coherent detection of a radar signal unless it knows the parametric details of the signal. When the signal modulation is random, this property becomes even more effective. Using true noise to modulate a radar signal is a good illustration of these characteristics. Radars using true noise modulation are called random signal radars (RSR). This kind of radar correlates the returning signal with a delayed sample of the transmitted signal. The amount of delay necessary to peak the correlation determines the range of a target. Since the transmitted signal is completely random, the intercepting receiver has no reference for correlating the received signal (Adamy 2001, ).

### 9. Monostatic/Bistatic Configuration

Monostatic and bistatic configurations may both be used in LPI radar designs. For monostatic radar, the leakage of the CW signal from the transmitter must be isolated from the receiver. For bistatic radars, the transmitting antenna and receiving antenna(s) are separated by distance. Bistatic radar designs face technological challenges preventing widespread operational use, such as the synchronization of time and direction, etc. From all considerations, the bistatic spread spectral CW radar is the most ideal form of LPI radar. In addition, bistatic radar can minimize the attack of ARMs and increase the detection of stealth targets (GuoSui Liu et al. 2001, 120; 120-124; 124).

## C. LPI RADAR WAVEFORMS

There are several LPI radar techniques available to the modern radar designer that may be used singly or in various combinations, depending on the application. Reducing the radar's peak effective radiated power (ERP) by using some form of pulse compression technique is the most common LPI radar technique. The objective is to spread the radar's signal over a wide bandwidth and a period of time. This is typically done with frequency modulation, phase shift keying and frequency shift keying techniques (McRitchie and McDonald 1999, ).

### 1. Frequency Modulation Continuous Wave (FMCW) Radar

Most of the LPI radars use FMCW which is a frequency modulation, pulse compression technique. This is the simplest and easiest technique to implement with simple solid-state transmitters. Another advantage of FMCW radars are their extremely high time bandwidth product which makes them very resistant to interception by ES systems. Large modulation bandwidth provides very good range resolution. The deterministic nature of this waveform provides practical advantages over other modulated CW waveforms because the form of the return signal can be predicted. FMCW technique provides:

- Resistance to jamming since any signals not matching are suppressed,
- It is simpler to find range information with FFT from IF signals,
- Implementation of sensitivity time control (STC) to control dynamic range and prevent saturation in the receiver will be easier in the frequency domain.

The most popular linear frequency modulation is triangular modulation. This consists of two linear frequency modulation sections with positive and negative slopes. With this configuration, and by using a continuous 100% duty-cycle waveform, target range and Doppler information can be measured unambiguously by taking the sum and difference of the two beat frequencies (Pace 2004, 455). These characteristics are shown in Figure 7.

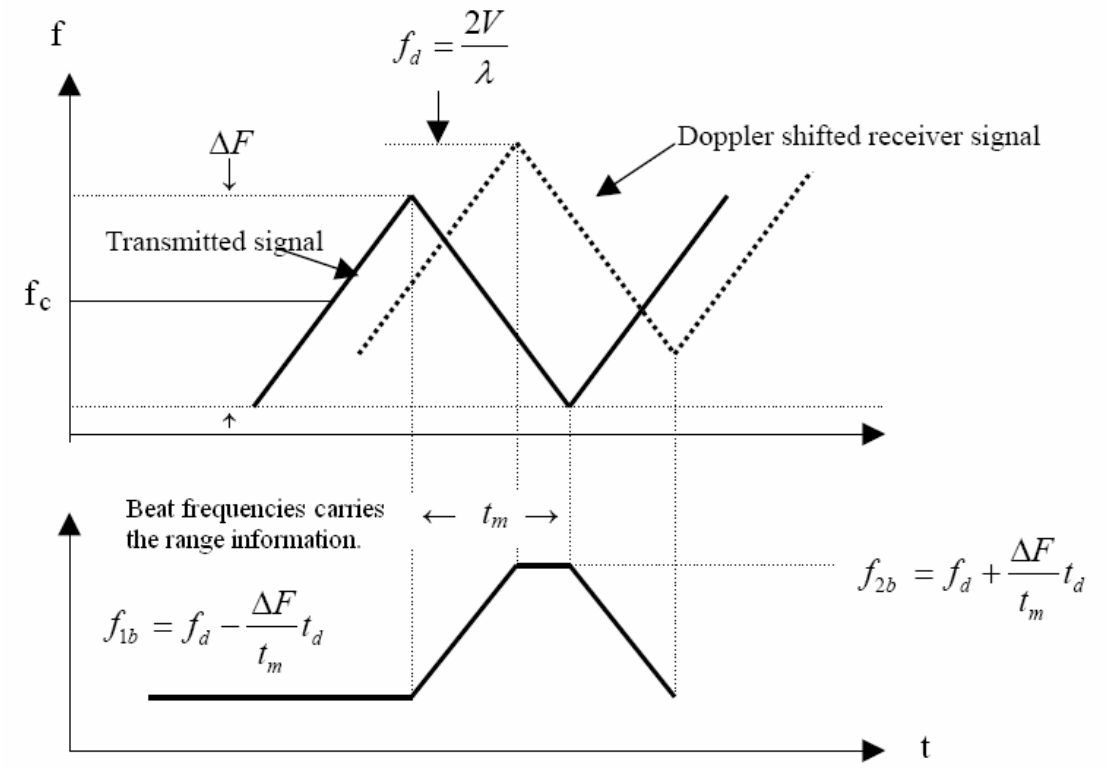


Figure 7. Linear Frequency Modulated Triangular Waveform and the Doppler Shifted Return Signal[7]

The frequency of the transmitted signal for the first section is

$$f_1 = f_c - \frac{\Delta F}{2} + \frac{\Delta F}{t_m} t \tag{2.2}$$

for $0 < t < t_m$ and zero elsewhere. Here $f_c$ is the RF carrier, $\Delta F$ is the transmitted modulation bandwidth, $t_d$ is the round-trip delay time and $t_m$ is the modulation period.

The phase of the transmitted RF signal is

$$\phi_1 = 2\pi \int_0^t f_1(x) dx \tag{2.3}$$

[7] (Pace 2004, 455)

Assuming that $\phi_0 = 0$ at t=0,

$$\phi_1(t) = 2\pi\left[\left(f_c - \frac{\Delta F}{2}\right)t + \frac{\Delta F}{2t_m}t^2\right] \tag{2.4}$$

for $0 < t < t_m$. The transmit signal is given by

$$s_1(t) = a_0 \sin 2\pi\left[\left(f_c - \frac{\Delta F}{2}\right)t + \frac{\Delta F}{2t_m}t^2\right] \tag{2.5}$$

The frequency of the transmitted waveform for the second section is similarly

$$s_2(t) = a_0 \sin 2\pi\left[\left(f_c + \frac{\Delta F}{2}\right)t - \frac{\Delta F}{2t_m}t^2\right] \tag{2.6}$$

Under normal operating environments, the FMCW radar will generally receive many signals from targets at different ranges simultaneously. These signals will combine to form a complex waveform at the output of the receiver mixer. The complex waveform at the output, after A/D conversion, is resolved into its frequency components using a Fast Fourier Transform (FFT). The width of each frequency bin of the FFT represents a range increment and the amplitude of that bin is the echo strength of the target at that range. The output of the FFT is normally further processed and converted into a 'regular' analog video signal which is suitable for PPI display or used for tracking purposes (Ong and Teng 2001, ).

For any radar waveform, the ideal range resolution, $\Delta R$, is linearly proportional to time resolution, $\Delta T$, and inversely proportional to the bandwidth of the transmitted waveform, $\Delta F$, as given below:

$$\Delta R = \frac{c\Delta T}{2} = \frac{c}{2\Delta F} \tag{2.7}$$

For example, a 50MHz FM sweep bandwidth corresponds to time resolution no less than 2ns and a range resolution of 3m. Very high sweep bandwidth of 1GHz will yield very good range resolution of 0.15m.

Figure 8(a) illustrates the triangular modulation signal for a FMCW signal with a modulation bandwidth of 250 Hz, modulation period of 50 ms and carrier frequency of 1000 Hz. Figure 8(b) shows the power spectral density (PSD) of the triangular FMCW signal described.

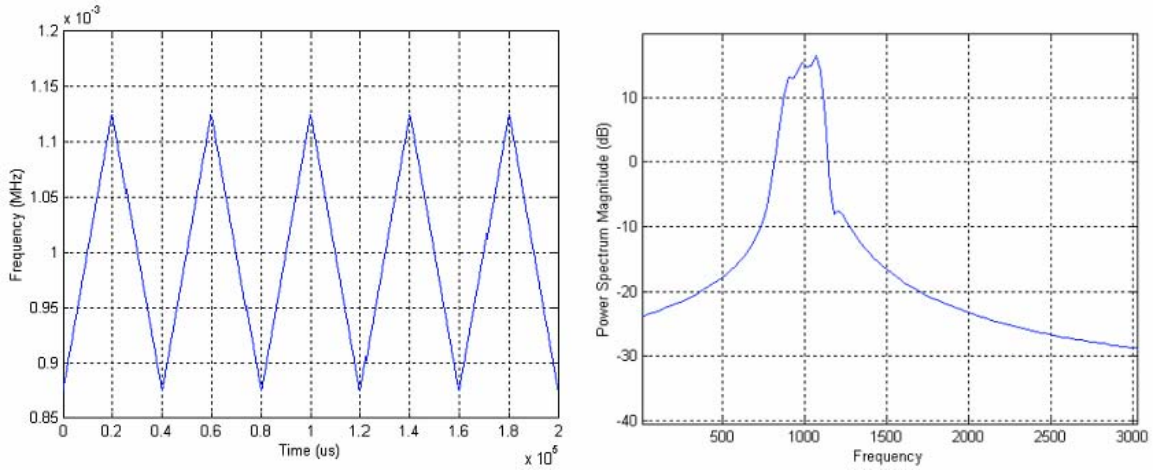


(a) (b)

Figure 8. Triangular Modulation and PSD of the FMCW signal[8]

## 2. Phase Shift Keying (PSK) Techniques

PSK CW waveforms have recently been a topic of active investigation, due to their wide bandwidth and inherently low periodic ambiguity function (PAF) sidelobe levels. The choice of PSK codes affects radar performance and implementation.

Binary phase shifting codes are popular while the most useful codes are the polyphase codes. Polyphase codes allow the phase shift value within the sub code to take

[8] (Taboada 2002, 271)

on many values and the code length to be made extremely long. These codes have better sidelobe performance and Doppler tolerance than binary phase codes.

The PSK techniques can result in a high range resolution waveform, while also providing a large SNR processing gain for the radar. The average power of the CW transmission is responsible for extending the maximum detection range while improving the probability of target detection. PSK techniques are also compatible with new digital signal processing hardware and solid state transmitters (Pace 2004, 455).

***a. Binary Phase Shift Keying (BPSK)***

Binary Phase Shift Keying (BPSK) is a modulation technique that has proven to be extremely effective in communication and radar systems. Even though BPSK is not a technique presently employed in LPI radar modulation, the technique is useful as a test signal in evaluating the performance of the signal processing (Taboada 2002, 271).

With BPSK, two output phases are generated for a single carrier frequency. One output phase represents logic 1 and the other logic 0. As the input digital signal changes state, phase of the output carrier shifts between two angles that are 180° out of phase. BPSK is a form of suppressed carrier, square wave modulation of a continuous wave signal (Jarpa 2002, 154).

Binary phase coded signals exhibit the same range sidelobes seen in FM chirp signals and mathematicians have spent years developing codes to minimize them. Three codes are commonly seen in use today are Barker codes, compound Barker codes and pseudo-random codes (McRitchie and McDonald 1999, ).

***(1) Barker Codes:*** Barker codes exhibit very low sidelobe performance. Barker codes have been found that consist of from 2 to 13 bits as shown Table 1. “+” represents zero phase shift and “-“ represents 180° phase shift.

Table 1. Barker Codes[9]

| Code Length | Code | Range Sidelobe Level (dB) | Processing Gain (dB) |
|---|---|---|---|
| 2 | + - OR + + | -6.0 | 3.0 |
| 3 | + + - | -9.5 | 4.8 |
| 4 | + + - + OR + + + - | -12.0 | 6.0 |
| 5 | + + + - + | -14.0 | 7.0 |
| 7 | + + +- - + - | -16.9 | 8.5 |
| 11 | + + + - - - + - - + - | -20.8 | 10.4 |
| 13 | + + + + + - - + + - + - + | -22.3 | 11.1 |

There are two major disadvantages associated with Barker codes. The first is that the maximum length is 13. Despite years of research, mathematicians have been unable to discover longer codes that exhibit better properties than the existing Barker codes. If, as is the case in LPI radar, it is desired to transmit a very wide pulse and still maintain good range resolution, then longer code lengths are required (McRitchie and McDonald 1999, ).

The second disadvantage is that they are quite sensitive to Doppler shifts. The Doppler shift of the return waveform can compress the waveform within the filter such that the matched filter gives incorrect results. Barker codes are not considered for use in LPI radars since they are easily detected by an intercept receiver that uses frequency doubling[10] (Pace 2004, 455).

***(2) Compound Barker Codes:*** While trying to alleviate the disadvantage associated with the limited length of the Barker codes, it was discovered that it was possible to embed one Barker code within another, as shown in Figure 9, to create a compound Barker code. These codes have the advantage that virtually infinite length code can be created and hence range resolution for long pulses can be enhanced and high levels of processing gain can be achieved.

[9] (McRitchie and McDonald 1999, )

[10] This technique involves multiplying the received signal by itself and processing the result with an envelope detector.

An important fact to note is that the sidelobe levels of the compound Barker codes do not improve with code length; they are identical to the sidelobe level of the original code. For example, the 9-bit compound Barker code shown in Figure 9 posses the same sidelobe levels as the 3-bit Barker code from which it is composed. In contrast, the gain associated with the processing does increase as the code length increases. Referring to the same example, the 3-bit Barker code only delivers a gain of 3.8 dB however the 9-bit compound Barker code yields a 9.5 dB gain (McRitchie and McDonald 1999, ).

| | | | | | | | | | |
|---|---|---|---|---|---|---|---|---|---|
| + | | | + | | | - | | | Primary Code |
| + | + | - | + | + | - | + | + | - | Embedded Code |
| + | + | - | + | + | - | - | - | + | Resulting Compound Code |

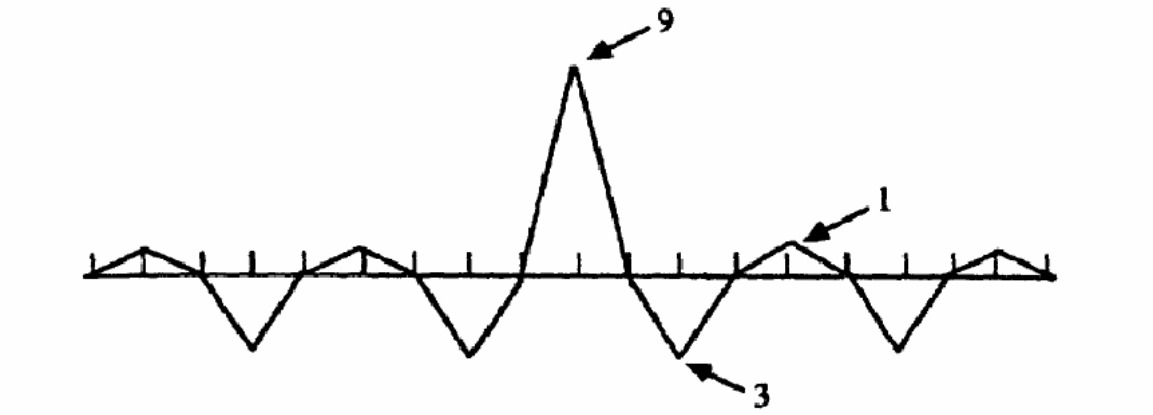


Figure 9. Compressed Output Using 9-Bit Compound Barker Code[9]

***(3) Pseudo-Random Codes:*** Pseudo-random or pseudo-noise (PN) codes are a third class of binary codes that are easily generated digitally using feedback register techniques. These codes offer enhanced performance when compared to Barker codes. In fact, a PN code of N=3 has performance similar to that of a 7-bit Barker code. Unfortunately, unlike the Barker codes whose sidelobe levels decrease with $N^2$ the sidelobe levels of these codes only decrease with N. PN codes posses three key features that make them attractive for use in an LPI system:

- They are less susceptible to Doppler effects than Barker codes
- The spectral content is noise-like

- The feedback register makes them programmable
- Although the spectral content of a PN coded signal is noise-like, the fact that the phase transitions are binary allows a hostile receiver to make use of the frequency doubling to remove the coded structure and thereby detect the signal (McRitchie and McDonald 1999, ).

***b. Polyphase Codes***

Polyphase codes have many useful features, such as low range–time sidelobes, ease of implementation, compatibility with digital implementation, and low cross–correlation between codes. Polyphase codes also have compatibility with bandpass limited receivers and code lengths of any size are possible.

The polyphase codes provide a class of frequency derived phase–coded waveforms that can be sampled upon reception and processed digitally, and may prove to be the LPI waveform most commonly used in future applications. (Jarpa 2002, 154)

The major disadvantage of this kind of code is that as the phase increment becomes smaller, the equipment needed to generate them becomes more complex and therefore more costly. In addition, the resulting processing is more sensitive to Doppler shifts. This property will restrict the number of the phase levels employed.

As an example, these codes would not be appropriate for use in air-to-air or supersonic missile seeker applications without the use of Doppler compensation. The ability of the processor to perform the compensation will be a limiting factor in the performance of these codes (McRitchie and McDonald 1999, ).

***(1) Frank Code:*** The Frank code is one of the modulation codes that have been successfully implemented in LPI radars. A Frank waveform consists of a constant amplitude signal that is phase modulated by the phases of the Frank code (Persson 2003, 127).

The Frank waveform is derived from a step approximation to a linear frequency modulation waveform using M frequency steps and M samples per frequency. The Frank code has a code length or processing gain of $N_c = M^2$. The phase values of a Frank coded signal are given by the following equation:

$$\phi_{i,j} = \frac{2\pi}{M}(i-1)(j-1),\ \text{i=1,2,...,M}\ \ \text{j=1,2,...,M} \qquad (2.8)$$

where $\phi_{i,j}$ describes the phase of the i-th sample of the j-th frequency.

Figure 10 (a) illustrates the discrete phase values of the Frank coded signal with M=8, ( $N_c$ =64) and Figure 10 (b) shows the signal phase modulo 2π.

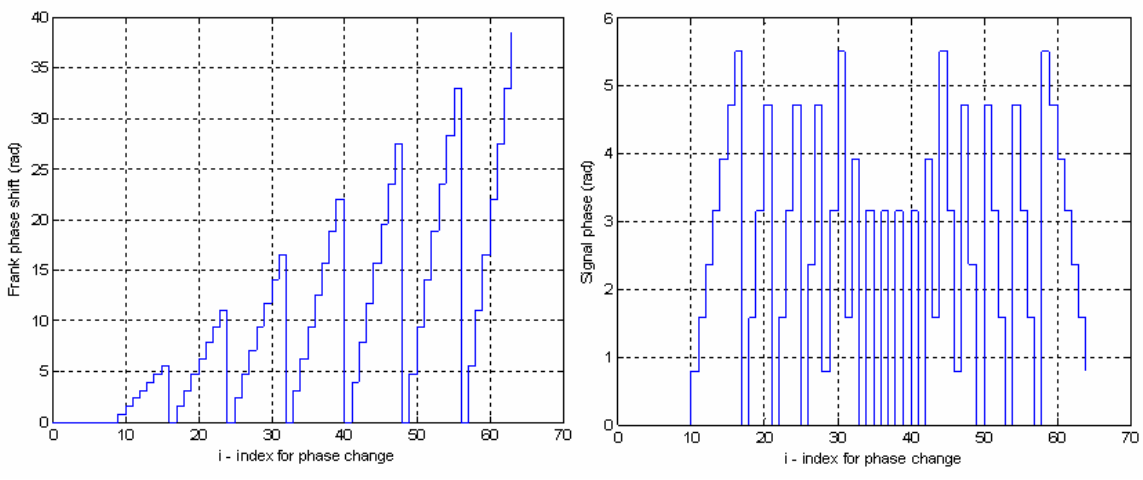


(a) (b)

Figure 10. Frank Code Phase Values for M=8 ( $N_c$ =64)[11]

***(2) P1 Code:*** By changing the synchronous oscillator frequency, different phase codes can be generated with equal amplitudes but with different phases. By placing the synchronous oscillator at the center frequency of the step chirp IF waveform and by sampling the base band waveform at the Nyquist rate, the polyphase code called P1 may be obtained. The P1 code and the Frank code consist of same number $N^2$ elements (Lewis 1986, ).

If *i* is the number of the sample in a given frequency and *j* is the number of the frequency, the phase of the *i*-th sample of the *j*-th frequency is given by the equation:

[11] (Pace 2004, 455)

$$\phi_{i,j} = \frac{-\pi}{N}[N-(2j-1)][(j-1)N+(i-1)] \qquad (2.9)$$

where $i$ = 1,2,…,$N$ and $j$ = 1,2,…,$N$ code. Figure 11(a) shows the phase values that result for the P1 code for M=8, ($N_c$=64) and Figure 11 (b) shows the signal phase modulo 2π.

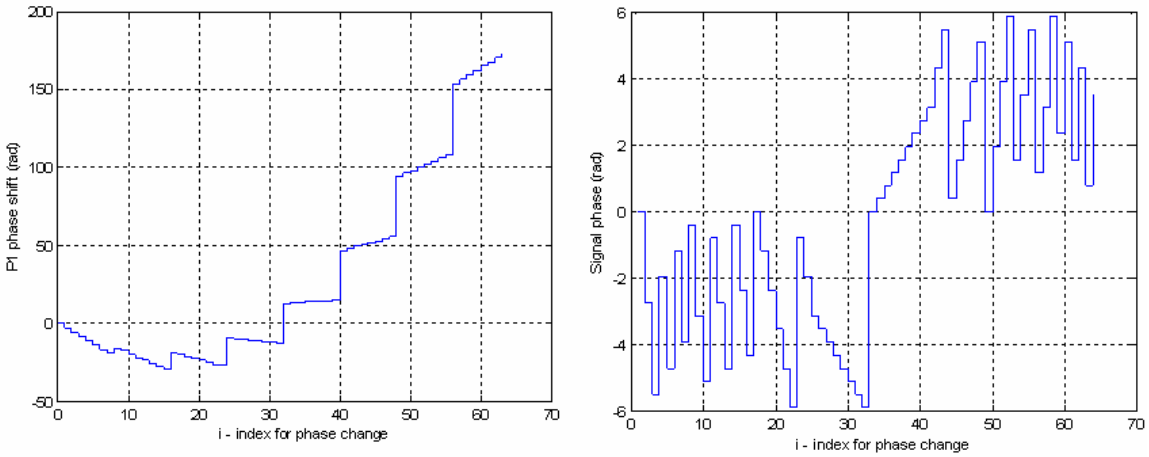


(a) (b)

Figure 11. P1 Code Phase Values for M=8 ($N_c$=64)[12]

***(3) P2 Code:*** This code is essentially derived in the same way as the P1 code is derived. The P2 code has the same phase increments within each group as the P1 code, except that the starting phase is different. The P2 code is valid for $N$ even, and each group of the code is symmetric about 0 phase. These phases can be calculated by

$$\phi_{i,j} = \frac{-\pi}{2N}[2j-1-N][2i-1-N] \qquad (2.10)$$

12 (Pace 2004, 455)

where *i*=1, 2, …, *N* and j= 1, 2, …, *N*. This code has the frequency symmetry of the P1 code while also containing the property of being a palindromic code since the phases are symmetric in the center of the code (Lewis 1986, ). The P2 polyphase code has more of a symmetrical frequency spectrum than a Frank coded signal due to its symmetry in the carrier. Figure 12 (a) shows the phase values that result for the P2 code for M=8, ( $N_c$ =64) and Figure 12 (b) shows the signal phase modulo 2π.

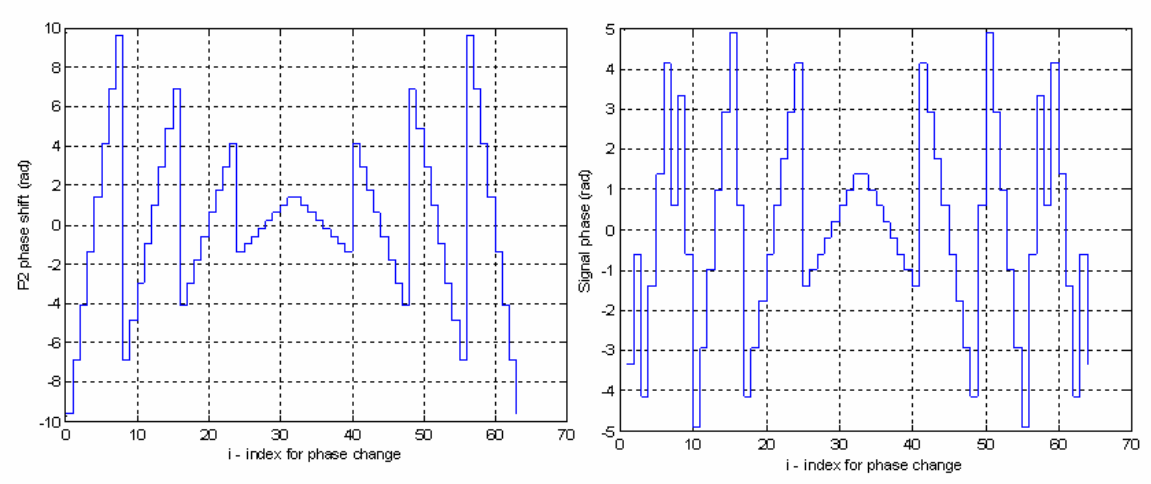


(a) (b)

Figure 12. P2 Code Phase Values for M=8 ( $N_c$ =64)[13]

***(4) P3 Code:*** The P3 code waveform is conceptually derived by converting a linear frequency modulation waveform to base band, by using a synchronous oscillator on one end of the frequency sweep (single sideband detection), and sampling the I and Q video at the Nyquist Rate[14]. The phase of the i-th sample of the P3 code is given by

$$\phi_i = \frac{\pi}{N_c}(i-1)^2 \qquad (2.11)$$

[13] (Pace 2004, 455)

[14] Nyquist Rate is the minimum sampling rate (in samples per second) required to avoid aliasing when sampling a continuous signal. It is generally equal to twice the highest frequency in the signal.

where i=1,2,…, $N_c$, and $N_c$ is the compression ratio (Lewis 1986, ). Figure 13 (a) shows the quadratic discrete phase values that result for the P3 code for $N_c$=64 and Figure 13 (b) shows the signal phase modulo 2π.

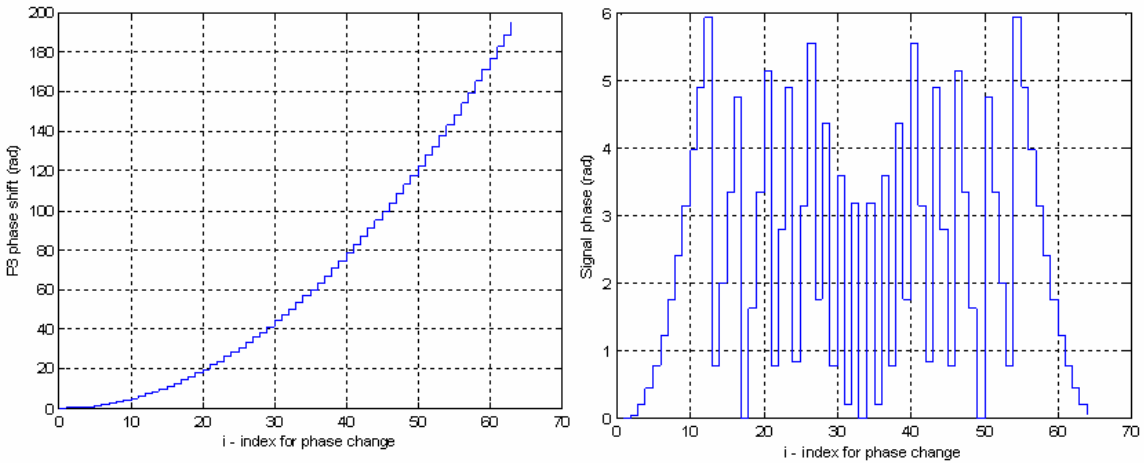


(a) (b)

Figure 13. P3 Code Phase Values for $N_c$=64[15]

***(5) P4 Code***: The P4 code waveform is conceptually derived from the same linear frequency modulation waveform as the P3 code, except that the local oscillator frequency is offset in the I and Q detectors, resulting in coherent double sideband detection. Sampling at the Nyquist rate yields the polyphase code named the P4 (Lewis 1986, ). The phase sequence of a P4 signal is described by

$$\phi_i = \frac{\pi(i-1)^2}{N_c} - \pi(i-1) \qquad (2.12)$$

where i=1,2,…, $N_c$, and $N_c$ is the compression ratio. Figure 14 (a) shows the discrete phase values that result for the P4 code for $N_c$=64 and Figure 14 (b) shows the signal phase modulo 2π.

[15] (Pace 2004, 455)

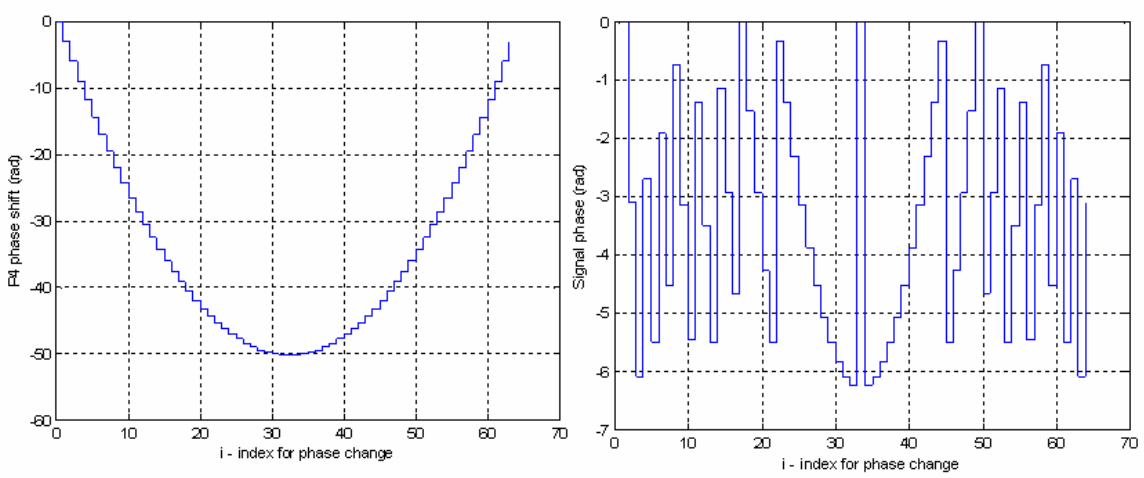


(a) (b)

Figure 14. P4 Code Phase Values for $N_c$=64[16]

### *c. Polytime Codes*

The polytime waveforms are developed by letting the phase change approximate a stepped frequency or linear frequency modulation waveform. With polytime waveforms the subcode period is not uniform in size. That is the size of the phase step varies as needed to approximate the underlying waveform while the time spent at any given phase state is a constant. To generate polytime waveform the approximation of a stepped frequency or linear frequency modulation waveform is generated by quantization of the underlying waveform into a user selected number of phase states.

Four types of polytime waveforms exist. The first two variants of polytime coded waveforms, denoted T1(n) and T2(n) where n is the number of phase states, can be generated using the stepped frequency model. The T3(n) and T4(n) polytime waveforms are approximations of a linear frequency modulation model. Increasing the number of phase states increases the quality of the polytime approximation to the underlying waveform; but it also reduces the time spent at any given phase state, complicating the generation of the waveform (Fielding 1999, 716-721).

16 (Pace 2004, 455)

***(1) T1(n) Code***: The T1(n) sequence waveform is generated using the stepped–frequency waveform where the first code segment is at "zero" frequency. The equation for the wrapped phase, φ(t) versus time for the T1(n) polytime sequence is

$$\varphi(t) = MOD\left\{\frac{2\pi}{n} INT\left[(kt - jT)\frac{jn}{T}\right], 2\pi\right\} \tag{2.13}$$

where j=0,1,2,…,k-1 is the segment number in the stepped RF waveform, k is the number of segments in the T1 code sequence, t is time, T is the overall code duration, and n is the number of phase states in the code sequence (Pace 2004, 455).

An example of converting a stepped RF waveform and its conversion into a T1(2) polytime waveform with k=4 segments and n=2 phase steps is shown in Figure 15. The figure shows how the polytime code phase steps are derived to fit the ideal RF phase. In this case two phase states are used (each phase step is π radians) and, as seen in the figure, the time between the two distinct phase steps is shortened to fit the derived phase to the ideal phase (Persson 2003, 127).

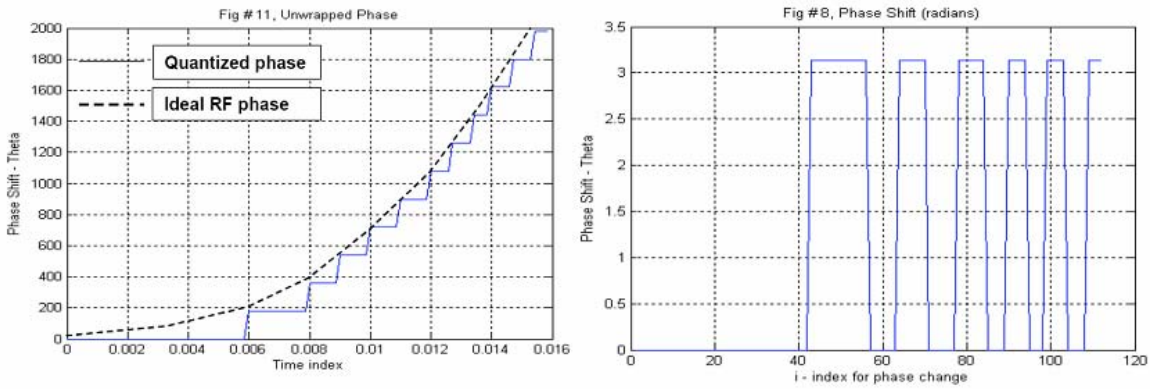


Figure 15. Polytime Waveform T1(2) Derived From Linear FM Waveform[17]

***(2) T2(n) Code:*** The T2(n) sequence waveform is generated by approximating a stepped frequency waveform that is zero–beat at the center frequency. If

[17] (Pace 2004, 455)

the waveform has an odd number of segments, the zero–beat frequency is the frequency of the center segment. If an even number of segments are used, the zero frequency is the frequency halfway between the two center most segments. The expression for the wrapped phase versus time for the T2(n) polytime sequence is

$$\varphi(t) = MOD\left\{\frac{2\pi}{n} INT\left[(kt - jt)\left(\frac{2j-k+1}{T}\right)\frac{n}{2}\right], 2\pi\right\} \tag{2.14}$$

where the variables are the same as defined under T1(n) (Fielding 1999, 716-721). An example of converting a stepped RF waveform into a T2(2) polytime waveform with k=4 segments and n=2 phase steps is shown in Figure 16.

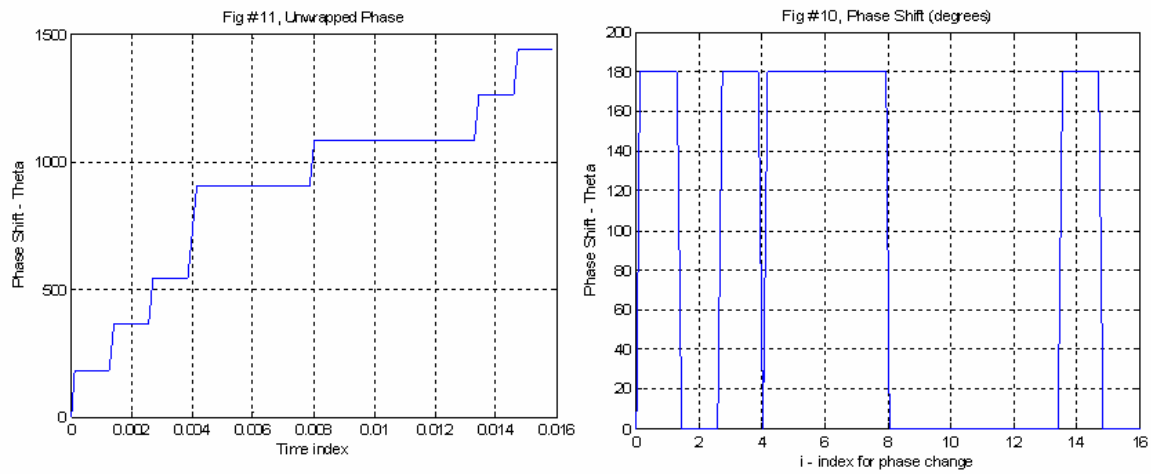


Figure 16. Polytime Waveform T2(2) Derived from Linear FM Waveform[18]

***(3) T3(n) Code:*** The T3(n) code waveform has a linear FM underlying waveform. The T3(n) is zero beat at its leading edge. The equation for the wrapped phase versus time for a T3 polytime sequence is

$$\varphi(t) = MOD\left\{\frac{2\pi}{n} INT\left[\frac{n\Delta F t^2}{2T}\right], 2\pi\right\} \tag{2.15}$$

[18] (Pace 2004, 455)

where t is the time, T is the overall pulse duration, ΔF is the modulation bandwidth and is the number of phase states in the code sequence (Fielding 1999, 716-721). An example of converting a stepped RF waveform and its conversion into a T3(2) polytime waveform with k=4 segments and n=2 phase steps is shown in Figure 17.

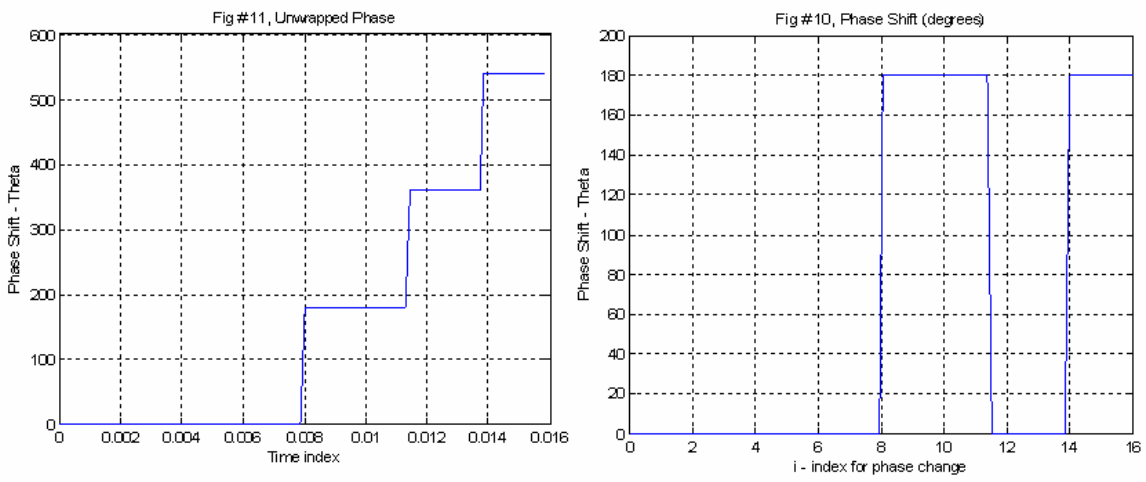


Figure 17. Polytime Waveform T3(2) Derived from Linear FM Waveform[19]

***(4) T4(n) Code:*** Polytime signal T4(n) waveform also has an underlying linear FM waveform to generate the signal. Compared with T3(n), it has its zero–beat at the center frequency. The equation for the wrapped phase versus time for a T4(n) polytime sequence is

$$\varphi(t) = MOD\left\{\frac{2\pi}{n} INT\left[\frac{n\Delta F t^2}{2T} - \frac{n\Delta F t}{2}\right], 2\pi\right\} \tag{2.16}$$

The variables are the same as defined under T3(n) (Fielding 1999, 716-721). An example of converting a stepped RF waveform into a T4(2) polytime waveform with k=4 segments and n=2 phase steps is shown in Figure 18.

[19] (Pace 2004, 455)

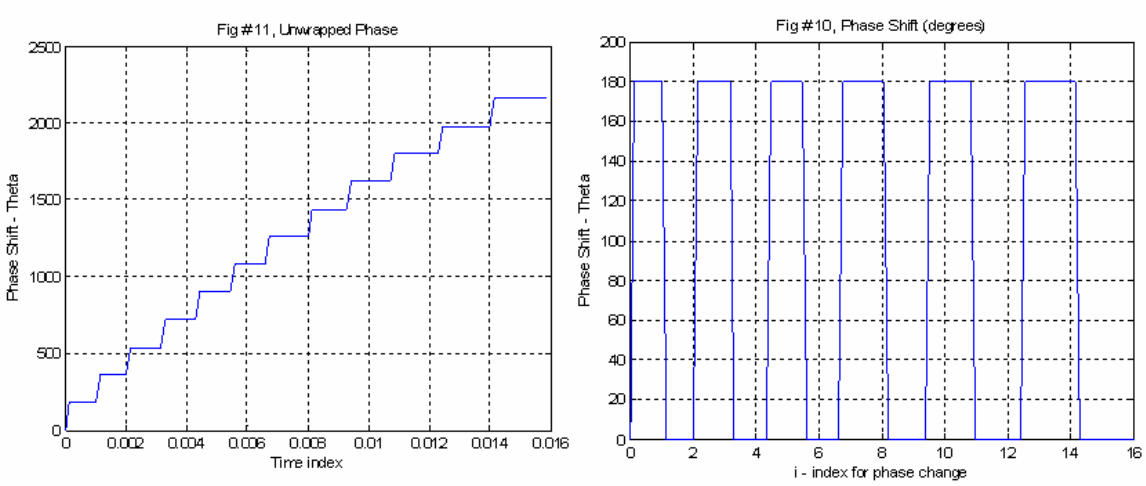


Figure 18. Polytime Waveform T4(2) Derived from Linear FM Waveform[20]

### 3. Frequency Shift Keying (FSK) Techniques

An FSK radar using Frequency Hopping (FH) techniques hops or changes the transmitting frequency in time over a wide bandwidth in order to prevent an unintended receiver from intercepting the waveform. The radar frequency slots are chosen from an FH sequence, gives the radar an advantage in terms of processing gain. That is, since the frequency sequence appears random to the intercept receiver, the possibility of following the changes in frequency is impossible. This prevents a jammer from reactively jamming the transmitted frequency.

In an FSK radar, transmitted frequency $f_j$ is chosen from the FH sequence $\{f_1, f_2, ..., f_{N_F}\}$ of available frequencies for transmission at a set of time intervals $\{t_1, t_2, ..., t_{N_F}\}$. The frequencies are placed in the various time slots corresponding to a binary time-frequency matrix. Each frequency is used once within the code period, with one frequency per time slot and time slot per frequency. The expression for the complex envelope of the transmitted CW FSK signal is given by

$$s(t) = Ae^{j2\pi f_j t} \tag{2.17}$$

[20] (Pace 2004, 455)

The transmitted waveform has $N_f$ contiguous frequencies with a band B, with each frequency lasting $t_p$ in duration.

In contrast to the FMCW and PSK techniques, the FSK technique of rapidly changing the transmitter frequency does not lower the power spectrum density (PSD) of the emission, but instead moves the PSD about according to the FH sequence (Pace 2004, 455). Besides the advantages of FH radars mentioned above, other important advantages are:

- Large bandwidths can easily be generated,
- Range resolution depends on the hopping rate and not on bandwidth,
- The use of secret hopping codes,
- The capability to be built with very simple architecture and circuits (Burgos-Garcia et al. 2000, 23-28).

### *a Costas Code*

In a frequency hopping system, the signal consists of one or more frequencies being chosen from a set $\{f_1, f_2, ..., f_m\}$ of available frequencies, for transmission at each of a set $\{t_1, t_2, ..., t_n\}$ of consecutive time intervals. For modeling purposes, it is reasonable to consider the situation in which *m*=*n*, and a different one of *n* equally spaced frequencies $\{f_1, f_2, ..., f_n\}$ is transmitted during each of the equal duration time intervals $\{t_1, t_2, ..., t_n\}$. Such a signal is represented by an *nxn* permutation matrix *A*, where the *n* rows correspond to the *n* frequencies, the *n* columns correspond to the *n* intervals, and the entry $a_{ij}$ equals 1 means transmission and 0 means no transmission (Burrus, Gopinath, and Guo 1998, ).

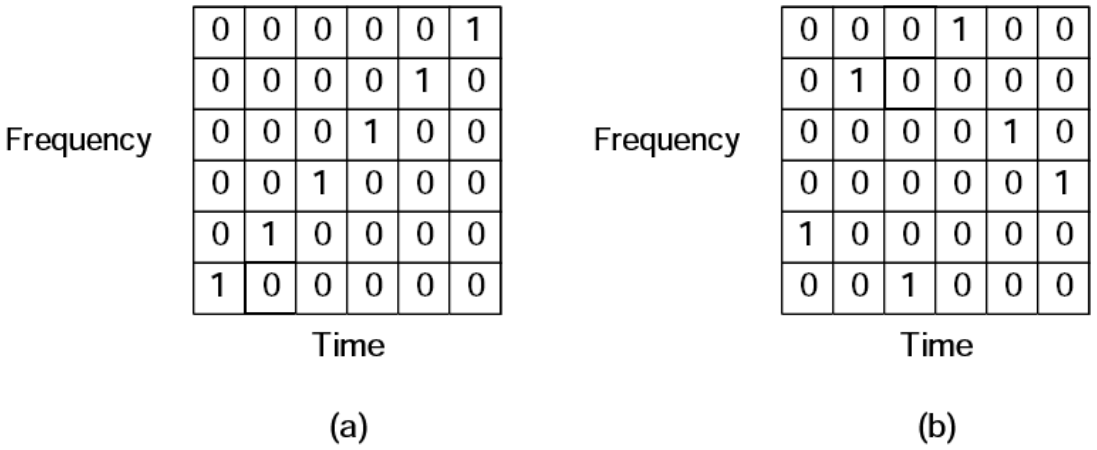


Figure 19. Binary Matrix Representation of (a) Quantized Linear FM and (b) Costas Signal[21]

At any given time, a tone frequency is transmitted, and each frequency is transmitted only once (Figure 19(a)). The hopping order strongly affects the ambiguity function of FSK signals. Frequency-hopping signals allow a simple procedure that results in a rough approximation of their ambiguity function. This is possible because the cross correlation signals at different frequencies approaches zero when the frequency difference is large relative to the inverse of the signal duration. The ambiguity function, at any given coordinates, is an integral of the product between the original signal and a replica of it, which is shifted in time and frequency according to the delay and the Doppler coordinates of the function.

Performing an exercise on the matrix in Figure 19(b), results show that except for the zero-shift cases when the number of coincidences is N, finding a combination of shifts yielding more than one coincidence is not possible. This is actually the criteria of the Costas sequences, which yields no more than one coincidence. For example: if $\{a_j\} = 4,7,1,6,5,2,3$ is a Costas sequence, then its coding matrix and difference matrix are shown in Figure 20 (Jarpa 2002, 154).

[21] (Burrus, Gopinath, and Guo 1998, )

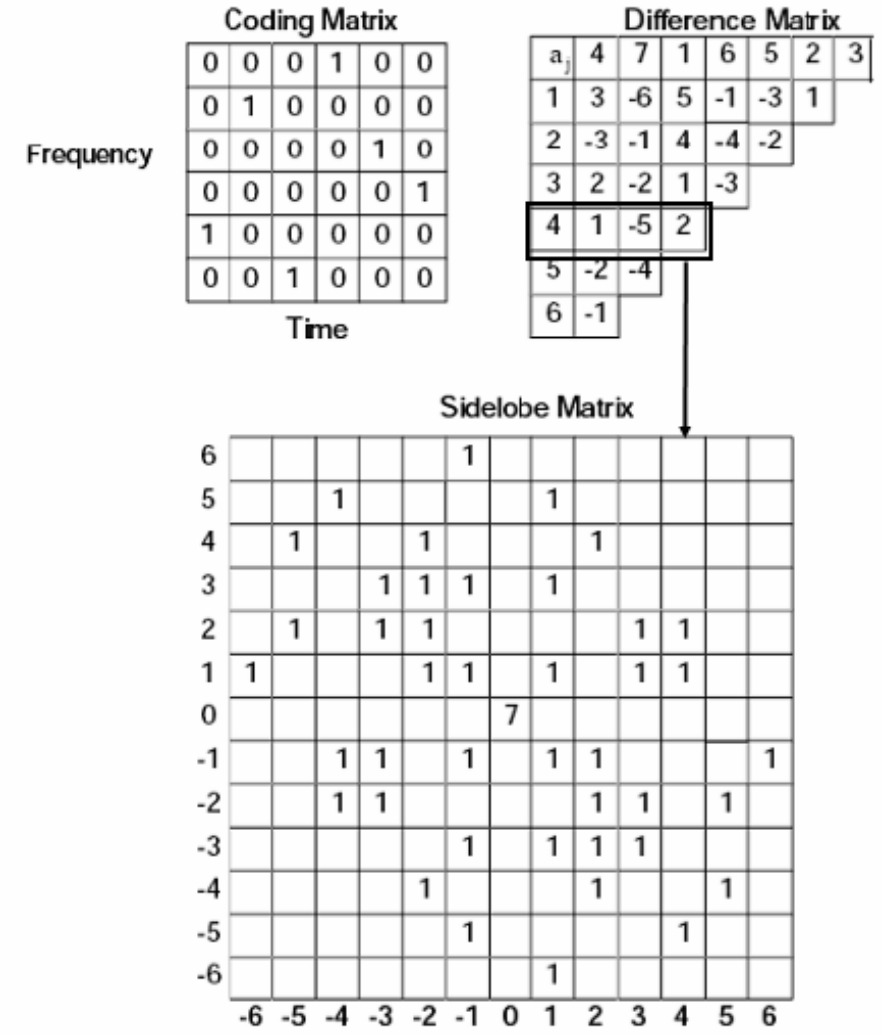


Figure 20. The Coding Matrix, Different Matrix and Ambiguity Sidelobes Matrix of a Costas Signal[22]

### *b. Hybrid FSK/PSK Technique (With Costas Code)*

This modulation technique is the result of a combination of frequency shift keying based on a Costas frequency hopping matrix and phase shift keying using Barker sequences of different lengths. In a Costas frequency-hopped signal, the firing order of the $N_F$ frequencies each with sub-period $T_F$ defines what frequencies will appear and with what duration. During each sub-period, as the signal stays at one of the frequencies, a binary phase modulation occurs according to a Barker sequence of length $N_P$ = 5, 7, 11 or 13. The final waveform may be seen as a binary phase shift modulation within each frequency hop (Lima 2002, 162).

[22] (Jarpa 2002, 154)

As illustrated in Figure 21, with $N_F$ frequency hops and $N_P$ as the number of phase slots of duration $T_P$ in each sub-period $T_F$, the total number of phase slots in the FSK/PSK waveform is given by $N = N_F x N_P$ (Donohoe and Ingels 1990, 268-273).

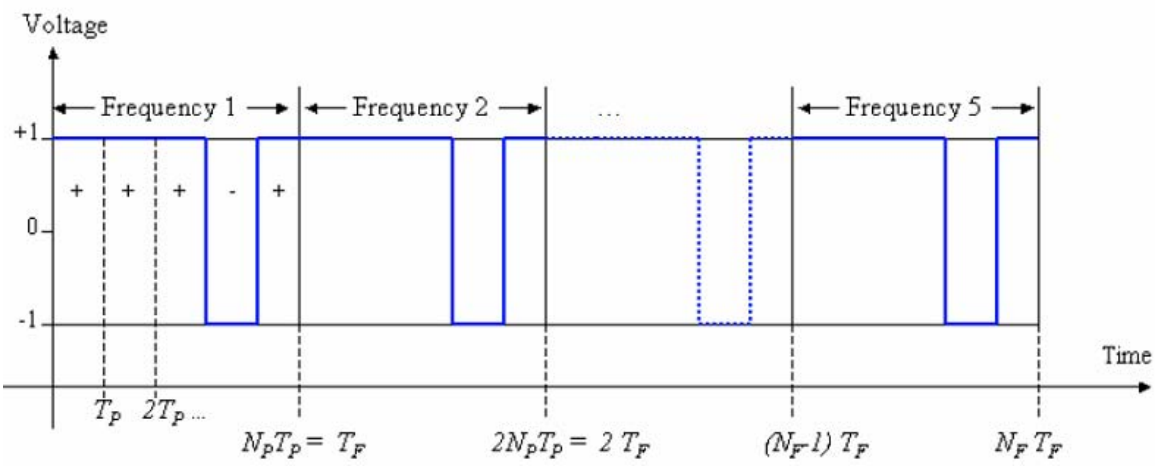


Figure 21. General FSK/PSK Signal Containing $N_F$ Frequency Hops with $N_P$ Phase Slots per Frequency[23]

Figure 22(a) shows the Costas frequency-hopping waveform PSD before it is phase modulated. Figure 22(b) presents the PSD for a FSK/PSK Costas-coded signal after phase modulation. The PSD plots reveal the spread spectrum characteristic of these signals. The Costas sequence is always seven frequency hops (4, 7, 1, 6, 5, 2, and 3 KHz). The sampling frequency is 15 KHz, satisfying the Nyquist rate (Taboada 2002, 271).

[23] (Lima 2002, 162)

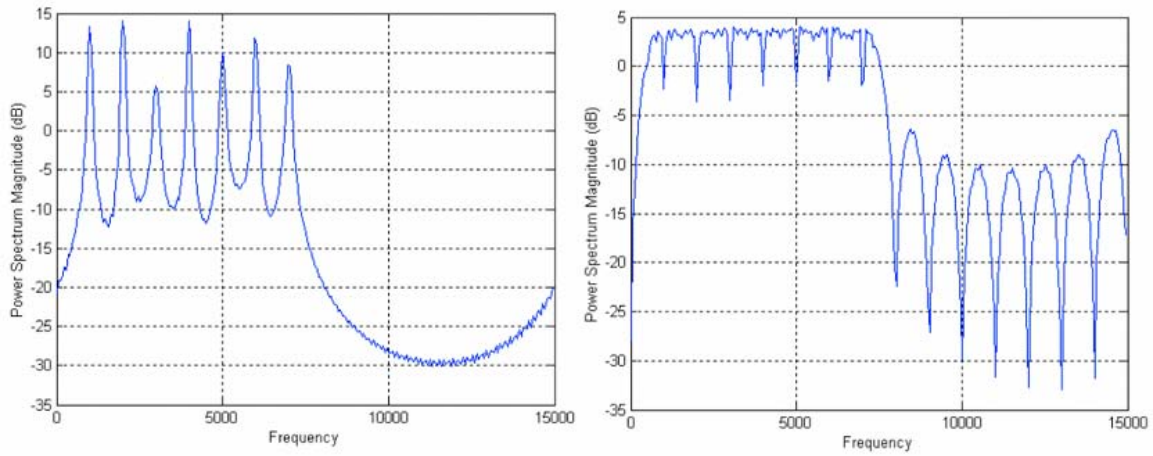


(a) (b)

Figure 22. ((a) PSD for a Costas Coded Signal (b) PSD of a FSK/PSK Costas Coded Signal[24]

### *c. Target Matched FSK/PSK Technique*

Instead of spreading the energy of the signal equally over a broad bandwidth, the target matched frequency hopping technique concentrates the signal energy in specific spectral locations that are important for radar target detection within its broad spectrum bandwidth. Since the transmitted signals have a pulse compression characteristic, they can achieve low probability of intercept.

Figure 23 illustrates the block diagram for the generation of FSK/PSK; in addition Figure 24 shows the FSK/PSK target simulated response, the probability distribution and frequency firing order with the number of occurrences per frequency. The implementation starts with a simulated target time radar response. This data is then Fourier transformed and the correspondent $N_F$ frequencies and initial phases are produced. A random selection process chooses each frequency with a probability distribution function defined by the spectral characteristics of the target of interest (obtained from the FFT). The frequencies with the highest spectral peaks (largest magnitudes) are transmitted more often. Each 'frequency hop,' transmitted is also modulated in phase, having its initial phase value modified by a pseudorandom phase sequence of values equally likely to be zero or $\pi$ radians (Lima 2002, 162).

[24] (Pace 2004, 455)

The matched FSK/PSK radar will then use a correlation receiver with a phase mismatched reference signal instead of a perfectly phase matched reference. This allows the radar to generate signals that can match a target's spectral response in both magnitude and phase.

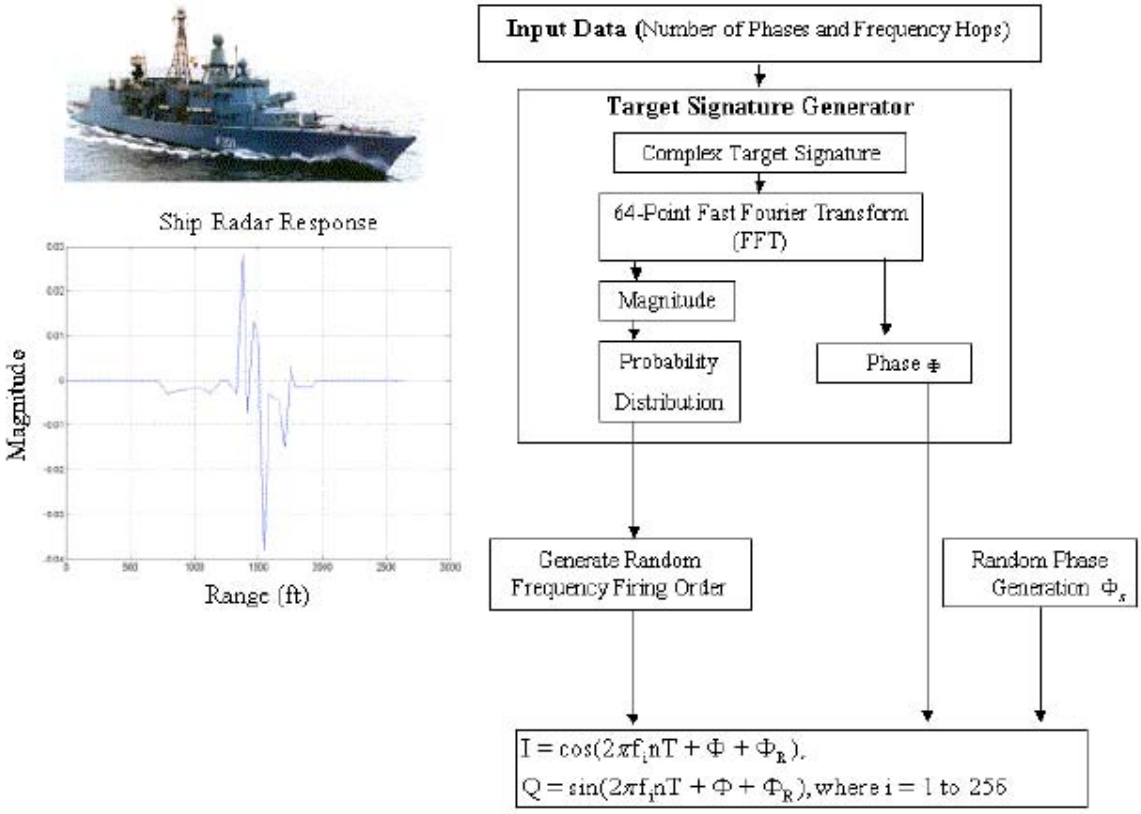


Figure 23. Block Diagram of the Implementation of the FSK/PSK Target Matched Waveform[25]

[25] (Pace 2004, 455)

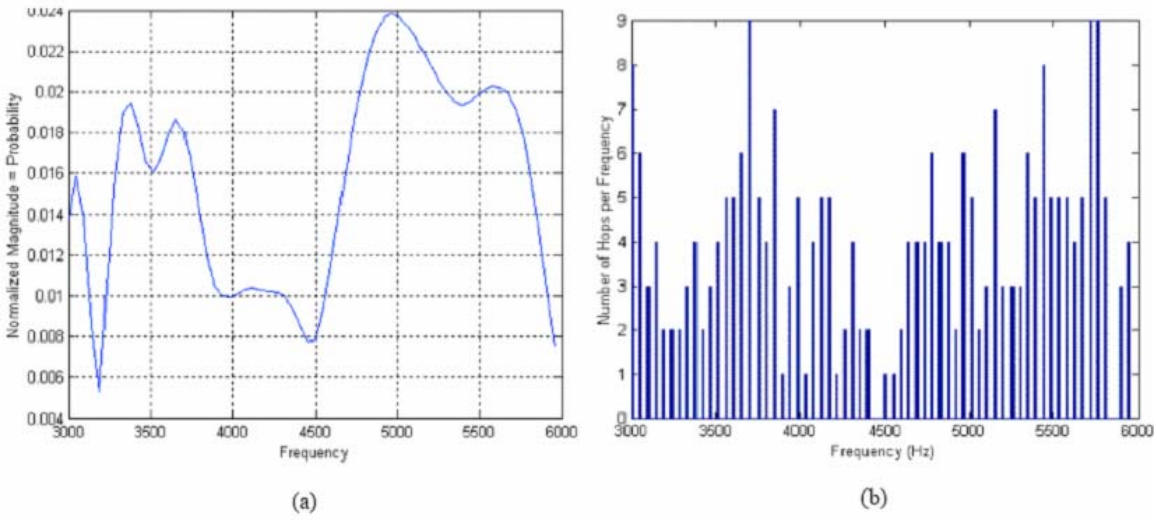


Figure 24. Frequency Probability Distribution AND Components Histogram[26]

## D. EXAMPLES OF LPI RADAR

On the battlefield, situational awareness and threat evaluation are achieved using tactical surveillance radars to detect and track targets. For covert operations, detection and tracking of targets should be as quiet as possible. These systems should employ LPI technology to decrease the probability of passive detection by hostile forces; that is, "to see without being seen." The role of multimode airborne fire control radar is to provide the eyes for tactical fighter aircraft within an air dominance mission and also should employ LPI radars (Pace 2004, 455). In this section some examples of air, maritime, and land based LPI radars will be given from the open literature.

### 1. Airborne LPI Radars

Airborne LPI radars are used for target searching, tracking, location, identification, acquisition, designation, target imaging, periscope detection and weapon delivery. These LPI radars also have modes for covert navigation, weather detection, terrain following and terrain avoidance. Here are the examples of airborne LPI radars:

[26](a) FSK/PSK Target 64 Frequency Components and Frequency Probability Distribution (b) FSK/PSK Target 64 Frequency Components Histogram with Number of Ocurrences per Frequency for 256 Frequency Hops (Taboada 2002, 271)

***a. AN/APG-77 Multimode Radar:*** F/A-22 Raptor tactical fighter's AN/APG-77 (Northrop Grumman with Raytheon) multimode radar incorporates a low-observable, Active Electronically Scanned Array (AESA - incorporating approximately 2,000 transceiver modules) and is described as offering long-range, multi target, all-weather, stealth vehicle detection, electronic intelligence gathering and multiple missile engagement capabilities. The active array provides frequency agility, low radar cross section, agile beam steering, and a wide bandwidth capability typical of LPI radar.

Figure 25. The AESA Antenna Used in the AN/APG-77 Radar[27]

As yet unconfirmed sources suggest that APG-77 has a typical operating range of 193 km and is specified to achieve an 86 per cent probability of intercept against a 1 $m^2$ target at its maximum detection range using a single radar paint (Jane's Radar and Electronic Warfare Systems 2004c, ).

***b. AN/APG-79 AESA Radar***: APG-79 Active Electronically Scanned Array (AESA) radar (Raytheon) is designed for installation aboard the F/A-18E/F family of multirole combat aircraft including the EA-18G electronic warfare derivative. The equipment's active array is described as making use of sixth generation transceiver modules, as being a wideband, multifunction equipment and as supporting a variety of waveforms for air-to-air, air-to-ground and electronic warfare modes.

Figure 26. AN/APG-79 AESA Radar[28]

[27] (Jane's Radar and Electronic Warfare Systems 2004c, )

[28] (Jane's Radar and Electronic Warfare Systems 2004a, )

The radar's receiver/exciter features four channels with programmable waveform generation and is billed as offering a wide bandwidth/fast frequency agility/low noise/spurious signals. The sensor has a range exceeding 100nm (180km) - almost twice that of some of today's radars - and can track more than 20 targets simultaneously (Jane's Radar and Electronic Warfare Systems 2004a, ).

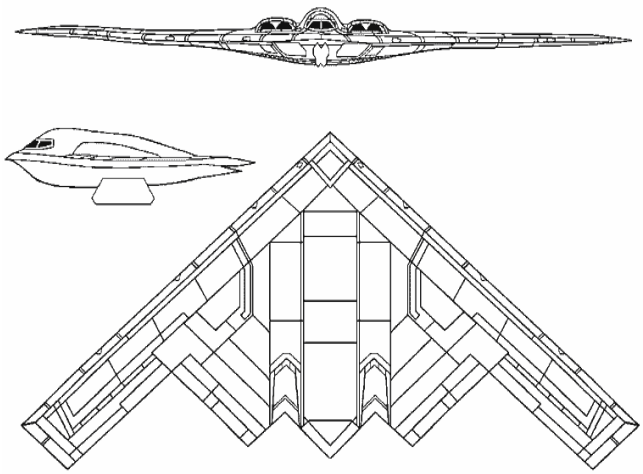

***c.*** ***AN/APQ-181*** is the LPI radar designed specifically for the B-2 Spirit stealth bomber which is in use by the US Air Force and shown in Figure 27. The radar operates in the J-band using 21 separate modes for terrain following, avoidance, navigation, target search, location, identification, acquisition and weapon delivery.

Figure 27. B-2 Spirit Stealth Bomber[29]

The radar employs two electronically scanned array antennas and advanced LPI techniques that match the aircraft's overall stealth qualities. The antenna is electronically steered in two dimensions and features a monopulse feed design to enable fractional beamwidth angular precision. It is designed to have a low RCS with respect to both in- and out-of-band RF illumination (Raytheon ).

***d.*** ***AN/APS-147 Multimode Radar*** is an inverse synthetic aperture radar (ISAR) that equips the US Navy's (USN) MH-60R multi-mission helicopter with a radar that has the latest in high-throughput signal and data processing.

Figure 28. AN/APS-147 Multimode Radar[30]

[29] (Raytheon )

[30] Aboard the MH-60R, the Scanner for the APS-147 Multimode Radar is Mounted Below the Helicopter's Cockpit (Sikorsky) (Jane's Radar and Electronic Warfare Systems 2005, )

The AN/APS-147 uses flexibility through programmability, providing a product optimized for the maritime surveillance mission. Advanced processing allows the APS-147 to use a collection of waveforms to perform its mission at an output power substantially lower than traditional counterparts in maritime surveillance radars. This results in a radar with an extremely Low Probability of Intercept (LPI). Using a low peak power waveform with frequency agility, the radar can detect medium- to long-range targets without the threat of electronic warfare support system interception (Jane's Radar and Electronic Warfare Systems 2005, ).

***e. AN/APG-78 Longbow Radar:*** The AN/APG-78 radar forms part of the Longbow fire-and-forget anti-armor system that is fitted to AH-64D Apache battlefield attack helicopters. The radar subsystem comprises a low probability of intercept millimeter wave (35 GHz frequency) radar mounted on top of the helicopter's main rotor mast (Jane's Radar and Electronic Warfare Systems 2004b, ).

Figure 29. AN/APG-78 Longbow Radar[31]

***f. Low-Altitude Navigation and Targeting Infra-Red for Night (LANTIRN):***

The LANTIRN system uses two pods to allow aircrew to fly their aircraft by day or night and in adverse meteorological conditions. LANTIRN consists of a navigation pod and a targeting pod. The navigation pod contains a wide field of view forward looking infrared (FLIR) and Ku-band LPI terrain following radar, AN/APN-237A, that can be linked directly to the F-16's autopilot to automatically maintain a preset altitude down to 100 feet while flying over virtually any kind of terrain. It has five modes: normal, weather, EP, LPI, and very low clearance (F-16.Net ).

[31] (Jane's Radar and Electronic Warfare Systems 2004b, )

## 2. Maritime LPI Radars

Just as LPI techniques are useful for covert navigation and targeting for air applications, they are equally useful for covert maritime applications. LPI is well suited for this environment as the relatively slow speed of the ship allows for long integration times and extremely large radar cross sections (RCSs).

In the maritime environment the most significant threat to navies are anti-ship cruise missiles (ASCMs) with LPI seekers. These ASCM seekers will have power managed operation in the 8-20GHz range as well as 35-96GHz ranges, by incorporating a number of advanced electronic technologies. These technologies will enable the missile to generate a broad collection wideband programmable waveforms with bandwidths reaching 500MHz to 1GHz. Using a variety of wideband techniques and coherent range Doppler processing, these seekers will effectively target low RCS ships while simultaneously allowing the seeker to escape detection and reject decoys such as chaff (Pace 2004, 455). The following are examples of maritime LPI radars.

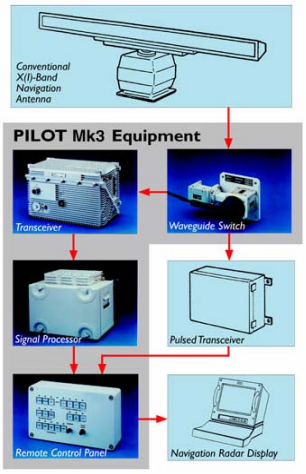


***a. PILOT MK3 LPI Navigation and Detection Radar:*** Saab Bofors has developed the new Pilot Mk3 LPI, a navigation and detection radar for all applications and a new version of the Mk2, with improved LPI performance for use on small ships and submarines. The standard PILOT Mk3 can be used for navigation, helicopter approach monitoring and general target detection. The FMCW principle for LPI purpose makes possible a very low output power level (1W continuous wave, selectable down to 1 mW).

Figure 30. PILOT MK3 LPI Radar[32]

The low power causes the ES system to have a very short detection range while the PILOT has the same navigation radar detection range as a conventional pulsed radar with peak power levels of several kW. The new Mk3 has frequency agility, which makes the probability of detection by ES much harder (SPG Media ).

[32] (SPG Media )

***b. SCOUT LPI Surveillance and Navigation Radar:*** Scout (Signaal) is an I-band (8 to 10 GHz) radar with max of 20nm range using FMCW techniques with low transmitter power (operator selectable 10 mW, 100 mW or 1 W) for LPI purposes. It was modified and improved from the FMCW Pilot radar concept by Thales (Netherlands). SCOUT is used on especially low cross section corvettes and fast patrol crafts. Scout Mk 2(S) variants are being offered for use in mobile or fixed-site coastal surveillance applications (Jane's Radar and Electronic Warfare Systems 2006b).

Figure 31. SCOUT LPI Radar[33]

***c. SMART-L D-Band Radar:*** SMART-L is a solid state, automatic 3D volume search radar capable of detecting and tracking up to 1,000 targets, including maritime patrol aircraft out to 400km, and stealth missile targets out to 55km. The radar has an integrated low probability of intercept (LPI) I/J-band surface surveillance mode, using FMCW techniques drawn from Signaal's Scout covert navigation radar program (Jane's Radar and Electronic Warfare Systems 2006b, ).

Figure 32. The SMART-L D-Band Radar[34]

[33] (Jane's Radar and Electronic Warfare Systems 2006b, )

[34] The SMART-L Installation Aboard the Dutch Destroyer De Zeven Provinciën (Thales Nederland) IBID

***d. RBS-15 MK3 ASCM:*** Saabs RBS-15 medium range, radar guided, air to surface missile is one of a family of long ranged ASCMs produced in Sweden that can be launched from the air, land, or sea.

Figure 33. RBS-15 MK3 ASCM[35]

The missile makes use of low RCS materials to reduce the likelihood of early detection by enemy radar and also has a low infrared signature to reduce the probability of detection by infrared search and track systems. The seeker uses FMCW technology and has output power in the milliwatt range that is progressively reduced as the missile approaches the target.

Saab is developing a future land attack version of the RBS-15 MK3 and is working on several new seeker technologies that maybe applicable and that may be retrofitted to existing variants. These include synthetic aperture radar, which would boost seeker resolution by more than 100% and substantially increase the seeker's target discrimination capability as well as the terminal aimpoint accuracy.

Another option is an LPI radar seeker that would use long, coded pulses that are difficult to detect and difficult to jam. Prototypes for both the synthetic aperture and LPI seekers are currently under test. The improved MK3 version uses a global positioning system (GPS) data link, and the range is 400km (Jane's Air-Launched Weapons 2002, ).

### 3. Land Based LPI Radars

There are many examples of land based LPI radars generally performing ground surveillance and short range air surveillance. In the case of ground surveillance role, these radars can be used to covertly detect ground targets because long integration times are possible. In the air surveillance role, the high speed of ingressing aircraft does not permit for extended integration times but typically these radars are used to cue short range SAM systems. LPI can also be used effectively in the detection of hovering helicopters. Since there is a little motion, long integration times can be used and this

[35] (Jane's Air-Lauched Weapons 2002, )

helps the radar to detect the target even though it is embedded within the surrounding clutter (McRitchie and McDonald 1999, ). The following are examples of land based LPI radars.

***a. SQUIRE Ground Surveillance Radar:*** SQUIRE (Thales, Netherlands) is man-portable solid-state J-band (10 to 20 GHz) radar based on FMCW techniques to ensure low probability of intercept. SQUIRE's processing is based on Fast Fourier Transform techniques to ensure a high rate of discrimination in both range and speed.

Figure 34. SQUIRE Ground Surveillance Radar[36]

Power output is changeable between 10mW, 100mW, 1W. Operating ranges are 10 km for pedestrians, 14 km for helicopters, 15 km for light vehicles, 20 km for small boats, and 24 km for heavy vehicles/large boats (Jane's Radar and Electronic Warfare Systems 2006a, ).

***b. Gerfaut (TRS 2620 and TRS 2630) Acquisition Radars:*** The Gerfaut radars are designed to operate with short and very short-range anti-aircraft weapons. Both radars have a high anti-jamming capability accorded by a wide transmission band, burst-to-burst frequency agility, digital pulse compression, dual-frequency change receiver, velocity filtering, false alarm regulation and the use of antennas optimized for very low sidelobes (Jane's C4I Systems 2001, ).

Figure 35. TRS 2630 Mounted on a Cross-Country Vehicle[37]

[36] (Jane's Radar and Electronic Warfare Systems 2006a, )

[37] (Jane's C4I Systems 2001, )

***c. GB-SCOUT:***

The GB-Scout, developed in the Netherlands by Signaal, differs from its contemporaries in using an FMCW waveform with a very low output power (min 10mW, max 1W). This reduces the likelihood of it being intercepted while still giving a 90% detection probability against a truck with 50 square meter RCS at 25km (Jane's International Defense Review 1994, ).

***d. MRSR Multi-Role Survivable Radar:***

MRSR (Raytheon), tactical target acquisition and tracking radar, is a US Army Missile Command program to meet future tactical air defense requirements in the High-to-Medium Air Defense (HIMAD) and Forward Area Air Defense (FAAD) mission areas. The radar is a 3D track-while-scan, phased array in elevation radar designed to acquire and track multiple airborne targets over a 360º azimuth at extended ranges and at tactical altitudes. Targets include tactical aircraft, unmanned aerial vehicles, and hovering and slowly moving helicopters. The radar incorporates solid-state, low noise transmitter technology, and operates over a wide bandwidth with frequency agility.

The radar aperture, optimized to resist advanced EA and ARMs, employs very low sidelobe antenna technology, combined with an LPI waveform. Multiple beams are moved electronically in elevation. While one beam continuously scans the horizon with its bottom edge touching the ground; thus producing hot spots to confuse ARM seekers (Jane's Air Defense Radar – Land and Sea 1997, ).

***e. MSTAR - Man-portable Surveillance and Target Acquisition Radar:*** MSTAR (Thales – UK) is a coherent J-band man-portable ground and air surveillance radar which is designed for ground surveillance, artillery observation, coast watching and the detection of hovering helicopters. Electronic protection features include infra-red reflective paint on the various components, low power output, low sidelobes, narrow beam, pulse compression and operator selectable frequencies, sensitivity and scan arcs.

Figure 36. MSTAR Battlefield Surveillance Radar[38]

[38] (Jane's Radar and Electronic Warfare Systems 2006a, )

MSTAR features selectable power outputs (1 and 10W) while maintaining low probability of intercept (Jane's Radar and Electronic Warfare Systems 2006a, ).

***f. EL/M-2140 (Advanced Ground Surveillance Radar):***

This is a ground surveillance radar system which automatically detects armored vehicles, light vehicles and personnel. EL/M-2140 (ELTA – Israel) works at X-Ku bands, has over 100 frequencies, and has pulse compression techniques and a peak power of 70 W. This radar has a detection range of 33 km for a tank, 30 km for a light vehicle, 25 km for a helicopter and 15 km for personnel (Jane's Police and Security Equipment 2005, ).

Figure 37. ELTA EL/M-2140[39]

***g. Improved HARD-3D Radar System:***

The Ericsson Microwave Systems Improved HARD (Helicopter and Aircraft/Radar Detection) is an all-solid-state-3D search-and-acquisition radar, which has been designed for use in short-range air defense systems.

Figure 38. HARD-3D Radar[40]

Improved HARD features a LPI capability which is due to its very low electromagnetic signature, low peak output power (240W, 30W average), broadband frequency agility, low sidelobes and narrow antenna beam. The radar is difficult to detect with warning receivers and virtually impossible to attack with anti-radiation missiles, according to Ericsson Microwave Systems (Jane's Land Based Air Defense 2004, ).

[39] (Jane's Police and Security Equipment 2005, )

[40] HARD-3D Radar on Hägglunds Vehicle Bv 206 Which Forms Part of the Swedish Army's Saab Bofors Dynamics RBS 90 SAM System (Jane's Land Based Air Defense 2004, )

***h. EAGLE Fire-Control Radar:*** The Ericsson Eagle fire-control radar is a silent millimetric system intended for use in mobile ground and naval-based air defense systems. The equipment operates in the K-band (20 to 40 GHz) enabling tracking of low-flying targets. The Eagle system has been designed with an extremely low radar signature which has been achieved by pulse compression, high antenna gain and almost no sidelobes, in combination with low peak output power (Jane's Radar and Electronic Warfare Systems 2004e, ).

Figure 39. EAGLE Fire-Control Radar[41]

***i. POINTER Radar System:*** In 1996, Ericsson Microwave Systems completed development of its short-range air surveillance radar system, the Pointer. This system features a LPI 3D all-solid-state radar and has been designed to be integrated into short-range air defense missile systems such as the Mistral, Stinger and Starburst.

Figure 40. Close-up of the Pointer-3D Radar Antenna[42]

Pointer builds on Ericsson Microwave Systems' experience in the development of HARD-3D and Eagle LPI radars which are claimed to be almost impossible to intercept by warning receivers and ARMs (Jane's Land Based Air Defense 1999, ).

[41] BAMSE Missile Control and Launch Vehicle With the Mast-Mounted Eagle Radar/TV/IFF and the Giraffe 3-D Radar in the Background (Jane's Radar and Electronic Warfare Systems 2004e, )

[42] (Jane's Land Based Air Defense 1999, )

***j. CRM-100 Surveillance Radar:*** CRM-100 (Poland), I-band (9.3 to 9.5 GHz sub-band) surface surveillance radar, is described as being a quiet, solid-state, frequency modulated continuous wave radar that is designed to detect surface targets, determine their co-ordinates and automatically hand-off tracking data (target number, range (from own position), bearing (from own position), course and speed) to a command system.

Figure 41. CRM-100 Surveillance Radar[43]

The CRM-100 is an LPI radar with low power (1 mW - 1 W switched according to range - 1.4 to 44.5 km) output and the ability to match the range coverage provided by standard pulse navigation radars. Additionally, the equipment is noted as being suitable for ground mobile as well as shipboard installations (Jane's Radar and Electronic Warfare Systems 2004f, ).

***k. JY-17A Surveillance Radar :*** The medium-range JY-17A (China) battlefield surveillance radar is described as being a fully coherent, solid-state sensor that is suitable for ground- or vehicle-based applications, with the latter including jeep-type vehicles, trucks and armored fighting vehicles (including tanks). The radar features a solid state, LPI transmitter in the 8 to 12 GHz range, and a high-stability frequency synthesizer.

Figure 42. JY-17A Medium-Range Ground Surveillance Radar[44]

It also has a selective linear/circular polarization antenna with low sidelobes, digital phase coding, random frequency shift keying, and pulse Doppler processing that has automatic target detection/tracking. It can detect a single pedestrian at

[43] (Jane's Radar and Electronic Warfare Systems 2004f, )

[44] (Jane's Radar and Electronic Warfare Systems 2004d, )

10 km, a light vehicle at 15 km, a helicopter at 20 km, and a ship at 30 km (Jane's Radar and Electronic Warfare Systems 2004d, ).

***l. CROTALE:***

Power managed systems such as French CROTALE have been placed in land based LPI radar category. Experience has shown that CROTALE is capable of quickly acquiring a target and decreasing its transmitting power to maintain a minimal SNR. This makes it very difficult for a hostile receiver to detect unless special techniques are employed (McRitchie and McDonald 1999, ).

Figure 43. The Monopulse-Doppler Radar Fitted to the Crotale Firing Unit[45]

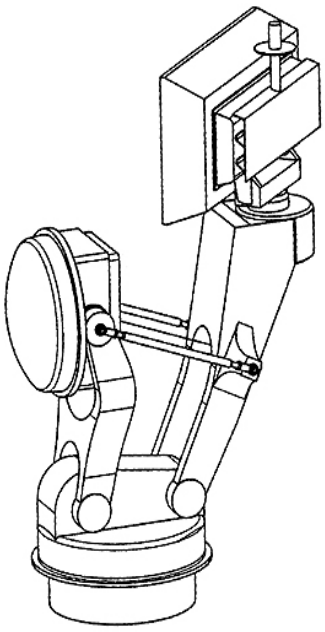

***m. PAGE (Portable Air-defense Guard Equipment) Radar:*** PAGE is a lightweight and inexpensive I-band FMCW LPI radar with a transmit power of only 10-20W, providing range of 10-15 km. Signaal's PAGE LPI surveillance set is used in the upgrade program of ZSU-23-4 with an ASADS Ka band tracker radar. An upgrade such as this will revitalize the lethality of this vintage weapon and will extend its useful lifetime by 15-20 years. There were between 7000 and 8000 ZSU-23-4 systems delivered between 1965 and 1983; many of these systems are in active service in Africa, Asia, Eastern Europe and the Middle East.

Figure 44. PAGE and ADADS Antenna[46]

[45] (Jane's Radar and Electronic Warfare Systems 2003, )

[46]Artist's Impression of the Integrated Foldable Dual Radar Mast Mount as Proposed for the Thales ZSU-23-4V1 Model 1972 Upgrade with PAGE Antenna on Top and ADADS Antenna Below (Jane's Land Based Air Defense 2004, )

THIS PAGE INTENTIONALLY LEFT BLANK

# III. DETECTION OF LPI RADARS

> LPI modulations cannot be properly processed with 'snap shots' of data. These signals will require the collection of continuous streams of data. We can collect and process all current threat signals with current receivers but will need digital receivers to detect LPI signals.
>
> Menahem Oren
>
> General Manager of ELISRA Electronic System, Israel

Electronic Warfare Support (ES) receivers must perform the tasks of detection, parameter identification, and classification in a complex environment of high noise interference and multiple signals in order to exploit LPI radar signals.

Detection of LPI radar signals requires a large processing gain because of the wideband nature of the LPI radar. The basic idea behind the use of wideband signals is to spread the radiated power over a large bandwidth in order to produce a Power Spectral Density (PSD) below the noise at receiver input. Under these conditions, detection is only possible if the signal is integrated over a long observation time. During that time, a special integration procedure must be used to ensure that the noise is not being added in the same amount (Burgos-Garcia et al. 2000, 23-28).

Another problem faced by the ES receiver is to provide sufficient sensitivity for detecting LPI radar signals with wide spectrum properties while discriminating against the multitude of high peak power, short duration conventional radar signals in the same band.

LPI radars are assumed to be low power, high duty cycle signals with phase or frequency coding. As the coding is unknown and can be complex, and assuming the frequency is also unknown, then coherent detection is not possible and non-coherent detection must be performed first. To achieve the maximum sensitivity the RF and video bandwidth must be matched to the signal modulation allowing detection of the total signal energy (Rayit and Mardia 1994, 359; 359-362; 362).

The detection process is followed by the task of classification. Classification requires sorting the signal into groups having similar parameters. Parameters such as:

- LPI radar type
- Carrier frequency
- Modulation bandwidth
- Modulation period
- Code period
- Time and angle of arrival.

These are the parameters that distinguish one LPI radar signal from another and they are required for effective exploitation (jamming). Correlation with existing signals in a database (identification) can then aid in signal tracking and response management.

To identify the emitter parameters, Fourier analysis techniques have been used as the basic tool. From this basic tool, more complex signal processing techniques have evolved, such as the short-time Fourier transform (STFT), so as to track signal parameters over time. More sophisticated techniques have also been developed, called time-frequency and bi-frequency distributions, to identify the different modulation schemes used by the LPI radar. These techniques include the Wigner Ville Distribution (WVD), Quadrature Mirror Filter Bank (QMFB), and Cyclostationary Processing (CP) (Pace 2004, 455).

## A. ES RECEIVER CHALLENGES

To detect LPI radar signals, ES receivers have to overcome three main difficulties. These are:

- Processing gain of the LPI radar
- High sensitivity requirement
- LPI radar's coherent integration

### 1. Radar Processing Gain

In the second chapter of this thesis, range factor α was defined as $\alpha = \frac{R_I}{R_R}$ where $R_I$ was the detection range of the interceptor and $R_R$ was the detection range of the

radar. If $\alpha > 1$, the radar will be detected by the intercept receiver. On the contrary, if $\alpha \leq 1$ the radar can detect the platform while the intercept receiver platform cannot detect the radar.

When the same radar antenna is used to both transmit and receive ($G_{T_r} \approx G_{Rr}$) and an omnidirectional intercept antenna ($G_i = 1$) is used for the interceptor, then for a certain energy or average power transmitted range factor α can be expressed directly in terms of the radar waveform, antenna pattern and radar cross section as;

$$\alpha = \frac{R_I}{R_R} = K\left[\left(G_{Ti} / G_{Tr}\right)\left(1/(\tau B_i)\right)\right]^{1/2}\left(1/\sigma\right)^{1/4} \tag{3.1}$$

where K is the constant parameter of the equation, $G_{Ti}$ is the antenna gain in the direction of the interceptor, $B_i$ is the equivalent noise bandwidth of the intercept receiver and τ is the integration time of the LPI radar. From (3.1), the α is directly proportional to square root of the antenna gain of the radar antenna in the direction of the interceptor, fourth-root of the radar cross section and inversely proportional to the time-bandwidth factor $(\tau B_i)$ which is also the processing gain of the radar receiver over the intercept receiver (Lee 1991, 55).

LPI radars are effective against some ES receivers when a low-peak power and long duration signal is used with a large time-bandwidth product. Large bandwidth signals greater than 10MHz which give 15 meters range resolution may not be needed unless very high range resolution is required. This implies that signals of relatively narrow bandwidths and high duty cycles are effective for LPI applications. An effective time-bandwidth product (processing gain) of around 1000 or 30dB with 10MHz modulation bandwidth and 1ms integration time is practicable and can be achieved with some LPI radars. (Lee 1991, 55).

**2. ES Receiver Sensitivity**

Some ES receivers do not have sufficient sensitivity for the detection of LPI radar signals. Mr. Jim P. Lee states that a system sensitivity requirement of about -100dBmi

will be adequate even for over-the-horizon operation. Sensitivity of ES receiver ($\delta_I$) can be calculated as;

$$\delta_I = n_i SNR_i G_i (B_1)^{\gamma} (2B_2)^{1-\gamma} \tag{3.2}$$

where $n_i$ is the receiver noise power density, $SNR_i$ is the threshold signal-to-noise ratio, $G_i$ is the intercept receiver antenna gain, $B_1$ is the pre-detection bandwidth, $B_2$ is the post detection bandwidth, and $\gamma$ is a parameter $0 < \gamma < 0.5$. (Lee 1991, 55).

The pre-detection bandwidth $B_1$ defines the instantaneous bandwidth of the intercept receiver over which it can detect signals. The post-detection bandwidth $B_2$ defines the maximum modulation rate that the intercept receiver can measure.

The parameter $\gamma$ determines the effective bandwidth of the receiver and varies from a value of 0.5 when $B_1 > B_2$, characteristic of a wide-open, high probability of intercept receiver, to 0 when the two bandwidths are comparable, characteristic of a high sensitivity search receiver.

The ES receiver has three basic means for increasing its sensitivity: increasing the antenna gain, reducing the pre-detection bandwidth and reducing the post-detection bandwidth. In order to improve sensitivity further, both the noise figure and transmission loss of the ES receiver should be minimized.

The first two means involve a probability of intercept (POI) loss by reducing either the angular or frequency instantaneous coverage. The third merely represents a reduction in the measurement bandwidth of the intercept receiver. Therefore, for operation against high duty cycle LPI waveforms, there is scope within conventional ES receivers for increasing sensitivity at negligible cost by reducing the post-detection bandwidth without compromising the POI (Ruffe and Stott 1992, 200; 200-202; 202).

Table 2 below shows the results from calculations of free space detection ranges for the PILOT radar, one of the most common FMCW tactical navigation LPI radar,

compared with a conventional pulsed radar at 10kW peak power. The detection ranges are calculated assuming that frequencies and antenna beams all coincide in time.

Table 2. Comparison of Radar Detection and ES Receiver Ranges[47]

| **Radar Output Power** | **Radar Detection Range (km)** | | **ES Receiver Intercept Range (km) (RCS=100m²)** | | |
|---|---|---|---|---|---|
| | **100m² Target** | **1m² Target** | $\delta_I$ **-40dBmi** | $\delta_I$ **-60dBmi** | $\delta_I$ **-80dBmi** |
| **PILOT MK2** | | | | | |
| **1W** | 28 | 8.8 | 0.25 | 2.5 | 25 |
| **0.1W** | 16 | 5 | 0 | 0.8 | 8 |
| **10mW** | 9 | 2.8 | 0 | 0.25 | 2.5 |
| **1mW** | 5 | 1.5 | 0 | 0 | 0.8 |
| **Conventional Pulsed 10kW Radar** | 25 | 7.9 | 25 | 250 | 2500 |

It can be seen from Table 2 that the PILOT radar with 1W output power can detect its 100m² RCS target at 28km, whereas its transmissions can only be intercepted at 0.25km with -40dBmi sensitivity. It can also be seen that ES receiver interception range is coming closer to radar's maximum detection range with -80dBmi sensitivity. ES receiver interception range can be calculated as 250km, too much above radar's maximum detection range, if the sensitivity of ES receiver were -100dBmi.

Table 2 also shows that the effectiveness of LPI radar performance is strongly influenced by the radar cross-section of the target to be detected. If the PILOT radar were required to detect a smaller target, for example an aircraft, with an RCS of 1m², transmitted power of 1W would give 8.8km radar detection range and the ES receiver with -80dBmi sensitivity would intercept PILOT radar much before it detects aircraft.

### 3. Coherent Integration

LPI radars can integrate their reflected signals coherently over the whole of the integration time, thus narrowing the receiver noise bandwidth and increasing sensitivity. On the other hand ES receivers cannot coherently detect the radar's signals and hence they cannot narrow their bandwidths in the same manner (Fuller 1990, 1-10).

[47] (SPG Media )

## B. ES RECEIVERS FOR LPI RADAR DETECTION

Some wide-open ES receivers such as the Instantaneous Frequency Measurement (IFM) and Crystal Video Receivers (CVR) work well in a low density signal environment where the pulses are short in duration. However, they are susceptible to interference in a dense signal environment where radar pulses overlap in time. This problem has become more severe with the introduction of pulse compression waveforms and pulse Doppler radars with their higher duty cycles. The problem associated with signal overlap may become worse with LPI signals which are expected to maintain even higher duty cycles.

On the other hand, LPI signals are expected to be of much lower in peak power, and thus those LPI radars which are far away will not affect the performance of the ES receiver. However, there are likely to be “friendly” LPI radars on the same platform or nearby which will cause interference.

As a result, with the proliferation of pulse compression and LPI signals, current wide-open IFM and crystal video receivers will be more susceptible to interference and thus are poor candidates for future ES receiver systems. In addition, they do not have the sensitivity for the detection of current and projected LPI signals (Lee 1991, 55).

With a scenario involving an FMCW LPI radar and an IFM receiver, the effects of processing gain and sensitivity on detection ranges can be seen. In the scenario the range at which 100% probability of intercept can be achieved against the main beam of the radar will be taken as the baseline measure of performance (MOP). Parameters of both FMCW LPI radar and IFM receiver are based on a reported calculation described in (Stove, Hume, and Baker 2004, 249-260). These parameters are given in the Table 3 below.

Table 3. Parameters of the FMCW Radar and IFM Receiver System[48]

| **Radar Type** | **FMCW** | **ES Receiver Type** | **IFM** |
|---|---|---|---|
| Mean Transmitter Power | 1W | IF Bandwidth | 2GHz |
| Antenna Gain | 30dB | ES Receiver Antenna Gain | 0dB |
| Antenna Sidelobe Level | -35dB | Video Bandwidth | 10MHz |
| Effective Radiated Power (ERP) | 60dBmi | Effective Bandwidth | 200MHz |
| Frequency | 9GHz | Processing Losses | 3dB |
| Integration Time | 1ms | Minimum SNR for Detection | 17dB |
| Bandwidth | 1KHz | Net Sensitivity | -60dBmi |
| Received Power at 20km Range | -125dBm | Incident Power Density from 60dBmi at 2.5km | -19 $dBm/m^2$ |
| Target RCS | $100m^2$ | Received Power at 2.5km | -60dBm |
| Noise Figure | 4dB | Noise Figure | 10dB |
| Noise Floor | -144dBm | Noise Floor | -80dBmi |
| Incoherent Integration Gain | 4dB | Effective Aperture | $-41dBm^2$ |
| SNR at 20km Range | 15dB | | |
| Agile Bandwidth | 100MHz | | |

It can be calculated from the parameters in Table 3 that the FMCW radar can detect its target at 20km range, while its transmissions can only be intercepted at 2.5km by the IFM receiver. If the FMCW radar is replaced by a pulsed radar with 0.1% duty cycle, the peak power will be increased by a factor of 1000 and the free space intercept range increased by about a factor of 30. In other words, the IFM receiver will easily detect the radar emissions before the radar system detects its target. As a result, it can be seen that although an IFM receiver can be suitable for low duty cycle pulsed radars, it is not a suitable ES receiver for LPI radar detection.

Following are some potential ES receiver architectures to be discussed for the detection of LPI radars. These potential architectures are by no means the only candidates for LPI detection, even though they are the best known today. There are other types of receivers not discussed, such as the correlator and the fast scan superhet, which could be used for LPI signal detection (Stove, Hume, and Baker 2004, 249-260). Among these ES receivers acousto-optic and digital receivers are seen to be the strongest candidates for the LPI radar detection.

[48] (Stove, Hume, and Baker 2004, 249-260)

### 1. Channelized Receivers

This is a system of many narrowly spaced receiving channels used to measure RF. This aims to give the best of both worlds, having a large probability of intercept with a high degree of sensitivity. Each channel is a complete radio receiver tuned to a particular filter characteristic and the assembly of many channels constitutes a fully parallel receiver with inherently high data rate capabilities (Fuller 1990, 1-10).

Channelized receiver techniques offer greater sensitivity than the IFM receiver described in the scenario, by dividing the IF bandwidth (of 2 GHz in the scenario) into a large number of narrow channels. For example, a sensitivity improvement of about 20 dB is possible using a channel bandwidth of typically 10 MHz with a lower noise figure and losses than the IFM based system. The detection range against the FMCW radar in the scenario with 1W will then be increased to 25km, i.e. it will be approximately equal to the FMCW radar's detection range.

A potential counter to this is the random noise (RN) radar. This can have a very instantaneous bandwidth and thus the intercept range will be reduced if the transmission bandwidth is greater than the channel bandwidth. This is due to signal in any one channel potentially being below the detection threshold, even if the total power (which is spread over several channels) exceeds it.

The linear FMCW waveform does not have RN radar's advantage because the signal is not instantaneously wideband and in any practical scenario the received signal will 'dwell' in a channel for a period longer than the reciprocal of the channel's bandwidth, and so will be detected (Stove, Hume, and Baker 2004, 249-260).

### 2. Superhet Receivers

A lower-cost alternative to the channelized receiver is to use a superheterodyne receiver which uses filtering and mixing to translate the signal to a lower intermediate frequency (IF). This has the advantage of enabling a narrowband channel with higher sensitivity to be tuned over a desired operating range. Superheterodyne receivers are also able to analyze one signal at a time without interference from signals close in frequency, and hence are suitable for emitter identification. This form of receiver can be especially useful if a search is to be made for a specific radar type.

Table 4. Sensitivity of the Superheterodyne Receiver[49]

| | |
|---|---|
| IFM Receiver Sensitivity (from Table 3) | -60dBmi |
| Lower Losses | -3dB |
| Lower Noise Figure | -4dB |
| Narrower Bandwidth | -22dB |
| Net Sensitivity | -89dBmi |

Table 4 shows the sensitivity of the superheterodyne receiver with the IFM receiver system sensitivity. Even in the 'non-tuned' case the receiver outlined in Table 4 would still detect the main beam of the FMCW radar, in free space, at 70km range, i.e. considerably greater range than that at which the radar can detect its target (Stove, Hume, and Baker 2004, 249-260).

### 3. Matched Incoherent Receiver (MIR)

The matched incoherent receiver overcomes the mismatch currently found between the bandwidths of radars and intercept receivers (Stove, Hume, and Baker 2004, 249-260). Growth in computing power makes it feasible for a parallel processor to carry out matched filtering in a number of channels to combat a number of potential threats simultaneously. The MIR would be matched to the RF information and information bandwidths of the radar, but not to its actual transmitted waveforms. This is because it still does not match to the phase of the signal as does a coherent matched receiver. Moreover, the radar no longer has the advantage of a mismatch between its bandwidth and that of the intercept receiver, only the advantage of knowing its own waveform and which part of its agile bandwidth it is actually using at any given time.

For the scenario above, the MIR would have an effective bandwidth of 200KHz, making it 30dB more sensitive than an IFM receiver. If MIR has 7dB improvement over the IFM receiver due to lower losses and noise figure which was assumed for the channelized receiver and the superhet receiver, the MIR will have a sensitivity of -97dBmi, giving it a free-space detection range of 177km against FMCW radar in the scenario (Stove, Hume, and Baker 2004, 249-260).

[49] (Stove, Hume, and Baker 2004, 249-260)

### 4. Acousto-Optic Receiver

The receiver requirement for a relatively a large number of narrow channels with a narrow video bandwidth for the detection of LPI radars can be easily met by the use of a time-integrating acousto-optic receiver. The narrow video bandwidth and the relatively large number of channels can be implemented relatively easy by using a time-integrating photodetector array.

Considerable progress has been made on the development of both 1-D and 2-D acousto-optic receivers. In a 1-D configuration, the acousto-optic receiver performs spectrum analysis on the received signals while in the 2-D configuration both spectrum analysis and direction-finding are carried out. An Acousto-optic receiver which is suitable for the detection of LPI signals can be implemented easily using “off-the-shelf” photodetector arrays with variable integration times.

The effective integration time (video bandwidth) of the acousto-optic receiver can be adjusted to match the duration of the signal intercepted for maximum sensitivity. This can be accomplished by either changing the integration period on the photo detector array or changing the number of samples integrated digitally (Lee 1991, 55).

### 5. Digital Receivers

Most recent receivers deployed for LPI radar detection are digital, using mainly Fast Fourier Transform (FFT) as a signal processing technique. With these digital processing techniques such as FFT, the processing gain of the LPI radar is overcome.

The most important advantage of implementing the digital receiver is the possibility of performing different digital signal processing algorithms, as the intercepted signals are stored in memory. There are some disadvantages for this receiver, such as restricted memory and the dynamic range due to low resolution of the analog to digital converter (ADC).

Digital receivers, often called software radios, place a high performance burden on the ADC, but allow a good deal of flexibility in post detection signal processing. ES receiver parameters of interest include sensitivity, dynamic range, resolution, simultaneous signal capability, complexity, and cost. Figure 45 shows a block diagram of wideband digital ES receiver (Pace 2004, 455).

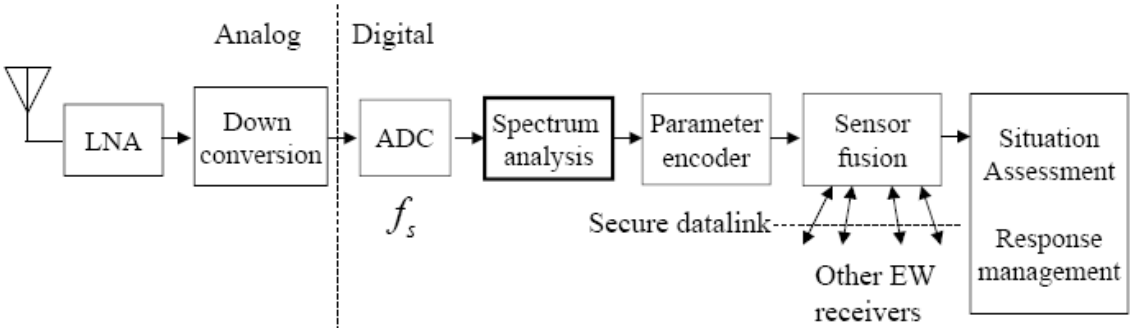


Figure 45. Wideband Digital ES Receiver[50]

After the signal is down-converted, digitized and sorted, the parameter encoder forms a pulse descriptor word (PDW). For LPI CW emitters, the PDW contains the center frequency, the signal coding details such as the modulation period and bandwidth (FMCW), code period and subcode period details (PSK), and frequency-hopping frequencies (and order), as well as the signal's angle of arrival. In all cases, the signal is down-converted to a baseband frequency that depends on the analog-to-digital converter (ADC) technology that is available.

The trend in ES digital receivers is to push the ADC as far towards the antenna as possible, and eliminate the down-conversion stage. This is due to bothersome spurious signals, nonlinearities, and image frequencies that the mixing and filtering operations cause. Although the development of standard components, such as ADCs, that are essential for such a concept have made considerable advancements recently, more wideband solutions are required using electro-optics (extremely wideband) and superconductivity (high sensitivity) (Pace 2004, 455).

## C. ES RECEIVER EXAMPLES

The following are some of ES receivers that have the capability of LPI radar detection, identification and classification.

### 1. High Sensitivity Microwave Receiver (HSMR)

Tenix Defense Electronic System Division's High Sensitivity Microwave Receiver (HSMR) is an ES receiver capable of operating in aircraft, ships, submarines and ground vehicles, and can stand-alone or be integrated with existing ES systems.

[50] (Pace 2004, 455)

The signal detection of the HSMR system is designed specifically to detect LPI radars and, combined with its very high sensitivity, provides the early detection of LPI emitters. The HSMR has an instantaneous bandwidth of 0.5, 1.0 or 2.0 GHz and is fed from a wide-band receiver operating nominally between 0.5 to 18.0 GHz. For LPI radars with very low effective radiated power, the HSMR provides significant warning times. The level of integration with existing ES equipment can range from none at all to a fully automated operation. As a stand-alone system, the HSMR will display the presence of LPI signals. This allows the operator to manually task the ES system to search for and identify the LPI signal. As a fully integrated system, HSMR detections can be integrated to include automatic library identification and then pass parametric information to the ES system on predetermined, or operator selected, emitters for further analysis (Tenix Defense 2005, 2).

The HSMR Acousto-Optic Module (AOM) is a custom, three slot VXI module containing the Radio Frequency (RF) amplifiers, 0.5, 1.0 or 2.0 GHz Bragg Cell, a 1024 element photo detector array and a digital signal processor. A wide-band analog signal (3.0 GHz intermediate frequency) is fed into the HSMR AOM and the resultant spectral power information is sent via an Ethernet connection to the HSMR executive processor. The VXI backplane is only used for power and ground, with no use of the data paths. The specifications for the 2.0 GHz system are shown in the Table 5. HSMR specifications at the Table 5 show that the receiver system covers the most common radar band of 0.5-18GHz with a very high sensitivity of >-90dBm which is a requirement for LPI radar detection.

Table 5. Specifications of HSMR[51]

| **Wide-band Receiver** | |
|---|---|
| Input Frequency Range | 0.5-18.0 GHz |
| Output Frequency Range | 2.0-4.0 GHz |
| **HSMR Core Module** | |
| Instantaneous Frequency Range | 2.0-4.0GHz |
| Instantaneous Dynamic Range | >45dB |
| Detector Array | 1024 Photo-diode elements |
| Pixel Resolution | 2.0MHz |
| Detector Integration Time | 3ms |

[51] (Tenix Defense 2005, 2)

| | |
|---|---|
| Frame Update Time | 48ms |
| Overall System Sensitivity | >-90dBm |
| **Interfaces** | |
| Control, Access to Spectral and Processed Data | Commercial Standard VXI |
| High Speed Access to Spectral Data | Ethernet, RS232, RS422 |

The HSMR executive processor software can be hosted on a Tenix Defense supplied standard Pentium-based single board computer mounted in the wide-band VXI chassis or on an existing ES workstation. The executive processor receives wide-band data from the wide-band receiver and the AOM as well as ESM narrow-band data via the Ethernet. This data is then made available to the operator console. The executive processor can also manage all of the ES system receivers using Ethernet and serial platform interfaces and has expansion capabilities for additional interfaces as required. Figure 46 shows the HSMR system components (Tenix Defense 2005, 2).

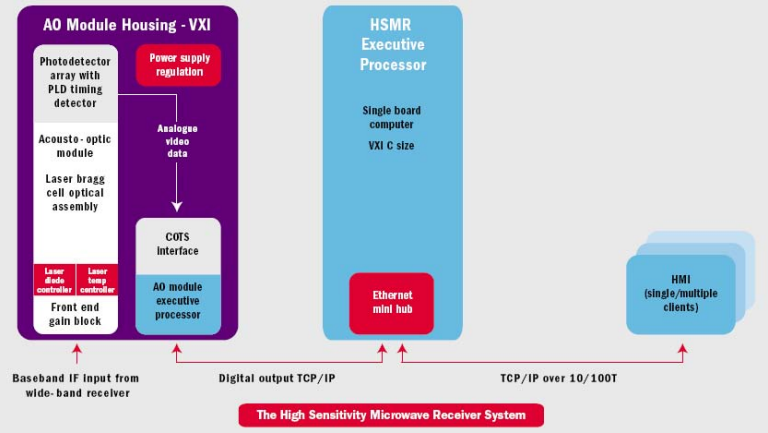


Figure 46. HSMR System[52]

## 2. Vigile-300

Vigile-300 is a digital scanning receiver giving an enhanced sensitivity over a narrow band, allowing detection of LPI radars and fine-grain analysis ('fingerprinting'). Thales representatives state that "There are lots of systems that do fingerprinting, but the challenge is to be able to do it automatically". Vigile 400 features high-accuracy DF with a wideband interferometer array that exploits a dual-polarized anti-roll antenna design,

[52] (Tenix Defense 2005, 2)

minimizing ambiguity and giving sub-degree accuracy on E-J bands, suitable for passive targeting (JANE'S NAVY INTERNATIONAL 2004, ).

### 3. Sabre

Thales Airborne Systems has also developed the earlier Sabre EW as shown in Figure 47 for the Royal Netherlands Navy's four De Zeven Provincien class air defense and command frigates. The first three are at sea, and in tests Thales states that Sabre has shown a very high level of accuracy and sensitivity, including an ability to detect LPI emitters such as the company's own Scout FMCW radar.

Figure 47. SABRE ES System[53]

Sabre comprises a high-quality ES system integrated with a multi beam phased array type EA system, with cross polarization jamming against monopulse seekers. The passive element incorporates six receivers with a 12-port antenna array to give very high accuracy, and uses 'smart blanking' to enable it to function alongside the ship’s active array radar. The system interfaces with a standard multifunction console developed by TNO-FEL, which also developed the associated threat evaluation and weapons allocation software application (JANE'S NAVY INTERNATIONAL 2004, ).

### 4. NS-9003A-V2 ES System

The NS-9003A-V2 shipboard ES system is designed to receive, analyze and identify signals in the 2 to 18 GHz frequency band and is claimed to offer 100 percent probability of intercept throughout 360º in azimuth as shown in the Table 6.

[53] (JANE'S NAVY INTERNATIONAL 2004, )

Table 6. Specifications of NS-9003A-V2 ES System

| | |
|---|---|
| Frequency Coverage | 2-18 GHz (0.5-40 GHz option) |
| Frequency Accuracy | 2 MHz |
| Azimuth Coverage | 360° |
| DF Accuracy | 2° RMS |
| POI | 100% (claimed) |
| Sensitivity | -65 to -75 dBm |
| Dynamic Range | 60dB |

The equipment's man/machine interface is noted as including a operator console and interfaces are provided to link the NS-9003A-V2 with onboard electronic countermeasures systems, decoy launchers, command and control (C2) systems and other shipboard devices. The NS-9003A-V1 configuration is described as being essentially similar to that of the NS-9003A-V2 with the exception of offering a reduced direction-finding accuracy of 5º RMS (JANE'S NAVY INTERNATIONAL 2004, ).

## D. SIGNAL PROCESSING ALGORITHMS

Detection and interception of LPI signals requires sophisticated receivers that use time frequency signal processing, correlation techniques and algorithms to overcome the processing advantage of the LPI radar.

These signal processing algorithms require a large amount of computing speed and memory. Managing processing speed is not a problem with the current digital capabilities, but carrying enormous amounts of data is still problematic. Increasing the sensitivity of the receiver allows for detecting sidelobes of the emitter, but at the same time obligates the receiver to process a significantly large number of signals.

In addition to these challenges, new signal detection and feature extraction systems are needed to effectively analyze these new waveforms in a complex signal environment.

Time-frequency data analysis can be performed using complex instrumentation through computer analysis. Computer algorithms are currently being developed to analyze and graphically display the results of the data for user interpretation. Improvements are being considered to provide representations beyond the conventional

use of the Fast Fourier Transform (FFT) (Taboada 2002, 271). Below are some signal processing algorithms that are used for LPI radar detection.

### 1. Adaptive Matched Filtering

To detect LPI radar signals at operationally useful ranges, the intercept receiver must overcome the processing gain advantage of the radar. One method to regain the advantage is to form a matched filter to the LPI radar waveform. Achieving similar processing gain, the interceptor's signal detection capability will be identical to that of the LPI radar; that is, dependent only on the energy contained within the signal. If the adaptive filter is matched with the LPI waveform, mismatch disadvantage will be eliminated.

To construct a matched filter, the transmitted frequency, the slope of the FM and the repetition period have to be known. However, these features of interest are not normally known to the LPI radar interceptor. As such, the matched filter has to be adaptively formed. The LPI radar signals have to be estimated and incorporated into the matched filter and adaptively changed as part of the detection process. In the construction of the adaptive matched filter, any inaccuracy in the feature estimates (mismatched filter) will lead to a loss in processing gain.

An adaptive matched filter for the PILOT radar waveform was developed by Mr. Peng Ghee Ong using a technique employed by pulse compression radar, called deramping. The deramping process mixes the input signal with a locally generated linear FM signal to produce an output signal of reduced FM slope in comparison with the input signal (Ong and Teng 2001, ).

From the analysis of the deramping process, the frequency range of the output can be predicted when the features of the matched filter are closely tuned to that of the target LPI radar waveform. The output of the deramped signal can then be easily processed using a FFT filter bank that covers the expected frequency range. Figure 48 shows an example of a LPI radar detector using analog deramping (Ong and Teng 2001, ).

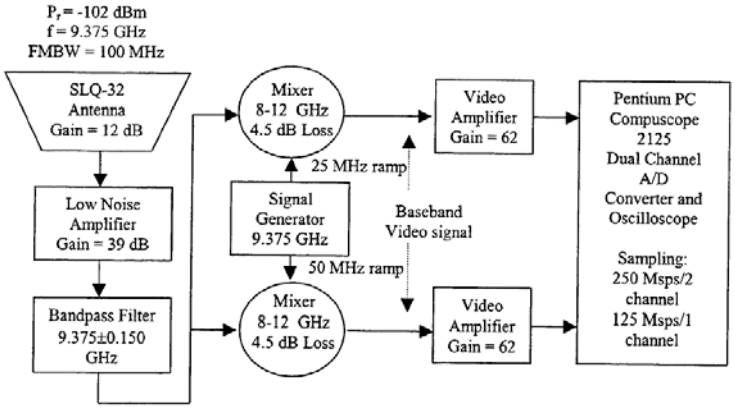


Figure 48. LPI Radar Detector Block Diagram[54]

Besides facilitating the determination of the frequency content, the output frequency spectrum (FFT output) can also be observed to assess the faithfulness of the matched filter. If two widely separated FFT filters, a number of filters covering a wide bandwidth or a combination are energized, the features of matched filter have to be re-tuned to synchronize it to the LPI signal. A re-adjustment of the FM repetitive frequency or the phase of the matched filter or both may be necessary (Ong and Teng 2001, ).

**2. Parallel Filter Arrays and Higher Order Statistics**

This technique is based on the use of parallel filter (sub-band) arrays and higher order statistics (third-order cumulant estimators). Each sub-band signal is treated individually and is followed by the third-order estimator in order to suppress any symmetrical noise that might be present. The significance of this technique is that it separates the LPI waveform in small frequency bands, providing a detailed time-frequency description of the unknown signal. Finally, the resulting output matrix is processed by a feature extraction routine to detect the waveform parameters. Identification of the signal is based on the modulation parameters detected.

The use of Higher Order Statistics (HOS) and parallel filter arrays along with the extraction of the most important features provide an accurate analysis and interpretation of unknown signals in real time (Taboada 2002, 271).

The use of parallel filter arrays and HOS is an effective technical approach for detecting and classifying LPI radar signals where the waveform of the signal is unknown.

[54] (Ong and Teng 2001, )

The HOS processing is one time-frequency approach to the detection of LPI signals as shown in Figure 49. The objective of parallel filter arrays is to separate the input signal into small frequency bands, providing a complete time-frequency description of the unknown signal. Then, each sub-band signal is treated individually by a third-order estimator in order to suppress the noise and preserve the phase of the signal during the correlation process. Finally, the resulting matrix is entered into a feature extraction module whose resulting characteristics from the signal are used to determine what type of modulation was detected.

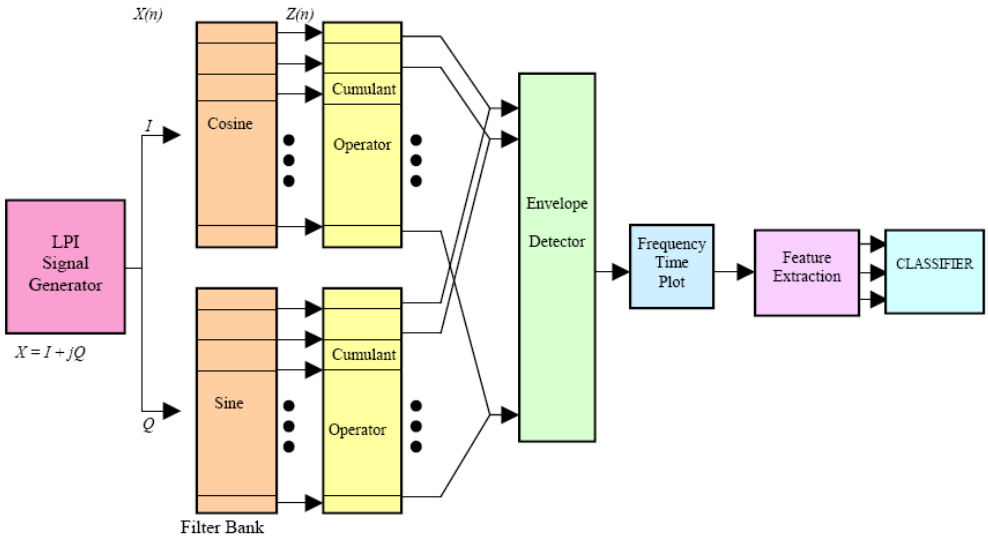


Figure 49. Overview of the Parallel Filtering and HOS[55]

The detection can be performed without knowing any of the characteristics of the input signal. The parallel array of filters can approximate the behavior of a matched filter. The purpose of this filter bank is to separate the observed signal into frequency bands. An increment in the number of filters in bank also increases the resolution of the system. The implementation of HOS, particularly third-order cumulant estimators, shows the potential of the method to suppress white Gaussian noise. The detection method also indicates that the third-order cumulant of a signal grows out the third-order cumulant of the noise with increasing SNR (Taboada 2002, 271).

55 (Taboada 2002, 271)

The efficiency of the proposed method varies with the modulation used in the LPI radar signal. High efficiency was gained for detecting and identifying all the parameters of BPSK and FMCW signals. The detection and identification of polyphase-coded signal is satisfactory, even though some of the parameters cannot completely be distinguished. This method also exhibits a good discrimination among different polyphase-coded signals as Frank, P1, P2, P3 and P4 (Taboada 2002, 271).

### 3. Wigner Ville Distribution (WVD)

The WVD is a two-dimension function describing the frequency content of a signal as a function of time. The WVD has been noted as one of the more useful time-frequency analysis techniques for signal processing. Using the WVD, frequency and time changes in most of the LPI radar signals can be identified (Gau 2002, 147).

The WVD of input signal x(t) is defined as

$$W(t,\omega) = \int x\left(t+\frac{\tau}{2}\right)x^*\left(t-\frac{\tau}{2}\right)e^{-jwt}d\tau \tag{3.3}$$

where t is the time variable and ω is the frequency variable. The WVD is a two dimension function describing the frequency content of a signal as a function of time.

This continuous time and frequency representation can be modified for the discrete sequence x(*l*), where *l* is a discrete time index, *l*=…,-1,0,1,…. The discrete WVD is defined as

$$W(l,\omega) = 2\sum_{-\infty}^{\infty} x(l+n)x^*(l-n)e^{-j2wn}. \tag{3.4}$$

If the functioned is windowed with a rectangular window function with magnitude one and some additional modification, the WVD becomes

$$W(l,\omega) = 2\sum_{n=-N}^{N} f_l(n)e^{-j2wn}, \tag{3.5}$$

where

$$f_l(n) = x(l+n)x^*(l-n) \tag{3.6}$$

and where the continuous frequency variable ω is sampled by

$$\omega = \frac{\pi k}{2N},\ k = 0,1,2,...,2N\text{-}1. \tag{3.7}$$

From equation (3.5) and (3.7) the WVD becomes

$$W\left(l, \frac{\pi k}{2N}\right) = 2\sum_{n=-N}^{N} f_l(n)e^{-\frac{j2\pi k}{2N}}. \tag{3.8}$$

Adjusting the limits of n in order to use the standard FFT algorithms, equation (3.8) becomes

$$W\left(l, \frac{\pi k}{2N}\right) = 2\sum_{n=0}^{2N-1} f_l^{'}(n)e^{-\frac{j2\pi k}{2N}}. \tag{3.9}$$

In (3.9) the kernel function has been adjusted to $f_l^{'}(n),$ where

$$f_l^{'}(n) = \begin{cases} f_l(n), & 0 \le n \le N\text{-}1 \\ 0, & n = N \\ f_l(n-2N), & N+1 \le n \le 2N\text{-}1. \end{cases} \tag{3.10}$$

The resulting WVD is, therefore

$$W(l,k) = 2\sum_{n=0}^{2N-1} f_l^{'}(n) e^{-\frac{j\pi kn}{N}}. \tag{3.11}$$

Equation (3.11) is the final WVD equation used to calculate the WVD of the detected signals (Gau 2002, 147). Figure 50 shows the 2D frequency-time output of an FMCW signal with 1KHz carrier frequency at the IF band, 250Hz modulation bandwidth and 20ms modulation period processed after WVD signal processing algorithm.

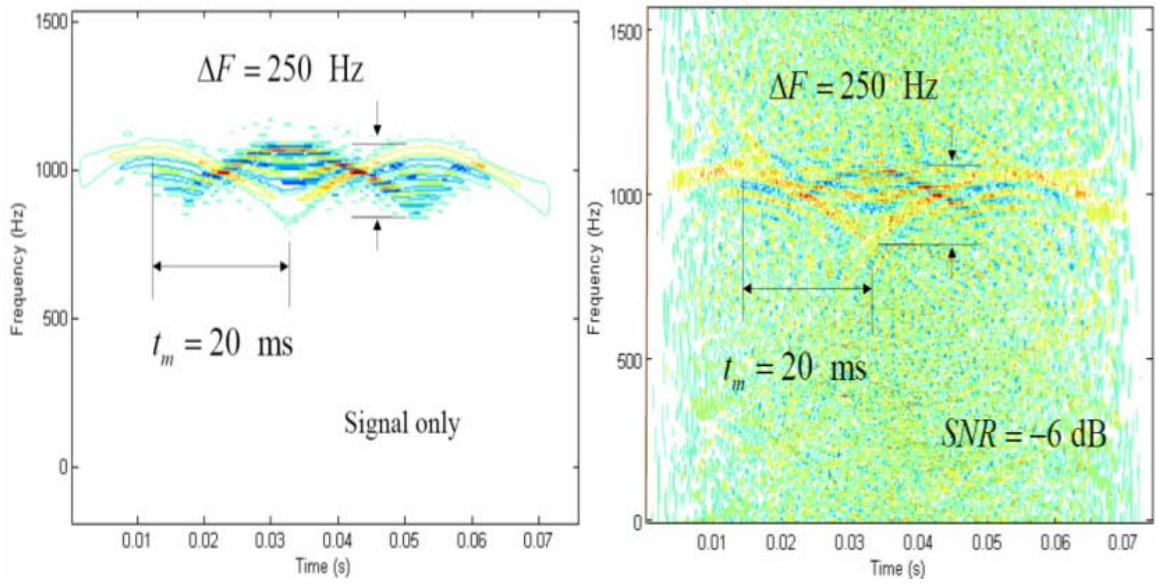


(a) (b)

Figure 50. Frequency-Time Output of FMCW signal (a) Signal Only (b) SNR=-6dB[56]

The WVD is a good time-frequency signal processing algorithm for observing the modulation characteristics of non-stationary signals. It is, however, extremely costly with respect to computation time. Improvements in ES receiver hardware are helpful but the analysis computations to extract the detailed modulation parameters are still expensive. Additionally, the signal must be known for somewhat large periods of time to derive useful results. For real-time signal processing, an efficient coding algorithm and a very

[56] (Pace 2004, 455)

fast digital processor of field programmable gate array (FPGA) are required (Milne and Pace 2002, IV3944; 3944-7 vol.4; 7o.4).

### 4. Quadrature Mirror Filter Bank (QMFB)

Complex sinusoids are used by the Fourier transform to perform the analysis of signals using appropriate basis functions. This approach is difficult since local information, such as an abrupt change in the signal, is spread out over all frequencies based on the infinite extension of the Fourier transform. This problem has been addressed by introducing windowed complex sinusoids as basis functions. This leads to the doubly indexed windowed Fourier transform:

$$X_{WF}(\omega,\tau) = \int_{-\infty}^{\infty} e^{-j\omega t} w(t-\tau) x(t) dt, \tag{3.12}$$

where $w(t-\tau)$ constitutes an appropriate window, $X_{WF}(\omega,\tau)$ is the Fourier transform of x(t) windowed with ω and shifted by τ. An advantage of the windowed or short time Fourier transform (STFT) is that if a signal has most of its energy in a given time interval [-T,T] and a given frequency interval [-Ω,Ω], the STFT will be localized in the region [-T,T]x[-Ω,Ω] and will be close to zero in time and frequency intervals where the signal has little energy. A negative aspect of the STFT is that a single window is used for all frequencies, meaning that the resolution of the analysis is the same at all locations in the time–frequency plane. Therefore arbitrarily high resolution in both time and frequency is not possible (Jarpa 2002, 154).

By varying the window used, resolution in time can be traded for resolution in frequency. To isolate discontinuities in signals, it is possible to use some basis functions, which are very short, while longer ones are required to obtain a fine frequency analysis. The wavelet transform achieves this by obtaining the basis functions from a single prototype wavelet, $h_{ab}(t),$ with the use of translation and dilation/contraction as in

$$h_{ab}(t) = \frac{1}{\sqrt{a}} h\left(\frac{t-b}{a}\right), \tag{3.13}$$

where is *a* positive real number and *b* is a real number. For large *a*, the basis function becomes a stretched version of the prototype wavelet (low frequency function) while for small *a*, the basis function becomes a contracted wavelet (short high frequency function). The wavelet transform (WT) is defined as

$$X_W(a,b) = \frac{1}{\sqrt{a}} \int_{-\infty}^{\infty} h^*\left(\frac{t-b}{a}\right) x(t)dt. \tag{3.14}$$

The time–frequency resolution of the WT involves a tradeoff not applicable to the STFT. At high frequencies, the WT is sharper in time, while at low frequencies, the WT is sharper in frequency (Jarpa 2002, 154).

By using the Wavelet techniques to develop an appropriate basis set and combining it with a quadrature mirror filter bank as illustrated in Figure 51, it is possible to decompose the waveform in such a way that the tiles have the same dimensions regardless of the frequency. By properly comparing these matrices, extracting signal features is possible using both fine frequency and fine time resolutions. Parameters, such as bandwidth, center frequency, energy distribution, phase modulation, signal duration and location in the time–frequency plane can be determined using these techniques, making them valuable for intercepting receivers (Jarpa 2002, 154).

Figure 51 shows the basic two–channel QMFB. Here, the input signal x[n] is first passed through a two–band analysis filter bank containing the filters, $H_0(z)$ and $H_1(z)$, which typically have lowpass and highpass frequency responses, respectively, determined by a cutoff frequency π/2.

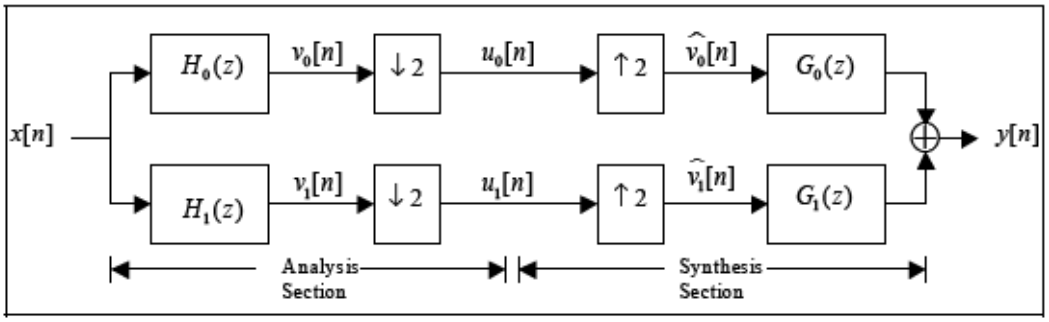


Figure 51. The Two-Channel Quadrature Mirror Filter Bank[57]

The sub-band signals $\{v_k[n]\}$ are then down-sampled by a factor of 2 in the "signal analysis section" to be transmitted to the "signal synthesis section." Here the signals will be up-sampled by a factor of 2 and passed through a two-band synthesis filter bank composed of the filters $G_0(z)$ and $G_1(z)$, whose outputs are then added yielding y[n]. The analysis and the synthesis filters in the QMFB are chosen to ensure that the reconstructed output is a reasonable replica of the input x[n].

One practical consequence of these requirements is that when a suitable *H* filter is found, the *G* filter is obtained by negating and time reversing every other coefficient value. The filters should collect energy in approximate tiles. They must pass as much energy from inside a tile as possible, while rejecting as much as possible from outside a tile with a reasonably flat pass region.

Some filters, such as the Haar filter, meet the wavelet requirements that perfectly tile the input energy in time but, unfortunately, does not tile well in frequency. The opposite of the Haar filter, in this respect, would be the sinc filter. The correct filter is the "modified sinc filter," which will return a good tile in time and frequency (Jarpa 2002, 154).

Figure 52 shows the 2D frequency-time output of an FMCW signal with 2KHz carrier frequency at the IF band, 250Hz modulation bandwidth and 50ms modulation period processed after QMFB signal processing algorithm.

[57] (Jarpa 2002, 154)

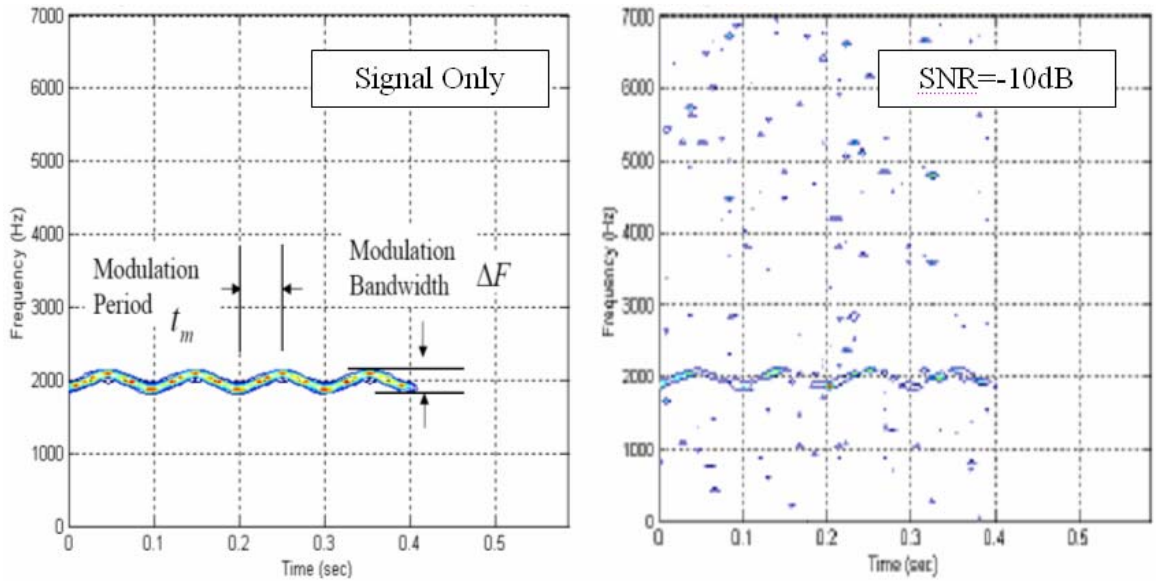


(a) (b)

Figure 52. Frequency-Time Output of an FMCW signal (a) Signal Only (b) SNR=-10dB[58]

The QMFB tree receiver does a good job of distinguishing the signals in the time domain. It is very good at picking out when frequency shifts occur and what those frequencies are. However, the image frequencies that appear can be strong enough to totally mask the actual signal frequency, making interpretation difficult. While the receiver's ability to pick out signals at low SNR appears to be poor, further analysis on the output matrices can add significant signal detail (Copeland and Pace 2002, IV-3960; IV-3963 vol.4).

### 5. Cyclostationary Processing (CP)

The cyclostationary attribute in the periodicities of the second order moments of the signal can be interpreted in terms of the generation of spectral lines from the signal by putting the signal through a quadratic non-linear transformation. This property explains the link between the spectral-line generation property and the statistical property called "spectral correlation", corresponding to the correlation that exists between the random fluctuations of components of the signal residing in distinct spectral bands. The correlation integral is very important in theoretical and practical applications and may be defined as

[58] (Pace 2004, 455)

$$h(x) = \int_{-\infty}^{\infty} f(u)g(x+u)du \tag{3.15}$$

Applying an FFT, it forms a Fourier transform pair given by:

$$\Im\{h(x)\} = F(s)G^*(s) \tag{3.16}$$

If *f(x)* and *g(x)* are the same function, the integral above is normally called the autocorrelation function, and called cross-correlation if they differ. The autocorrelation function is a quadratic transformation of a signal and may be interpreted as a measure of the predictability of the signal at time t + τ based on knowledge of the signal at time *t* (Lima 2002, 162).

Looking at a time series of length T, the autocorrelation function is given by the time–average autocorrelation function:

$$R_x(\tau) \triangleq \lim_{T\to\infty} \frac{1}{T} \int_{\frac{-T}{2}}^{\frac{T}{2}} x\left(t+\frac{\tau}{2}\right)x^*\left(t-\frac{\tau}{2}\right)dt \tag{3.17}$$

The cyclic autocorrelation function

$$R_x^{\alpha}(\tau) \triangleq \left( \lim_{T\to\infty} \frac{1}{T} \int_{\frac{-T}{2}}^{\frac{T}{2}} x\left(t+\frac{\tau}{2}\right)x^*\left(t-\frac{\tau}{2}\right)e^{-j2\pi\alpha t}dt \right) \neq 0 \tag{3.18}$$

where α is the cycle frequency. $R_x^{\alpha}(\tau)$ is the cyclic auto-correlation function, also known as the "time-frequency limit autocorrelation function". Since (3.18) is a generalization of (3.17), when α = 0, the DC component of (3.18) yields the time average autocorrelation

function of (3.17). Therefore, the process defined by (3.18) is able to extract more information from the signal than the process defined by (3.17).

Due to the fact that the power spectrum magnitude may be obtained from the Fourier transform of the autocorrelation function, the spectral-correlation density (SCD) or the cyclic-spectral density may also be obtained from the Fourier transform of the cyclic autocorrelation function (3.18)

$$S_x^\alpha(f) \triangleq \int_{-\infty}^{\infty} R_x^\alpha(\tau) e^{-j2\pi T} d\tau = \lim_{T\to\infty} \frac{1}{T} X_T\left(f + \frac{\alpha}{2}\right) X_T^*\left(f - \frac{\alpha}{2}\right) \tag{3.19}$$

where α is the cycle frequency and

$$X_T(f) \triangleq \int_{\frac{-T}{2}}^{\frac{T}{2}} x(u) e^{-j2\pi fu} du \tag{3.20}$$

which is the Fourier transform of the time domain signal *x(u).* The additional variable α leads to a two-dimensional representation $S_x^\alpha(f)$ which is the bifrequency plane or *(f,α)* plane (Lima 2002, 162).

In practice, the cyclic-spectral density must be estimated because the signals being processed are defined over a finite time interval (Δt). Estimates of the cyclic-spectral density can be obtained via time-smoothing or frequency-smoothing techniques. An estimate of the SCD using the time-smoothed cyclic periodogram is given by

$$S_x^\alpha(f) \approx S_{x_{T_W}}^\alpha(t, f) = \frac{1}{\Delta t} \int_{t-\Delta t/2}^{t+\Delta t/2} S_{x_{T_W}}^\alpha(t,u) du, \tag{3.21}$$

where

$$S^{\alpha}_{x_{T_W}}(u,f)=\frac{1}{T_W}X_{T_W}\left(u,f+\frac{\alpha}{2}\right)X^{*}_{T_W}\left(u,f-\frac{\alpha}{2}\right), \tag{3.22}$$

and Δt is the total observation time of the signal, $T_W$ is the short-time FFT window length, and

$$X_{T_W}(u,f)=\int_{t-T_W/2}^{t+T_W/2}x(u)e^{-j2\pi fu}du \tag{3.23}$$

is the sliding short-time Fourier transform. Figure 53 shows that, for any signal *x(t)*, the frequency components are evaluated over a small time window $T_W$ along the entire observation time interval Δt. The spectral components generated by each short-time Fourier Transform have a resolution, $\Delta f=1/T_W$. The variable *L* is the overlapping factor between each short-time FFT. In order to avoid aliasing and cycle leakage on the estimates, the value of *L* is defined as $L \le T_W/4$ (Lima 2002, 162).

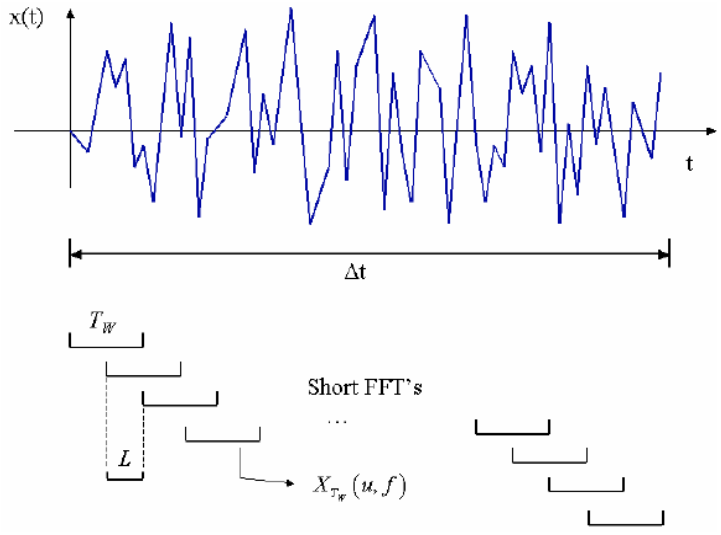


Figure 53. Estimation of the Time-Variant Spectral Periodogram[59]

[59] (Lima 2002, 162)

Figure 54 shows that the spectral components of each short-time FFT are multiplied for the cyclic-spectrum estimates. Note that the dummy variable *u* has been replaced by the time instances $t_1,...,t_p$. At each window ($T_W$), two components centered on some frequency $f_0$ and separated by some $\alpha_0$ are multiplied together and the resulting sequence of products is then integrated over the total time (Δt).

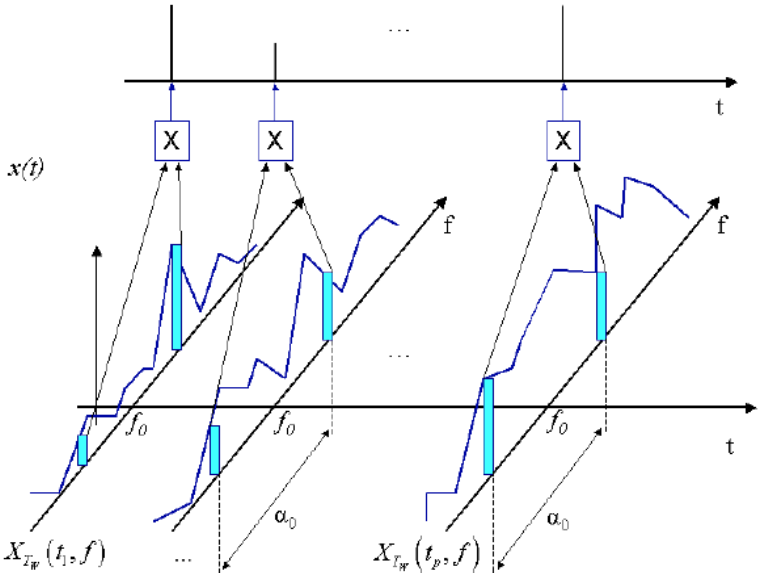


Figure 54. Sequence of Frequency Products for Each STFTs[60]

The estimation $S_x^\alpha(f) \approx S_{x_{T_W}}^\alpha(t, f)_{\Delta t}$ can be made as reliable and accurate as desired for any given *t* and, for all *f*, by making Δt large. Finally, an illustration of the relationship between the frequency plane and the bi-frequency plane is shown in Figure 55 (Lima 2002, 162).

60 (Lima 2002, 162)

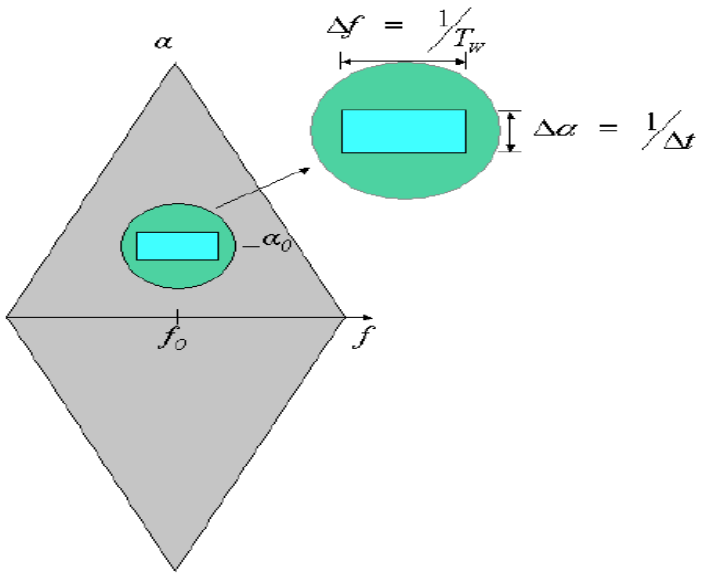


Figure 55. Bi-frequency and Frequency Plane[61]

Figure 56 shows the 2D bi-frequency output of an FMCW signal with 1KHz carrier frequency at the IF band, 250Hz modulation bandwidth and 10ms modulation period processed after cyclostationary processing.

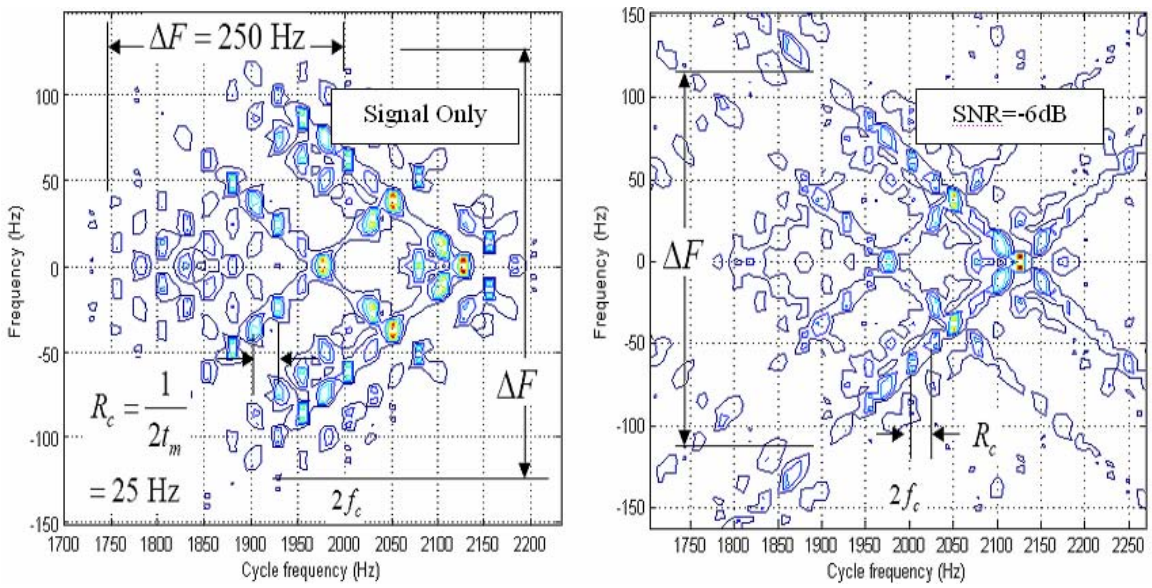


(a) (b)

Figure 56. Bi-Frequency Output FMCW signal (a) Signal Only (b) SNR=-6dB[62]

[61] (Lima 2002, 162)

[62] (Pace 2004, 455)

Table 7 below summarizes requirements to detect LPI radars. These include receiver challenges to overcome, ES receiver candidates and their operational examples, and some of the signal processing algorithms used in ES receivers.

Table 7. LPI Radar Detection Requirements

| | |
|---|---|
| Receiver Challenges to Overcome | Processing Gain of the LPI Radar<br>High Sensitivity Requirement<br>LPI Radar's Coherent Integration |
| ES Receiver Candidates | Digital Receivers<br>Acousto-Optic Receivers |
| ES Receiver Examples | High Sensitivity Microwave Receiver (HSMR)<br>Vigile-300<br>Sabre<br>NS-9003A-V2 ES System |
| Signal Processing Algorithms | Adaptive Matched Filtering<br>Parallel Filter Arrays and Higher Order Statistics<br>Wigner Ville Distribution (WVD)<br>Quadrature Mirror Filter Bank (QMFB)<br>Cyclostationary Processing (CS) |

THIS PAGE INTENTIONALLY LEFT BLANK

# IV. CLASSIFICATION AND JAMMING OF LPI RADARS

## A. CLASSIFICATION OF LPI RADARS

A trained operator can use one or a combination of signal processing tools to detect the LPI waveform characteristics. For real-time tactical situations, such as EA being conducted against an LPI radar, the use of computers will provide the ultimate solution. A remaining problem is autonomous parameter extraction and classification. Trained operator eyes have no problem with this, once the signal processing results are obtained, but the question is how can this be done by a computer autonomously.

This task is normally called specific emitter identification (SEI). SEI is a method of recognizing individual electronic emitters through the precise measurement of selected signal and characteristics. The problem that arises is that in order to be identified by SEI techniques, the emitter must have parameters that are stable and unique, within the measurement capabilities of the ES receiver. For LPI signals, this is typically not the case, since the signal is on for only a few code periods (Pace 2004, 455).

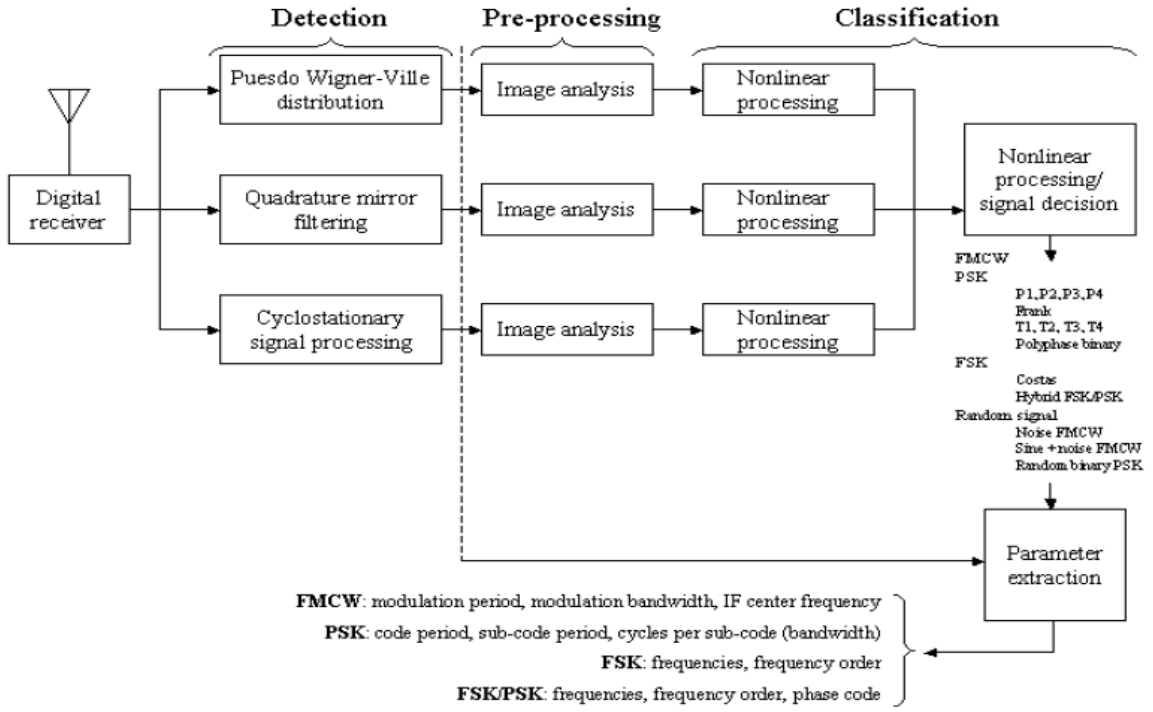


Figure 57. Autonomous Classification of LPI Radars[63]

[63] (Pace 2006, )

Figure 57 above shows an example of a possible ES receiver used to detect and identify LPI radar signals. After being received and digitized, the type of modulation is determined first. The classification is done by using WVD, QMFB, CS, and possibly others, in parallel. Each algorithm provides its own neural network (NN) with the time-frequency or bi-frequency image.

First a good amount of preprocessing must be done before the NN processed the image. The NN is trained with different LPI radar signals to recognize the numerous modulations that might be used by the LPI radar. Once the modulation type is identified, it is used to select the proper parameter measurement algorithm to process the time-frequency or bi-frequency output image. After the parameters of the signal are measured, the results are weighted to select the highest probable signal parameters, and then sorted into emitter classes by a clustering routine. It is only by directly digitizing the signal at the antenna, and taking advantage of high-speed parallel processing to run the sophisticated algorithms, that autonomous classification of LPI emitters can take place (Pace 2004, 455).

## B. NETWORK CENTRIC APPROACH

There are limitations to the use of intercept receivers in a platform-centric configuration. Geometrical limitations include extended stand-off ranges and alignment problems, which make it especially difficult to detect and jam LPI emitters. Also, the intercept receiver is limited by “look through”. The look through process allows the jammer to observe its effectiveness on the LPI emitter by stopping the jamming assignment to listen periodically. This results in inefficient jammer management and limited coordination during a mission.

During the jamming process, a certain amount of look through is required. For example, with an EA-6B reactively jamming a frequency-hopping radar, the jamming must stop in order to sense the radar’s transmit frequency. Duty cycle of the intercept receiver look through process must be less than the time necessary for the radar to sense it is being jammed, and switch radar parameters such as frequencies. Any amount of look through is not desired, since this allows the threat radar a window in which to detect the strike aircraft (Pace 2004, 455).

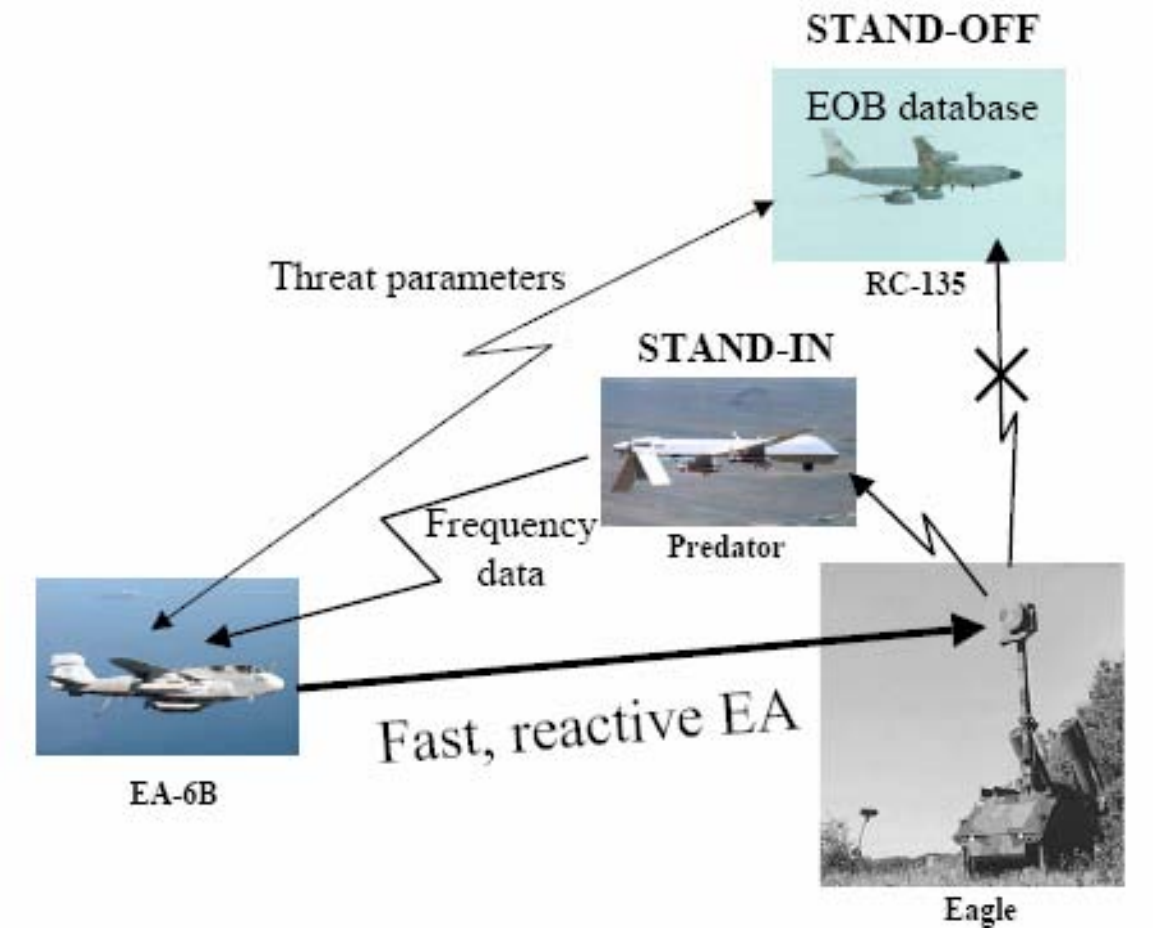


Figure 58. Tip-and-Tune: Solution for the Look Through Problem[64]

If, however, the EA-6B integrates threat parameters from an electronic order-of-battle database, a reconnaissance aircraft with near-real time on scene intelligence collection, analysis, and dissemination capabilities (e.g., Rivet Joint), and frequency data from an off-board stand-in sensor (e.g., UAV) to cue the on-board intercept receiver (tip and tune) as shown in Figure 58, a fast reactive electronic attack can be performed that eliminates the need for look through. For the reactive jamming assignments to be effective, however, the data link used to provide the cuing data must not induce a delay time of any significance to the reactive assignment. That is, if the frequency hopping radar can switch frequencies faster than the cueing data can arrive from the off-board intercept receiver, then effectiveness is significantly degraded (Pace 2004, 455).

[64] (Pace 2006, )

Eliminating the limitations inherent in a platform-centric configuration comes from a distributed system of systems. A distributed system of systems provides significant geometric flexibility, and can reduce or eliminate the need for look through.

In a network-centric architecture, the network acts as a force multiplier by networking sensors (e.g., ES receivers), decision makers, and shooters (e.g. Weapon Systems), to achieve shared awareness. The network requires sufficient bandwidth for all users to take advantage of data mining in appropriate databases afloat and ashore. The architecture is determined mostly by the mission altitudes, signal densities, reaction times, and modulation analysis that must be performed (Pace 2004, 455).

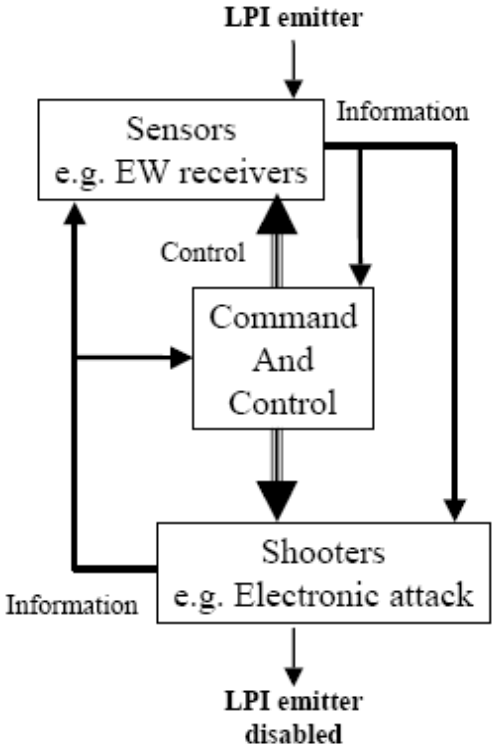


Figure 59. LPI Radar Jamming with Network-Centric Architecture[65]

Figure 59 above demonstrates the detection and jamming of an LPI emitter using a network-centric architecture. The LPI emitter is detected using a number of sensors that relay the information to both a C2 point, and the proper shooter. C2 allows the shooter to apply the appropriate electronic attack to disable the LPI emitter. The shooter also relays

[65] (Pace 2004, 455)

its information concerning the jammed emitter back to the both sensors and C2. That is, instead of each platform making decisions on information received by only its own intercept receiver (the platform-centric approach), modern ES receivers integrate information from many sensors and databases for targeting (Pace 2004, 455).

Stand-off platforms are augmented by specialized receivers that can go to the emitters (stand-in platforms). These specialized receivers are mounted, for example, in unmanned aerial vehicles (UAVs) such as the Predator.

The use of “swarm intelligence” technology is fast becoming an important concept in network-centric sensor configurations. Swarm intelligence allows the design of ES receiver networks to detect LPI emitters, and is inspired by the behavior of social insects (Bonabeau, Dorigo M, and Theraulaz 1999, ). In swarm sensor architecture, the signal collection capability is defined by group behavior and not individual behavior. One advantage in using a UAV swarm of ES receivers is the ability to behave autonomously, using digital information pheromones (DIP). The idea is to use another ES receiver’s experience in prior LPI emitter searches. This allows other ES receivers to gain knowledge of how many previous detections of this emitter were found, and characteristics of the emitter. Continuously detected DIPs should be updated by regular verifications (Pace 2004, 455).

Another advantage is the ability of the UAVs to behave cooperatively. Cooperative behavior allows the UAVs to form a robust, self organizing and self-adapting sensor architecture, while retaining the intercept function even in the presence of a loss. The swarm LPI detection architecture requires only low-cost medium-endurance airframes (expandable), existing wideband intercept receivers (e.g. R-300A, highly integrated microwave receiver), and the use of swarm logic with intra-swarm communications using, for example, an 802.11 link as shown in the Figure 60. With the swarm approach, LPI radars run the risk of detection and classification, especially when the intercept receiver incorporates advanced signal processing techniques that take the advantage of time frequency, bi-frequency processing (Pace 2004, 455).

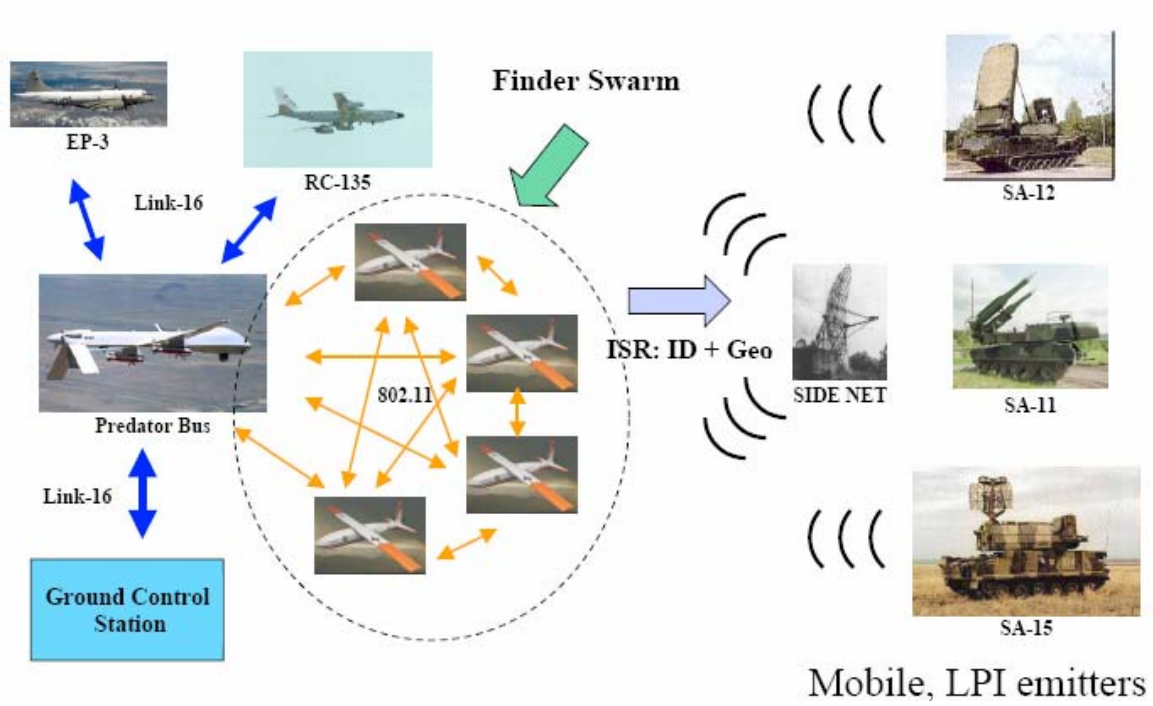


Figure 60. Swarm Intelligence Approach[66]

## C. JAMMING OF LPI RADARS

### 1. Probability of Jamming

So far, this thesis has considered the detection and the classification of LPI radar signals, and not the extraction of any information that would enable the jammers to exploit the transmissions. If we consider the information that can be extracted from the waveform, then we can examine the potential to further exploit the LPI radar signal (Stove, Hume, and Baker 2004, 249-260).

Following is Shannon's theorem:

$$C = W \log_2(1 + SNR) \tag{4.1}$$

where C is the channel capacity in bits/second, W is its bandwidth, and SNR is the signal to noise ratio. In this case, if W is set to 1 then C becomes the capacity in bits per

[66] (Pace 2006, )

interception. For the detection threshold level of 17dB SNR, each interception may be assumed to provide the opportunity for extracting 5.7 bits of information concerning the LPI radar. It can be assumed that in order to exploit transmissions, the following information is needed:

- Scan timing, i.e. where the radar is pointing at any time,
- Carrier frequency,
- Modulation bandwidth,
- Modulation or code period,
- Synchronization, i.e. when the modulation pattern starts.

If each of these parameters must be known to 4 bits precision, i.e. slightly better than 10% accuracy, 20 bits of information is needed to characterize the radar, not including trying to replicate its waveform in any detail. The scan timing and carrier frequency can readily be discovered from the way in which intercept is made. Information on the LPI radar would effectively be obtained from multiple looks at the receiver output. After this process 12 bits giving 36dB SNR of information has to be recovered from the signal. In some conventional ES receivers this sensitivity is achieved through integrating multiple looks, using a receiver with a wider bandwidth than the signal's information bandwidth (Stove, Hume, and Baker 2004, 249-260).

The problem with attempting to match the jamming receiver for a single look interception and exploitation is that it is more efficient in energy terms to obtain information from separate looks at lower SNR. For example, to send 8 bits of information in one go requires 24dB SNR in the channel's information bandwidth. To send it in two 4-bit messages requires twice as much time but only 12dB SNR, a saving of 9dB in the amount of energy used.

It should be noted in passing that the true matched filter removes all the modulation information from the signal, leaving only the information about the energy spectrum. It can be a fundamental fact that optimizing the detection sensitivity involves removing as much as possible of the information bearing capacity of the original waveform, by whatever means the filtering is achieved (Stove, Hume, and Baker 2004, 249-260).

### 2. Sensitivities Required for Jamming

The process of coding the information onto the radar waveform and decoding it in the receiver is 6dB less efficient than a typical communication channel, which may itself be assumed to be 6dB less efficient than the Shannon limit. Therefore, 48dB SNR is needed to recover the required information from the signal. This is approximately equivalent to removing the 30dB increase in sensitivity obtained by going from an IFM type receiver to a matched ES receiver. It can be hypothesized that the channelized receiver achieves an intermediate exploitation performance by being less lossy than the IFM type receiver in recovering the information, but that it will require additional SNR to stitch together the outputs of the different channels to recover all the information required (Stove, Hume, and Baker 2004, 249-260).

The results derived above show that it is possible to exploit the radar's transmissions. The simple radiometric detector is able to cope with any waveform, but at the cost of destroying most of the information contained within it. This makes it unsuitable for use in a busy environment, but it can be useful during normal 'radar silence' when very few emitters will be present. In fact, in busy environments, it can be argued that the best way of transmitting covertly is to make the transmissions look like a commercial radar, such as a conventional marine radar or aircraft weather radar. Thus, they may not be noticed. However, if an LPI waveform is detected, it is clearly not coming from an innocent source (Stove, Hume, and Baker 2004, 249-260).

### 3. LPI Radar Jammer Design Requirements

Two parameters are of critical importance when considering the design of an LPI receiver front-end for EA applications. First one must consider the RF bandwidth; too wide a bandwidth allows too much signal to enter the detector and unnecessarily degrades the receiver noise figure while too narrow a bandwidth eliminates too much of the signal lowering the average power to the detector.

The second factor to be considered is the detector video bandwidth. A wide video bandwidth provides for fast rise and fall times necessary for processing narrow pulses, but this is done at the expense of allowing more noise to the detector as well. A carefully designed jammer will address both of these design areas (McRitchie and McDonald 1999, ).

### *a. RF Bandwidth*

In order to define the RF bandwidth requirements for a jammer, the dynamics of the radar/target engagement must be considered. A limiting factor in this discussion is the time-bandwidth product of the radar.

A target traveling with radial velocity $\nu_r$ moves a distance ΔR in the time $T_1$ given by:

$$\Delta R = T_1.\nu_r \,. \tag{4.2}$$

For coherent integration, the target must not move out of the radar range cell during the integration time, so that:

$$\Delta R \le \frac{c.\tau}{2} \cong \frac{c}{2.B} \tag{4.3}$$

where c=speed of light ($3.10^8 m/s$), $\tau$ = integration time, and B=signal bandwidth. Therefore,

$$T_1 \le \frac{c}{2.B.\nu_r}. \tag{4.4}$$

An airborne intercept (AI) radar must be designed for closing velocities of Mach 2 to Mach 3, while a ground based radar would probably be designed for Mach 1 fighter aircraft or much slower closing velocities for helicopter targets (McRitchie and McDonald 1999, ). Thus, the maximum compression gain is limited to:

$$T_1.B \le 200,000 \quad \text{air-air}$$
$$T_1.B \le 500,000 \quad \text{surface-air}$$

Doppler resolution is equal to the inverse of the integration time, and is typically 100 to 1000 Hz. Thus $T_1$ and B are bounded by:

$$1\text{msec} < T_1 < 10\text{msec}$$

$$20\text{MHz} < B < 500\text{MHz}$$

This is significant in that the jammer's bandwidth should be wide enough to capture the whole radar signal, which may be spread out over the bandwidth B by polyphase coding, or FMCW. There is a limit in the radar technology that places bounds on the amount of RF agility or modulation that can be obtained on a given radar as a function of RF operating frequency. This limit is about one half of one percent of the bandwidth. Therefore, for a radar operating at 10GHz, the upper bound on either RF agility or FMCW is on the order of 500MHz. In practice, the operational limit is somewhat smaller than this due to need of RF components over this significant bandwidth and over the rigorous military environment constraints (McRitchie and McDonald 1999, ).

***b. Video Bandwidth***

The primary LPI technique employed by the radar designers is to spread the signal in frequency and use coherent integration and pulse compression so that the radar's peak power can be reduced to the point where the signal power levels at the jammer receiver are lost in the noise. If the jammer attempts to narrow its bandwidth in order to reduce the noise power, it loses a significant amount of the information because of the radar's large agile bandwidth.

**4. Jamming FMCW Radars**

FMCW radars are difficult to detect due to their wideband waveforms and consequently, potential jammers have a significant problem measuring the waveform parameters with sufficient accuracy in order to match the jamming waveform (Pace 2004, 455).

In a realistic environment with a large number of radar systems operating in the same frequency band, an FMCW radar is significantly more difficult to detect. Also, since the FMCW transmit waveform is deterministic; it possesses inherent resistance to electronic attack. This stems from the fact that since the transmitted signal is deterministic, the return target signature has a form that can be predicated, and provides

significant suppression of many interfering waveforms that are uncorrelated. (such as narrowband interference and pulsed radar emissions)

If the modulation period $t_m$ and modulation bandwidth ΔF can be determined, then coherent deception jamming is feasible and very effective, since the jammer waveform looks like the radar waveform (Pace 2004, 455).

Anti jamming aspects of linear FM waveforms using simulations were performed by Jeffrey S. Fu and Younan Ke. White Gaussian noise, continuous wideband jamming, and jamming signals that were identical to transmitted chirp signals were evaluated. They conclude that the FMCW signal can be recovered in moderate noise conditions, but the radar has a difficult time distinguishing a genuine chirp signal from hostile jammer produced signals that have a similar frequency spectrum to the chirp signal (Fu and Ke 1996, 605).

There are some basic approaches for jamming FMCW radars. One approach is to predict the frequency-versus-time characteristics of the signal and use a jammer that will input energy to the receiver at the same frequency as the FM signal it is attempting to receive. This will allow the maximum jammer-to-signal ratio (JSR) to be achieved for any given jammer power and jamming geometry (Adamy 2001, ).

Another approach is to cover all or part of the modulation range with a broadband jamming signal that is received by the LPI radar receiver with adequate power to create adequate JSR in the “de-chirped” output. As shown in Figure 61, the FM modulated signal has an anti-jam advantage equal to the ratio between its information bandwidth and the frequency range over which it is modulated.

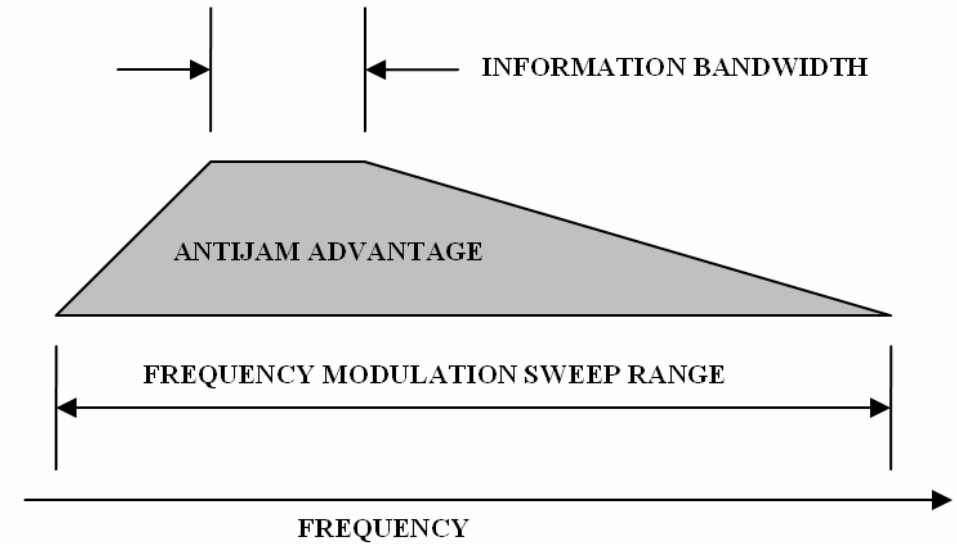


Figure 61. Anti-jam Advantage of FMCW Radar Signal[67]

Depending on the specifics of the information signal modulation, it may be practical to perform effective partial-band jamming. This jamming technique focuses the jamming power over a fraction of the frequency modulation range that will allow the JSR ratio in the jammed portion to cause a high rate of bit errors in the digital modulation which is carrying the signal's information. The fraction of the range which is jammed depends on the jammer power, the effective radiated power of the modulated transmitter, and the relative ranges of the transmitter and the jammer to the jammed receiver (Adamy 2001, ).

In addition to the jamming approaches above, some coherent deception EA techniques can be used effectively against FMCW radars. One of them is false range targets. They can be produced in an FMCW radar by slightly shifting the frequency of the return. This will create a shift in the apparent range of the signal as it passes through the radar processor.

Another coherent EA technique is velocity gate pull-off (VGPO). VGPO signals, which are effectively a change in the rate of change of signal's phase, will affect the signal processing in the radar. Although the introduction of a frequency error in the return

[67] (Adamy 2001, ) Unless a jammer can be swept in synchronization with the signal modulation rate, a jammer's power must be spread across the whole swept range. The ratio of the modulation sweep range to the information bandwidth is the antijam advantage.

signal will affect the integration efficiency, in order to be effective, the VGPO must create at least 180° phase shift over the signal (McRitchie and McDonald 1999, ).

Narrow band Doppler noise may also be quite effective since the SNR in the LPI receiver is already at quite a low value. A Digital RF Memory (DRFM) can be used to focus the available power of the jammer and inject Doppler noise that is only a few KHz wide, matching to the instantaneous bandwidth of the FMCW radar (McRitchie and McDonald 1999, ).

**5. Jamming PSK Radars**

These phase coded signals can be affected by VGPO type techniques. The introduction of an additional Doppler shift, which will be interpreted by the radar as an additional phase shift, will cause a spreading of the received signal and therefore decrease the effective processing gain. If enough Doppler shift can be added then there will be a corresponding loss of integration gain within the radar processor (McRitchie and McDonald 1999, ).

Range bin masking techniques should also be quite effective. If a section of the radar waveform recorded by DRFM or repeater is used by the jammer as it's transmit waveform, the truncation will cause an increase in the sidelobe levels of the processed return. The merging of the sidelobes can create a threshold problem for the radar leading to total signal loss; but at the very least will degrade the SNR of the true target return causing a loss in processing gain (McRitchie and McDonald 1999, ).

**6. Jamming FSK Radars**

FSK radars are said to have an anti-jam advantage as seen in Figure 62. This advantage is based on the assumption that the jammer knows only the full hopping range and must spread its jamming power over that full frequency range. Assume an FSK radar that has a 2000 frequency hopping sequence which is random or unknown to the ES receiver. The FSK radar can be said to have a jamming advantage of 2000, which converts to 33dB. This means that it takes 33dB more jammer power to achieve a given JSR against this frequency hopper than would be required if it were a fixed-frequency conventional radar.

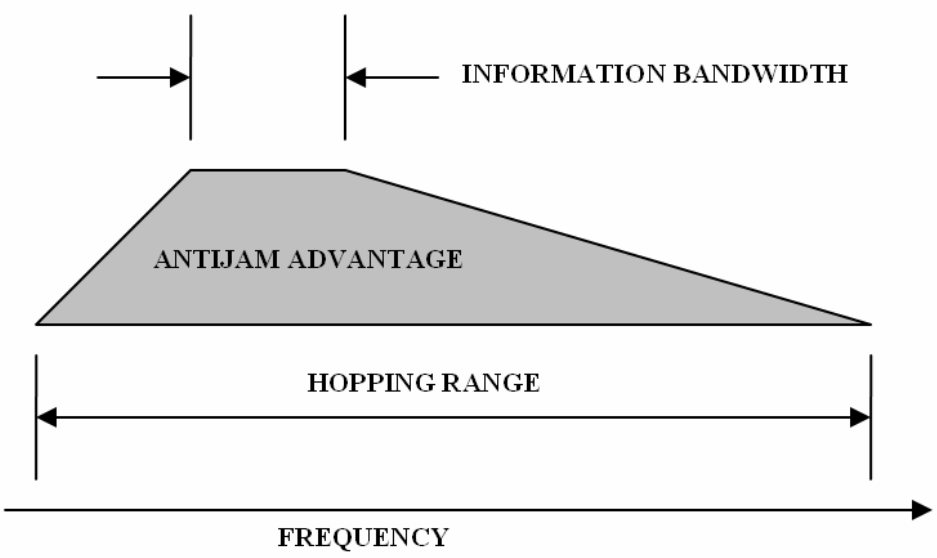


Figure 62. Anti-jam Advantage of FSK Radar Signal[68]

One jamming approach that can be used for this kind of radar is to perform "follower jamming". A follower jammer detects the frequency of each hop and then jams on that frequency. This solution requires an extremely fast frequency measurement technique in order to deny the enemy the transmitted information in each hop (Adamy 2001, ). Furthermore, the frequency hopping sequence of FSK radar is unknown and appears random to the ES receiver. Unless this frequency sequence is solved, the possibility of a jammer following the changes in frequency is very remote.

[68] (Adamy 2001, ) In order to jam a FSK radar signal with a conventional jammer, the jammer's power must be spread across the whole hopping range. The ratio of the hopping range to the information bandwidth is the antijam advantage.

# V. CONCLUSION

The signal environment is changing at a rapid pace with new Low Probability of Intercept (LPI) radars coming into service worldwide. These radars exhibit lower power and higher duty cycle than previous radar technology. By 2010, approximately 30% of all radars will emit LPI signals and will be employed in all classes of radar including battlefield, navigation, surveillance, target acquisition and missile seekers on airborne, maritime, and land-based platforms (Tenix Defense 2005, 2).

Airborne LPI radars are used for search, tracking, location, identification, acquisition, designation, target imaging, periscope detection, and weapon delivery. These LPI radars also have modes for covert navigation, weather detection, terrain following, and terrain avoidance. Just as LPI techniques are useful for covert navigation and targeting in airborne applications, they are equally useful for maritime applications. LPI is well suited for this environment as the relatively slow speed of a ship and extremely large radar cross sections (RCSs) allows for long integration times. Besides maritime applications, there are many examples of land-based LPI radar generally performing ground surveillance and short range air surveillance. In the case of the ground surveillance role, these radars can be used to covertly detect ground targets due to long integration times.

Electronic Warfare Support (ES) receivers currently in service are not optimized for the detection of LPI radars as they lack the sensitivity to detect the signals at sufficient range to provide military crews with an operational range advantage. LPI Radars use advanced radar and signal processing techniques *"to see and not be seen"*[69] by ES receivers. To survive Electronic Attack (EA) and Anti Radiation Missile (ARM) threats and mask their presence, LPI radars use:

- Low sidelobe antennas,
- Irregular antenna scan patterns,
- High duty cycle/wide band transmission,
- Accurate power management,

[69] (Fuller 1990, 1-10)

- Carrier frequencies at peak atmospheric absorption,
- Very high sensitivity,
- High processing gain,
- Coherent detection,
- And monostatic/bistatic configurations.

There are several LPI radar techniques available to the modern radar designer that can be used singly or in various combinations, depending on the application. Reducing the radar's peak effective radiated power (ERP) by using some form of pulse compression technique is the most common LPI radar technique. The objective is to spread the radar's signal over a wide bandwidth and a period of time. This is typically done with frequency modulation (FM), which is the most common technique, phase shift keying (PSK), and frequency shift keying (FSK) techniques.

In order to jam LPI radar signals the ES receivers and associated EA systems must accomplish specific steps. First and most important is LPI radar detection. Without detection no countermeasures are possible. To detect LPI radar signals, ES receivers have to overcome three main difficulties. These are:

- LPI radar's coherent integration,
- High sensitivity requirement,
- And processing gain of the LPI radar.

LPI radars have low power, high duty cycle signals with phase or frequency coding. As the coding is unknown and can be complex, and assuming the frequency is also unknown, then coherent detection is not possible and non-coherent detection must be performed first. To achieve the maximum sensitivity the RF and video bandwidth must be matched to the signal modulation, allowing detection of the total signal energy (Rayit and Mardia 1994, 359; 359-362; 362). Detection of LPI radar signals also requires a large processing gain because of the wideband nature of the LPI radar. Detection is possible if the signal is integrated over a long observation time.

Detection of LPI radar signals also requires sophisticated receivers that use time frequency signal processing, correlation techniques and algorithms to overcome the processing gain of the LPI radar. Fourier analysis techniques have been used as the basic tool. From this basic tool, more complex signal processing techniques have evolved, such

as the short-time Fourier transform (STFT), so as to track signal parameters over time. More sophisticated time-frequency and bi-frequency distribution techniques have also been developed to identify the different modulation schemes used by LPI radars. These techniques include the Wigner Ville Distribution (WVD), Quadrature Mirror Filter Bank (QMFB), and Cyclostationary Processing (CP) (Pace 2004, 455).

These signal processing algorithms require large amounts of computing speed and memory. Managing processing speed is not a problem with current digital capabilities, but carrying enormous amounts of data is still difficult. Increasing the sensitivity of the receiver allows for detecting sidelobes of the emitter, but at the same time obligates the receiver to process a significantly large number of signals.

Some wide-open ES receivers such as the Instantaneous Frequency Measurement (IFM) and Crystal Video Receivers (CVR) work well in a low density signal environment where the pulses are short in duration. However IFM and crystal video receivers are more susceptible to interference and thus are poor candidates for future ES receiver systems that perform LPI radar detection. In addition, they do not have the sensitivity required for the detection of current and projected LPI signals (Lee 1991, 55). Calculations made by Dr. Jim Lee show that in order to detect LPI radar; the receiver sensitivity must be on the order of -100dBm.

The trend in ES receivers for LPI radar detection is toward digital receivers and incorporates the concept of digital antennas in which the analog-to-digital converter (ADC) is at the antenna. The future digital receiver will incorporate optical technologies for speed and bandwidth, and will also incorporate high-temperature superconductors for required sensitivities (Pace 2006, ).

Once the detection hurdle has been overcome, the ES receiver must next perform classification. Classification requires sorting the signal into groups having similar parameters. These parameters are;

- LPI radar type,
- Carrier frequency,
- Modulation bandwidth,
- Modulation or code period,

- Scan timing, i.e. where the radar is pointing at any time,
- And synchronization, i.e., when the modulation pattern starts.

These parameters distinguish one LPI radar signal from another and they are required for effective jamming. Correlation with existing signals in a database, which is called identification, can then aid in signal tracking and response management.

A trained operator can use one or a combination of signal processing tools to detect and classify the LPI waveform characteristics. For real-time tactical situations, such as EA being conducted against an LPI radar, speed and the decision making of manual processing will not be fast, accurate, and sufficiently correct. In this case, autonomous parameter extraction, classification, and response management is required. This necessitates the use of computers. After being received and digitized, the type of modulation is first determined. The classification is accomplished by using WVD, QMFB, CS, and possibly other signal processing algorithms in parallel. Each algorithm provides its own neural network (NN) with the time-frequency or bi-frequency image.

The NN is trained with different LPI radar signals to recognize the numerous modulations that might be used by the LPI radar. Once the modulation type is identified, it is then used to select the proper parameter measurement algorithm to process the time-frequency or bi-frequency output image (Pace 2004, 455). Adaptive Resonance Theory (ART) is a very strong candidate for NN and has pattern recognition algorithms that the time-frequency or bi-frequency output images of LPI radar signals can be processed and classified effectively.

After classification and parameter extraction, immediate jamming response can be initiated with associated EA systems. There are two requirements for effective jamming of LPI radars. The first is that the platform carrying the EA and ES receiver systems should detect the LPI radar before LPI radar detects the platform. Otherwise the EA system's effectiveness is severely reduced. The second requirement relates to the efficiency of the jamming waveform. Because the LPI radar transmissions are spread over a very wide bandwidth in a noise-like manner, it is very difficult for an uncorrelated waveform spread over the same bandwidth to be effective (Schleher 1986, 559).

For FMCW LPI radars, noise techniques such as white Gaussian noise and continuous wideband noise are not effective, and FMCW signals can be recovered in such moderate noise conditions (Fu and Ke 1996, 605). On the other hand; if the modulation period $t_m$ and modulation bandwidth ΔF can be determined, then coherent deception jamming is feasible and very effective, since the jammer waveform looks like the radar waveform (Pace 2004, 455). False range targets, velocity gate pull-off, and narrow band Doppler noise created by using digital RF memory (DRFM) are the coherent EA techniques which can be used effectively against FMCW LPI radars.

Against phase coded LPI radars, noise type EA techniques are also not effective. Phase coded LPI radars can be affected by VGPO type techniques. The introduction of an additional Doppler shift, which will be interpreted by the radar as an additional phase shift, will cause a spreading of the received signal and therefore decrease the effective processing gain. If enough Doppler shift can be added then there will be a corresponding loss of integration gain within the radar processor (McRitchie and McDonald 1999, ). Range bin masking techniques should also be quite effective against phase coded radars. If a section of the radar waveform recorded by either DRFM or a repeater is used by the jammer as it's transmit waveform, the truncation will cause an increase in the sidelobe levels of the processed return. The merging of the sidelobes can create a threshold problem for the radar leading to a blank display, and at the very least will degrade the SNR of the true target return, causing a loss in processing gain (McRitchie and McDonald 1999, ).

For FSK radars "follower jamming" can be used. A follower jammer detects the frequency of each hop and then jams on that frequency. But this solution requires an extremely fast frequency measurement technique in order to deny the enemy the transmitted information in each hop (Adamy 2001, ). Furthermore, the frequency hopping sequence of the FSK radar is unknown and appears random to the ES receiver. Unless this frequency sequence is solved, the possibility of the jammer following the changes in frequency is very remote.

There are limitations to the use of ES receivers and EA systems in a platform-centric configuration. Geometrical limitations include extended stand-off ranges and

alignment problems, which make it especially difficult to detect and jam LPI radars. Also, the ES receiver is limited by “jamming look through”. Eliminating the limitations inherent in a platform-centric configuration is accomplished by a distributed system of systems. A distributed system of systems provides significant geometric flexibility, and can reduce or eliminate the need for look through.

In a network-centric architecture, the network acts as a force multiplier by networking sensors (e.g., ES receivers), decision makers, and shooters (e.g., Weapon Systems and HARM shooters) by achieving shared awareness in order to detect and jam LPI radars (Pace 2004, 455). Stand-off platforms are augmented by specialized receivers that can go to the emitters (stand-in platforms). These specialized receivers are mounted, for example, in unmanned aerial vehicles (UAVs) such as the Predator.

The use of “swarm intelligence” technology is fast becoming an important concept in network-centric sensor configurations. Swarm intelligence allows the design of ES receiver networks to detect LPI emitters, and is inspired by the behavior of social insects (Bonabeau, Dorigo M, and Theraulaz 1999, ). With the swarm approach, LPI radars run the risk of detection and classification, especially when the intercept receiver incorporates advanced signal processing techniques that take the advantage of time frequency, bi-frequency processing (Pace 2004, 455).

While modern LPI radar systems and waveforms present formidable challenges to older and presently deployed ES receivers, there are techniques and technologies available on the near-horizon equipped to meet this challenge. Digital receivers with high sensitivities, time-frequency and bi-frequency signal processing techniques with high processing gains working in the neural networks will overcome the LPI radar’s signal masking and hiding techniques. Furthermore, using miniaturized receivers at UAVs with network centric and swarm intercept strategies will carry LPI radar and ES receiver battle into a different dimension.

# LIST OF REFERENCES


Adamy, David L. 2001. *EW 101: A first course in electronic warfare*. Norwood, MA: Artech House.

Bonabeau, E., Dorigo M, and G. Theraulaz. 1999. *Swarm intelligence from natural to artificial systems*. New York: Oxford University Press.

Burgos-Garcia, M., J. Sanmartin-Jara, F. Perez-Martinez, and J. A. Retamosa. 2000. Radar sensor using low probability of interception SS-FH signals. *IEEE Aerospace and Electronic Systems Magazine* 15, (4) (APR): 23-28.

Burrus, S., A. Gopinath, and H. Guo. 1998. *Introduction to wavelets and wavelets transforms*. First Edition ed.Prentice Hall.

Copeland, D. B., and P. E. Pace. 2002. Detection and analysis of FMCW and P-4 polyphase LPI waveforms using quadrature mirror filter trees.

Donohoe, J. P., and F. M. Ingels. 1990. The ambiguity properties of FSK/PSK signals.

F-16.Net. AN/AAQ-13 & AN/AAQ-14 LANTIRN. [cited April/16 2006]. Available from http://www.f-16.net/f-16_armament_article2.html.

Fielding, J. E. 1999. Polytime coding as a means of pulse compression. *Aerospace and Electronic Systems, IEEE Transactions on* 35, (2): 716-721.

Fu, J. S., and Y. Ke. 1996. Anti-jamming aspects of linear FM and phase coded pulse compression by simulation. Paper presented at CIE International Conference of Radar, .

Fuller, K. L. 1990. To see and not be seen [radar]. *Radar and Signal Processing, IEEE Proceedings F* 137, (1): 1-10.

Gau, Jen-Yu. 2002. Analysis of low probability of intercept (LPI) radar signals using the wigner distribution. M.S. in Systems Engineering., Naval Postgraduate School.

GuoSui Liu, Hong Gu, WeiMin Su, and HongBo Sun. 2001. The analysis and design of modern low probability of intercept radar. *2001 CIE International Conference on Radar Proceedings (Cat no.01TH8559)* (2001): 120; 120-124; 124.

Hou Jiangang, Tao Ran, Shan Tao, and Qi Lin. 2004. A novel LPI radar signal based on hyperbolic frequency hopping combined with barker phase code. *2004 7th International Conference on Signal Processing Proceedings (IEEE Cat.no.04TH8739)* (2004): 2070; 2070-3 vol.3; 3o.3.

Jane's Air Defense Radar – Land and Sea. 1997. Section 9 – product descriptions (united states). (February 1997).

Jane's Air-Lauched Weapons. 2002. Air to surface missiles, RBS-15F. (September 12, 2002).

Jane's C4I Systems. 2001. Intelligence systems – surveillance and reconnaissance. (April 06, 2001).

Jane's International Defense Review. 1994. Radar eyes on the battlefield. (October 01, 1994).

Jane's Land Based Air Defense. 2004. Self-propelled anti-aircraft guns (netherlands). (August 17, 2004).

———. 1999. Anti-aircraft control systems (sweden). (March 25, 1999).

JANE'S NAVY INTERNATIONAL. 2004. Radar ESM faces up to the littoral challenge (SEPTEMBER 01, 2004).

Jane's Police and Security Equipment. 2005. Surveillance equipment. (December 29, 2005).

Jane's Radar and Electronic Warfare Systems. 2006a. Battlefield, missile control and ground surveillance radar systems. (February 22, 2006).

———. 2006b. Naval/Coastal surveillance and navigation radars. (February 22, 2006).

———. 2005. Airborne surveillance, maritime patrol and navigation. (August 11, 2005).

———. 2004a. Airborne fire-control radars, united states. (March 10, 2004).

———. 2004b. Airborne fire-control radars, united states. (October 22, 2004).

———. 2004c. Airborne fire-control radars, united states. (December 03, 2004).

———. 2004d. Battlefield, missile control and ground surveillance radar systems. (October 22, 2004).

———. 2004e. Battlefield, missile control and ground surveillance radar systems. (October 26, 2004).

———. 2004f. Naval/Coastal surveillance and navigation radars (poland). (November 17, 2004).

———. 2003. Battlefield, missile control and ground surveillance radar systems. (March 25, 2003).

Jarpa, Pedro F. 2002. Quantifying the differences in low probability of intercept radar waveforms using quadrature mirror filtering. M.S.: Electrical Engineering., Naval Postgraduate School.

Klein, L. A. 1997. *Milimeter-wave and infrared multisensor design and signal processing*. Norwood, MA: Artech House, INC.

Lee, Jim P. 1991. *Interception of LPI radar signals.*

Lewis, Bernard. 1986. *Aspects of radar signal processing*. Norwood, MA: Artech House, INC.

Lima, Antonio F. 2002. Analysis of low probability of intercept (LPI) radar signals using cyclostationary processing. M.S. in Systems Engineering., Naval Postgraduate School.

McRitchie, Dr W. K., and S. E. McDonald. 1999. *Detection and jamming of LPI radars.* Canada: MC Countermeasures INC, W7714-7-0133/003/SV.

Milne, P. R., and P. E. Pace. 2002. Wigner distribution detection and analysis of FMCW and P-4 polyphase LPI waveforms. *2002 IEEE International Conference on Acoustics, Speech, and Signal Processing.Proceedings (Cat.no.02CH37334)* (2002): IV3944; 3944-7 vol.4; 7o.4.

Ong, Peng G., and Teng, Haw K. *Digital LPI radar detector*.2001.

Pace, Philip E. 2006. *Introduction to LPI radar, EC4690 class notes*. Class Notes ed. Monterey: .

Pace, Phillip E. 2004. *Detecting and classifying low probability of intercept radar*. Artech house radar library. Boston: Artech House.

Persson, Christer N. E. 2003. Classification and analysis of low probability of intercept radar signals using image processing. Electrical Engineering)., Naval Postgraduate School.

Rayit, R. K., and H. K. Mardia. 1994. Detection of LPI radars using an adaptive front-end. *Microwaves 94.the Applications of RF.Microwave and Millimetre Ware Technologies.Conference Proceedings* (1994): 359; 359-362; 362.

Raytheon. AN/APQ-181 RADAR SYSTEM. in Raytheon Company [database online]. [cited April 16, 2006]. Available from http://www.raytheon.com/products/apq181.

Ruffe, L. I., and G. F. Stott. 1992. LPI considerations for surveillance radars. *International Conference Radar 92 (Conf.Publ.no.365)* (1992): 200; 200-202; 202.

Schleher, D. Curtis. 1986. *Introduction to electronic warfare*. Artech house radar library.

SPG Media. SAAB BOFORS DYNAMICS. [cited April 16, 2006]. Available from http://www.naval-technology.com/contractors/weapon_control/celsiustech/celsiustech2.html.

Stove, A. G., A. L. Hume, and C. J. Baker. 2004. Low probability of intercept radar strategies. *Iee Proceedings-Radar Sonar and Navigation* 151, (5) (OCT): 249-260.

Taboada, Fernando L. 2002. Detection and classification of low probability of intercept radar signals using parallel filter arrays and higher order statistics. M.S. in Systems Engineering., Naval Postgraduate School.

Tenix Defense. High sensitivity microwave receiver. in Tenix Defense Pty Ltd [database online]. Australia, 2005 [cited November 6, 2006]. Available from http://www.tenix.com/Main.asp?ID=849.

Wirth, W. D. 1995. Long term coherent integration for a floodlight radar.

# INITIAL DISTRIBUTION LIST

1. Defense Technical Information Center
   Ft. Belvoir, Virginia

2. Dudley Knox Library
   Naval Postgraduate School
   Monterey, California

3. Chairman
   Information Sciences Department
   Monterey, California

4. Professor Edward Fisher
   Department of Information Sciences
   Monterey, California

5. Professor Orin Marvel
   Department of Information Sciences
   Monterey, California

6. Capt. Aytug Denk
   Turkish Air Force
   Turkey

7. Hava Kuvvetleri Komutanligi
   Hava Kuvvetleri Komutanligi Kutuphanesi
   Bakanliklar, Ankara, Turkey

8. Hava Harp Okulu
   Hava Harp Okulu Kutuphanesi
   Yesilyurt, Istanbul, Turkey

9. Deniz Harp Okulu
   Deniz Harp Okulu Kutuphanesi
   Tuzla, Istanbul, Turkey

10. Kara Harp Okulu
    Kara Harp Okulu Kutuphanesi
    Bakanliklar, Ankara, Turkey